

Dissertation  
submitted to the  
Combined Faculties for the Natural Sciences and for Mathematics of the  
Ruperto-Carola University of Heidelberg, Germany  
for the degree of  
Doctor of Natural Sciences

Presented by

**MSc. Zhenni Li**

Born in: Chengdu, Sichuan, China

Oral-examination: April 27<sup>th</sup>, 2018

The role of cell identity in the response to cell wall perturbation in the  
*Arabidopsis thaliana* primary root

Referees: Prof. Dr. Karin Schumacher

Dr. Sebastian Wolf

## Summary

The cell wall is a defining feature of plant cells. It is a rigid, yet flexible, layer surrounding each cell outside the plasma membrane and is mainly composed of polysaccharides such as cellulose, hemicellulose, and pectin, as well as to a lesser extent, phenolic compounds such as lignin and structural proteins. Plant cell wall is central to nearly all aspects of plant. Its biosynthesis and remodeling are essential for cell division, expansion and differentiation, the fundamental events through plant growth and development. In brief, cell walls shape the cells, which is crucial for organ formation, provide mechanical support to the plant, control cell-to-cell adhesion, form the interface between cells, which is indispensable for cellular communication, and regulate plant-pathogen/environment interactions. As plants permanently face intrinsic and extrinsic cues from developmental programs and the environment, this information must be correctly conveyed into the cells in order to adjust the plant's growth behavior and reallocate the resources accordingly. Therefore, a cell wall surveillance and signalling system must exist to ensure transmission of the information.

Roots form the hidden half of the plant and perform numerous physical and physiological functions such as anchoring, nutrient uptake and transport. The primary root of the model organism in plant research, *Arabidopsis thaliana*, is formed with different tissues organized as longitudinal cell files that are radially patterned in a concentric manner, which provides an easily accessible model to study plant development. By using this model, previous studies in our lab have revealed the plasma membrane residing RECEPTOR LIKE PROTEIN (RLP)44 as key factor for cell wall surveillance and signalling. RLP44 monitors pectin status in the cell wall and transduces the signal of changes in cell wall integrity through interaction with the brassinosteroid receptor BRI1, which in turn activates a well-described signalling cascade to regulate plant growth transcriptionally. As in plants, different tissues fulfill distinct biological functions and have similar, yet distinguishable, characteristics in their cell walls, investigation of RLP44-mediated cell wall signalling in tissue-specific context would bring more insights into how plants co-ordinates its growth and development in responses to cell wall changes at tissue level. To do so, we made use of the recently developed GreenGate cloning technique and the dexamethasone-inducible system *pOp6/GR-LhG4*. By using promoters driving expression specifically in different cell types/tissues, we ectopically expressed pectin-modifying gene *PECTIN METHYLESTERASE INHIBITOR 5 (PMEI5)* and studied the responses of the plant to the loss of cell wall integrity. Here, we showed that cell wall homeostasis had pronounced impact on root growth, especially on in root morphogenesis, meristem size control, division plane determination through CDS maintenance, and tissue patterning. This influence was manifested as varying phenotypes at tissue level, implemented probably through crosstalks between brassinosteroid and other hormone signalling pathways in both cell-autonomous and non cell-autonomous manner. Besides, the previously described RLP44-mediated cell wall signalling exerts its role in a cell type/tissue-specific way and other cell wall sensing and signalling mechanisms are also possibly involved in the responses to cell wall perturbation. However, biochemical and histological characterization of cell wall properties as well as genetic studies for discovering the underlying molecular mechanisms will be necessary to further understand the role of cell identity in cell wall signalling and plant growth regulation.

## Zusammenfassung

Die Zellwand ist ein wichtiges Merkmal von Pflanzenzellen. Es ist eine starre, aber gleichzeitig flexible Schicht, die die Zelle außerhalb der Plasmamembran umgibt und hauptsächlich aus Polysacchariden wie Cellulose, Hemicellulose und Pektin besteht. In geringerer Menge sind auch Lignin und Strukturproteine vorhanden. Die Pflanzenzellwand ist essentiell für nahezu alle Aspekte des Pflanzenwachstums und der Pflanzenentwicklung. Die Biosynthese und Remodellierung sind Kapital für die Zellteilung, -expansion und -differenzierung, die fundamentalen Ereignisse durch den Lebenszyklus der Pflanze. Zellwände bestimmen die Zellform, und sind entscheidend für die Organbildung, geben mechanische Unterstützung, kontrollieren Zell-Zell Adhäsion und bilden die für die zelluläre Kommunikation unentbehrliche Schnittstelle zwischen Zellen und regulieren Pflanzenpathogene/Umwelt Interaktionen. Da Pflanzen permanent intrinsischen und extrinsischen Signalen sowohl von internen Entwicklungsprogrammen als auch externer Umgebung ausgesetzt sind, müssen diese Informationen korrekt in die Zellen gelangen, um das Wachstumsverhalten der Pflanze anzupassen. Um die Übertragung der Informationen sicherzustellen, muss ein Zellwandüberwachungs- und Signalsystem vorhanden sein.

Wurzeln bilden die verborgene Pflanzenhälfte und erfüllen zahlreiche physikalische und physiologische Funktionen wie Verankerung, Nährstoffaufnahme und Transport. Die Hauptwurzel des Modellorganismus in der Pflanzenforschung, *Arabidopsis thaliana*, wird aus verschiedenen Geweben gebildet. Diese Gewebe sind als longitudinale Zellreihen organisiert, radial konzentrisch angeordnet, wodurch sie ein und leicht zugängliches Modell zur Untersuchung der Pflanzenentwicklung bilden. Unsere Studien haben das in der Plasmamembran verankerte RECEPTOR LIKE PROTEIN (RLP) 44 als Schlüsselfaktor für die Zellwandüberwachung und Signalgebung identifiziert. RLP44 überwacht den Pektinstatus in der Zellwand und leitet Veränderungen der Zellwandintegrität durch Wechselwirkung mit dem Brassinosteroidrezeptor BRI1 weiter. BRI1 wiederum aktiviert eine gut beschriebene Signalkaskade um das Pflanzenwachstum transkriptionell zu regulieren. Verschiedene Gewebe erfüllen unterschiedliche biologische Funktionen und haben ähnliche, aber unterscheidbare Merkmale in ihren Zellwänden. Die Untersuchung von RLP44-vermittelter Zellwand-assoziierten Signalprozessen in gewebespezifischen Kontext sollte uns helfen zu verstehen, wie Pflanzen auf Zellwandveränderungen auf ihr Wachstum und ihre Entwicklung anpassen. Dazu nutzten wir die kürzlich entwickelte GreenGate-Klonierungstechnik und das Dexamethason-induzierbare System *pOp6/GR-LhG4*. Unter Verwendung von Promotoren, die die Expression spezifisch in verschiedenen Zelltypen/Geweben steuern, exprimierten wir das Pektin-modifizierende Gen *PECTIN METHYLESTERASE INHIBITOR 5 (PMEI5)* ektopisch und untersuchten die Reaktionen der Pflanze auf den Verlust der Zellwandintegrität. Wir konnten zeigen, dass die Zellwandhomöostase einen ausgeprägten Einfluss auf das Wurzelwachstum hatte, insbesondere auf die Größenkontrolle der Wurzelapikalmeristeme und die Gewebemusterung. Dieser Einfluss manifestierte sich als unterschiedliche Phenotypen auf Gewebeebene und wurde wahrscheinlich durch Wechselwirkung zwischen Brassinosteroid und anderen Hormon-Signalwegen verursacht. Darüber hinaus übt die zuvor beschriebene RLP44-vermittelte Signalkaskade ihre Rolle in einer zelltyp-/gewebespezifischen Weise aus, und andere Mechanismen zur Überwachung der Zellwandfunktion sind möglicherweise auch in die Reaktionen auf Zellwandstörungen involviert. Eine biochemische und histologische Charakterisierung der Zellwandeigenschaften, sowie genetische Untersuchungen zur Entdeckung der zugrundeliegenden molekularen Mechanismen wird jedoch notwendig sein, um die Rolle der Zellidentität bei der Zellwandsignalisierung und der Regulierung des Pflanzenwachstums besser zu verstehen.

**Table of content**

<b>Abbreviations .....</b>	<b>1</b>
<b>Introduction .....</b>	<b>3</b>
<b>1. Cell walls in cells of different organisms.....</b>	<b>3</b>
<b>2. The plant cell wall and its functions in plant growth and development.....</b>	<b>3</b>
2.1. Biochemical properties, biosynthesis and modifications.	3
2.2. Plant cell wall in cell division, expansion and differentiation.	5
2.3. Plant cell wall and root development.	7
2.3.1. Arabidopsis thaliana primary root architecture and the root apical meristem (RAM).	7
2.3.2. Cell wall in tissue/cell identity specification and plant development.	8
<b>3. Plant development according to its surrounding environment - the role of cell wall signalling (CWS) and its mechanisms. ....</b>	<b>9</b>
<b>4. Phytohormones and hormone signalling. ....</b>	<b>10</b>
4.1. Phytohormones in plant development.	10
4.2. Brassinosteroids and brassinosteroid signalling pathway.	11
4.3. Brassinosteroids and BR signalling in plant growth and development.	13
4.4. Crosstalks between BR and other signalling pathways.	13
<b>5. RLP44- &amp; BRI1-mediated cell wall signalling ensures cell wall homeostasis.....</b>	<b>15</b>
5.1. RLP44- & BRI-mediated cell wall signalling.	15
5.2. The receptor-like protein 44 (RLP44) and its role in cell wall signalling.	17
<b>6. Aim of the study: role of RLP44-mediated cell wall signalling in cell type/tissue-specific context. ....</b>	<b>17</b>
<b>Results .....</b>	<b>19</b>
<b>1. Loss of cell wall integrity by PME15 over-expression activates cell wall signalling and results in compensatory regulation of root growth.....</b>	<b>19</b>
1.1. Cell wall signalling-mediated compensatory responses resulted in pleiotropic phenotypes in root.	19
1.2. The pleiotropic phenotype in PME1ox roots is a consequence of impaired cell division, expansion, and differentiation in the root apical meristem.	20
1.2.1. The oblique cell walls observed in PME1ox were caused by an altered cell division plane during mitosis.	20
1.2.1.(1) <i>The oblique cell walls resulted from an oblique cell division plane in mitosis.</i>	20
1.2.1.(2) <i>The oblique division plane in PME1ox seemed to be related to the failure in maintaining a proper cortical division site position.</i>	22
1.2.1.(3) <i>The seedling root waving was unrelated to oblique cell walls in the RAM.</i>	24
1.2.2. The reduced primary root growth in PME1ox is caused by a premature transition of meristem cells from division to transition.	25
1.2.3. Over-expression of PME15 promoted columella stem cell differentiation.	26

1.3. The pleiotropic phenotype in PME1ox is a result of enhanced BR-signalling, altered cytokinin and auxin signalling, and altered cell identity specification.	27
1.3.1. The premature transition of meristematic cells into elongation and CSC over-differentiation in PME1ox might result from crosstalk with cytokinin and auxin signalling pathways.	27
1.3.2. Altered cell identity specification might contribute to altered tissue organization and overall impaired plant morphology.	30
<b>2. RLP44- and BRI1-mediated CWS is partially involved in regulation of root growth and development in the responses to cell type/tissue-specific perturbation of cell wall properties. ....</b>	<b>33</b>
2.1. A case study about the effect of cell type specific cell wall properties on plant growth and development — disrupting the wall only in XPP cells was sufficient to cause pleiotropic phenotype.	33
2.2. Triggering the loss of CWI in specific cell types/tissues with Dex-inducible system.	35
2.2.1. The cell type/tissue-specific dexamethasone-dependent cis-inducible system.	35
2.2.2. Functional test of the cell type/tissue-specific Dex-inducible system (dose- and time-dependent induction).	36
2.2.3. The promoters drove expression specifically to the expected cell types/tissues.	37
2.2.4. The cell type/tissue-specific Dex-inducible system triggered an increase of PME15 expression.	39
2.3. Loss of CWI in specific cell types/tissues triggered diverse responses.	41
2.3.1. Seedling root waving was triggered independently by expression of PME15 in root hair cells, epidermis, or XPP cells.	41
2.3.2. Specific expression of PME15 in different cell types/tissues triggered similar yet diverse directional growth phenotypes on soil.	41
2.3.3. Specific expression of PME15 in the beginning of cortex cell file was sufficient to provoke abnormal cell division and disrupted tissue patterning.	43
2.3.4. Expression of PME15 in the beginning of cortex cell file showed mild effect on root growth and RAM size.	43
2.3.5. Ectopic expression of PME15 triggered PME1ox-comparable yet distinctive growth phenotypes.	43
2.4. The oblique cell walls and QC/SCN disruption in pCO2>GR>PME15 seemed to originate from abnormal cell divisions in cortex cells harbouring ectopic PME15 expression.	46
2.5. Mechanical imbalance between different tissues was not likely to be responsible for the defective root morphology, cell division and tissue patterning.	48
2.5.1. Re-establishing the balance of cell wall mechanical properties between neighbouring tissues did not rescue the root waving phenotype.	48
2.5.2. Re-establishing the balance of cell wall mechanical properties in cells surrounding the beginning of the cortex file did not alleviate the QC/SCN disruption.	51
2.6. Cell identity specification in pCO2>GR>PME15.	51
2.7. RLP44- and BRI1-dependent but BRs-independent mechanisms seemed to be involved in the responses to loss of CWI in cell type/tissue-specific context.	54
2.7.1. RLP44- and BRI1-mediated signalling pathway had different effect on root and above-ground tissue growth in pXPP:PME15.	54
2.7.2. Cell type/tissue-specific expression of PME15 might not have altered BR signalling.	54
2.7.3. rlp44cnu2 but not bri1cnu4 rescued the root waving upon cell type/tissue-specific loss of CWI.	56
2.7.4. The oblique cell walls were possibly caused by RLP44- and BRI1-dependent mechanisms while unknown processes could play a role in QC/SCN organization.	57

<b>Discussion .....</b>	<b>59</b>
1. Cell identity and tissue specificity might play an important role in RLP44/BR1-mediated CWS in PMEIOx. ....	59
2. Both cell-autonomous and non cell-autonomous regulations are implicated in the responses to cell wall perturbation.....	60
3. RLP44 and BRI1 might have distinct role in cell-autonomous regulation of root morphology upon cell wall perturbation.....	61
4. RLP44/BRI1-mediated CWS affects RAM growth through regulation of transition domain via other hormone signalling and responses. ....	64
5. Cell wall properties affect cell division and tissue patterning in both cell-autonomous and non cell-autonomous manner possibly by interfering with BR and auxin responses. ....	66
<b>Material &amp; Methods .....</b>	<b>71</b>
1. Green Gate cloning, plant transformation and transgenic line selection.	71
2. Plant materials and growth conditions.	73
3. Genomic DNA extraction and genotyping.	73
4. Microscopy analysis.	74
5. EdU staining.	74
6. Microtubule immunolabelling.	74
7. mPS-PI staining.	75
8. Histology: GUS staining and basic fuchsin staining of stem cross sections.	75
9. qRT-PCR.	76
<b>Supplemental information.....</b>	<b>77</b>
<b>Reference .....</b>	<b>81</b>
<b>Acknowledgement.....</b>	<b>96</b>

## TABLE OF CONTENT

---

## Abbreviations

### A

ABA — Abscisic acid  
AHP6 — *Arabidopsis* Phosphotransfer Protein 6  
ARF — AUXIN RESPONSE FACTOR  
ARR — *Arabidopsis* response regulator

### B

BAK1 — BRI1-ASSOCIATED RECEPTOR KINASE 1  
BES1 — BRI1-EMS-SUPPRESSOR 1  
BIN2 — BRASSINOSTEROID INSENSITIVE 2  
BL — Brassinolide  
BR — Brassinosteroid  
BRI1 — BRASSINOSTEROID INSENSITIVE 1  
BSL — BSU1-LIKE  
BSU1 — BRI1 SUPPRESSOR 1  
BZR1 — BRASSINAZOLE-RESISTANT 1

### C

CDG1 — CONSTITUTIVE DIFFERENTIAL GROWTH 1  
CDL — CDG-LIKE  
CEI — Cortex/endodermis initial  
CSC — Columella stem cell  
CWI — Cell wall integrity  
CWS — Cell wall signalling

### D

DAG — Day after germination  
DM — Degree of methylesterification

### E

EdU — 5-ethynyl-2'-deoxyuridine  
ECD — Extracellular domain

### G

GA — Gibberellin  
GalA — galacturonic acid  
GSK3 — glycogen synthase kinase 3

### H

HG — Homogalacturonan

**J**

JA — Jasmonic acid

**L**

LRR — Leucine-rich repeat

LRR-RLK — Leucine-rich repeat-receptor-like kinase

Lti6B — Low temperature induced protein 6B

**M**

mPS-PI staining — modified pseudo-Schiff propidium iodide staining

MT — microtubules

**P**

PAMP — Pathogen-associated molecular pattern

PME — Pectin methylesterase

PMEI — Pectin methylesterase inhibitor

PP2A — PROTEIN PHOSPHATASE 2A

PPB — Preprophase band

promTS — Tissue-specific promoter

**R**

RAM — Root apical meristem

RLCK — Receptor-like cytoplasmic kinase

RLP44 — Receptor-like protein 44

**S**

SA — Salicylic acid

SAM — Shoot apical meristem

SERK — SOMATIC EMBRYOGENESIS RECEPTOR-LIKE KINASE

SHR — SHORT-ROOT

SL — Strigolactone

SCN — Stem cell niche

**T**

TMO5 — TARGET OF MONOPTEROS 5

TDIF — TRACHEARY ELEMENT DIFFERENTIATION INHIBITORY FACTOR

TDR — TDIF RECEPTOR

**X**

XPP — Xylem pole pericycle

## Introduction

### *1. Cell walls in cells of different organisms.*

The cell wall is a cellular compartment surrounding some types of cells and is situated outside the plasma membrane. It is present in most prokaryotes and in eukaryotes such as algae, bacteria, fungi and plants, but not in animals. Although existing in organisms of distinct domains, the function and composition of cell wall differ to a large extent. They also vary depending on cell types and developmental stages. In bacteria, the cell wall is the main stress-bearing and shape maintaining element that is crucial for cell viability and mainly consists of the unique cross-linked polymer peptidoglycan (Scheffers et al., 2005). The fungal cell wall is a dynamic structure that protects the cell from osmotic pressure and allows cell growth. Walls of fungal cells are comprised of glycoproteins and polysaccharides that are mainly  $\beta$ -1,3-linked glucans and chitin, making them significantly different from other organisms (Bowman and Free, 2006; Sanz et al., 2017). In plants, cell walls perform numerous essential functions in growth and development, including providing cell shape that is necessary to form different tissues/organs and mechanical support to allow the resistance to the turgor pressure, controlling cellular adhesion, cell expansion and division, forming the interface between neighbouring cells, which play a crucial role in cell-to-cell communication, and regulating plant-pathogen/environment interactions given its surface location and its role as a physical barrier (Cosgrove, 2005; Keegstra, 2010; Wolf, 2017).

### *2. The plant cell wall and its functions in plant growth and development.*

#### *2.1. Biochemical properties, biosynthesis and modifications.*

Cell walls in land plants (embryophytes) are characterized by a network of cellulose microfibrils embedded in a complex gel-like matrix of polysaccharides mainly consisting of hemicellulose, pectins. This network also comprises lignin and structural proteins (Cosgrove, 2005; Nishitani and Demura, 2015). The wall comprises three layers: the middle lamella, the primary cell wall and the secondary cell wall (Albersheim et al., 2010). The middle lamella is formed during cytokinesis and is surrounded by two layers of primary cell wall belonging to two adjacent cells. While secondary cell walls can be deposited in some cell types such as vessel and fiber cells in the vascular tissue, the primary cell walls are active mainly in growing cells (Cosgrove, 2005; Keegstra, 2010).

Cellulose microfibrils are insoluble polymers composed of linear  $\beta$ -1,4-linked glucan chains (**Figure 1**) organized in parallel through non-covalent hydrogen bonds and are synthesized by plasma membrane-residing protein complexes (Somerville, 2006; Cosgrove, 2014). It has long been considered that cellulose microfibrils are arranged as an hexagon of 36 glucan chains (Somerville, 2006; Lindeboom et al., 2008; Ding et al., 2014), which is based on the hexamer of cellulose synthase complexes with 6 glucan chains in each unit and cited as 6 x 6 (Cosgrove,

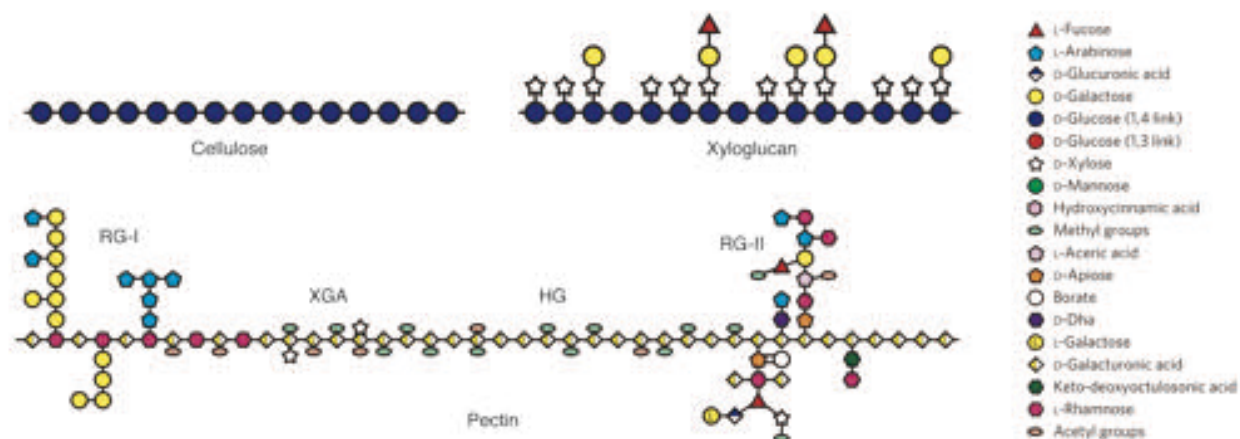


**Figure 1. Schematic representation of cell wall polysaccharides** (Adapted from Mohen, 2008; Burton et al., 2010).

2014). Recent technical improvement has favored a smaller estimation in which the microfibril is formed by only 18 to 24 chains (Fernandes et al., 2011; Newman et al., 2013; Thomas et al., 2013; Cosgrove, 2014). Hemicelluloses are classically grouped into xyloglucans, xylans, mannans and glucomannans, and  $\beta$ -(1,3; 1,4)-linked glucans (Scheller and Ulvskov, 2010). As the most abundant hemicellulose in primary cell wall of spermatophytes (except for grasses), xyloglucan have a linear  $\beta$ -1,4-linked glucan chain as backbone (Figure 1), which is similar to cellulose. This backbone can be divided into repetitive units each containing 4 glucose residues with 3 of them branched on the side with xylose (Cosgrove, 2005; Scheller and Ulvskov, 2010; Burton et al., 2010). Pectins, considered as the most complex family of cell wall polysaccharides and the main component of the gel-like matrix especially in dicots, include several different structural groups such as homogalacturonan (HG), rhamnogalacturonan I (RG-I), and with smaller amount of rhamnogalacturonan II (RG-II), xylogalacturonan (XGA), arabinan and arabinogalactan I (Cosgrove, 2005; Mohen, 2008; Burton et al., 2010). Most pectic polysaccharides share as common backbone a linear homopolymer composed of  $\alpha$ -1,4-covalently linked galacturonic acid (GalA) (Figure 1). This backbone, also known as the major group of the family – HG, makes up to 65% of pectin (Mohen, 2008; Sénéchal et al., 2014). HG has been revealed to have a degree of polymerization in the range of 81-117 GalA residues (Yapo et al., 2007), and is partially methylated at the C-6 carboxyl and O-acetylated at O-2 or O-3 (O'Neill et al., 1990).

Cellulose and matrix polysaccharides are synthesized by distinct pathways (Cosgrove, 2005; Somerville, 2004, 2006; Keegstra, 2010). Cellulose biosynthesis involves a large membrane complex consisting of different cellulose synthase enzymes as subunits and appears as a 'rosette' at the cell surface. This synthesis complex is thought to transfer glucose from cytosolic UDP-glucose to produce extracellular glucan chains (Doblin et al., 2002; Saxena and Malcom Brown, 2005; Guerriero et al., 2010). Non cellulosic polysaccharides are synthesized by membrane-bound glycosyltransferases (GTs) in the Golgi and transported towards the plasma membrane in small vesicles. After the fusion of the transport vesicle to the plasma membrane, the fragments of

polysaccharides are delivered to the extracellular space and integrated into the wall network (Cosgrove, 2005; Doblin et al., 2002; Scheller and Ulvskov, 2010; Harholt et al., 2010). About 67 different glycosyltransferases, methyltransferases and acetyltransferases have been predicted to be required for pectin biosynthesis (Mohnen et al., 2008). HG, the most abundant pectin, is assumed to be synthesized in the *cis*-Golgi, methylesterified in the *medial*-Golgi, substituted in the *trans*-Golgi and then secreted to the wall in a highly methylesterified form (Wolf et al., 2009). The degree of methylesterification (DM) of HG (Figure 1) has pronounced impact on cell wall structure and mechanical properties: once secreted into the wall network, the de-methylesterified HG can form crosslinks with  $\text{Ca}^{2+}$  to form the so-called 'egg-box' structure, which is pivotal for wall strength and cell-to-cell adhesion; or it can be targeted by pectin-degrading enzymes such as polygalacturonases, pectate lyases-like and pectate lyases. In either case, modulation of HG methylesterification can have dramatic consequences on cell growth (Liners et al., 1989; Bouton et al., 2002; Wolf et al., 2009; Sénéchal et al., 2014; Daher and Braybrook, 2015). Besides, HG methylesterification state plays important role in diverse developmental processes such as lateral organ initiation in shoot apical meristem (SAM) and phyllotactic patterning (Peaucelle et al., 2008, 2011a, b; Braybrook and Peaucelle, 2013), fruit ripening (Wakabayashi et al., 2003; Panicgua et al., 2014), hypocotyl development (Derbyshire et al., 2007; Pelletier et al., 2010) and pollen maturation (Francis et al., 2006). Breakdown products of HG, named pectic oligogalacturonides, have been shown to act as signal molecules in responses to pathogen attack or counteract the effects of auxin during plant growth and development (Ridley et al., 2001; Wolf et al., 2009; Gravino et al., 2015). In particular, the DM of HG is controlled by a large multigene family of cell wall-localized pectin methylesterases (PMEs, E.C. 3.1.1.11) whose activity is regulated by endogenous PME inhibitors (PMEIs) (Pelloux et al., 2007; Wolf et al., 2009). PMEs catalyze the removal of the methyl groups from the HG chain (Figure 1) mostly within the cell wall network leading to release of free carboxyl groups, methanol and protons (Wolf et al., 2009). In *Arabidopsis thaliana*, 66 open reading frames (ORFs) have been annotated as putative full-length PMEs (Pelloux et al., 2007). PMEIs, also belonging to multigenic families in plants, can form a stoichiometric 1:1 complex with PMEs, thus resulting in PME inhibition in the wall in a pH- and ion concentration-dependent way (Di Matteo et al., 2005).

## 2.2. Plant cell wall in cell division, expansion and differentiation.

Cell division, expansion and differentiation are fundamental processes that determine the growth and development in higher plants (Dupuy et al., 2010). Since plant cells are glued together through their shared cell walls, there is no cell migration possible for the accomplishment of different process including development, wound healing, and invasive growth as thoroughly studied in animals (Mandai et al., 2013). Thus, morphogenesis in higher plants is rather a process of local cell division, selective cell expansion and differentiation, which are tightly controlled by the cell wall (Cosgrove, 2005; Wolf et al., 2012a; Wolf and Höfte, 2014; Wolf et al., 2017). Adjacent

plant cells share the same wall, which is deposited at the end of cell division, and the mechanical forces generated due to different growth rate might have impact on morphogenesis (Mirabet et al., 2011; Uyttewaal et al., 2012). Moreover, right before the division cycle starts, cells need to increase in volume (Lipka et al., 2015), a process that is tightly controlled by cell wall biosynthesis and remodelling (Cosgrove, 2000, 2005, 2015; Wolf et al., 2012a; Braidwood et al., 2014). Cell expansion is also determining for plant body growth and the rate as well as the direction of cell expansion depend on the balance between the turgor pressure and the resistance of the wall to the tensile stress (Cosgrove, 2005, 2015; Braidwood et al., 2014). Plant cells grow by expanding the cell walls through a slow and irreversible process of 'polymer creep' in which cellulose microfibrils and matrix polysaccharides slide within the wall to increase its surface area (Cosgrove, 2015). In principle, plant cell expansion includes wall hydration, turgor-driven wall relaxation, mechanosensing and wall cross-linking, and deposition of new wall materials (Wolf et al., 2012a). In addition, specialized cell types (e.g. xylem, fibers and anther cells) differentiate by depositing a secondary cell wall after being fully elongated, which is dissimilar to the primary wall in composition, structure and mechanical properties (Roland, 1978; Cosgrove and Jarvis, 2012; Taylor-Teeples et al., 2015; Cosgrove, 2015).

It has been described that plant cells divide by default along the shortest plane that produces two daughter cells with equal size in the case of symmetric division, which implicates the cell geometry (Besson et al., 2011; Rasmussen et al., 2013; Shapiro et al., 2015). In an extended version of this theory, the cell wall has been proposed to be one of the key points for the division plane determination as tensile microtubule (MT) strands radiate from the nucleus and are stabilized on the shortest path to the cell wall (Lloyd, 1991; Lipka et al., 2015). It is widely accepted that cell division plane is pre-determined already in prophase by the position of cortical division site (CDS). The CDS is a site at the periphery of the cell where cortical MT network condenses and lays down a ring structure in the cell periphery, which is known as preprophase band (PPB). The PPB marks the future fusion point of the cell plate and the vertical parental wall during cytokinesis, thus defines the transverse orientation of the new cell wall (Smith, 2001; Rasmussen et al., 2013). However, the PPB is only a transient marker of the CDS since MTs disassemble after prophase (Rasmussen et al., 2013; Lipka et al., 2014). Other proteins such as PHRAGMOPLAST-ORIENTING KINESIN 1 and 2 (POK1 and POK2), TANGLED (TAN) are recruited during prophase and are continuously localized to the CDS throughout mitosis (Müller et al., 2006; Walker et al., 2007; Rasmussen et al., 2010; Lipka et al., 2014). Hence, the phragmoplast-guided cell plate will fuse to the parental wall at the site marked by those proteins. There is also evidence supporting a role of cell wall in division plane determination, as it has profound influence on cell shape and mechanical forces (Baluška et al., 2001; Sablowski, 2016). Regarding the asymmetric or formative divisions, several studies revealed roles of the cell wall in cell polarization (Smith, 2001). At the end of cytokinesis a new cell wall is deposited in the center of the cell and expands outward in a centrifugal way to fuse with the parental wall through phragmoplast-dependent guidance (Smith, 2001; Rasmussen et al., 2013). A mutation in *Arabidopsis KORRIGAN* (KOR)

gene, which encodes a cell plate-localized cell wall modifying enzyme endo-1,4- $\beta$ -D-glucanase, caused typical cytokinesis defect (Zuo et al., 2000). Similarly, defects in cell wall hydrolysis during cytokinesis have severe consequences on daughter cell separation and growth in bacteria and yeast (Cvrčková et al., 1995; Uehara et al., 2010; Yang et al., 2011).

### 2.3. Plant cell wall and root development.

#### 2.3.1. *Arabidopsis thaliana* primary root architecture and the root apical meristem (RAM).

The root is essential for plant anchoring in the soil and for the transport of nutrients and organic compounds to ensure normal plant growth (Petricka et al., 2012; Tian et al., 2014; Sparks and Benfey, 2017). Root growth depends on tight co-ordination between different tissues, which involves cell proliferation, elongation and differentiation. These processes require constant cell wall biosynthesis and remodeling throughout the plant life cycle (Petricka et al., 2012; Cederholm et al., 2012). In the model organism *Arabidopsis thaliana*, the primary root comprises various tissues as concentric layers that are radially patterned, which has provided a simple and clear model for root structural and developmental studies over many years (Figure 2; Dolan et al., 1993; Wachsman et al., 2015). Along the longitudinal axis are distributed cells with a stem cell state in the root apical meristem (RAM) and elongated/differentiated ones in the mature part of the root. Different tissues are formed through formative cell divisions and symmetric cell divisions as well cell elongation and differentiation contribute to tissue growth (Birnbaum, 2016).

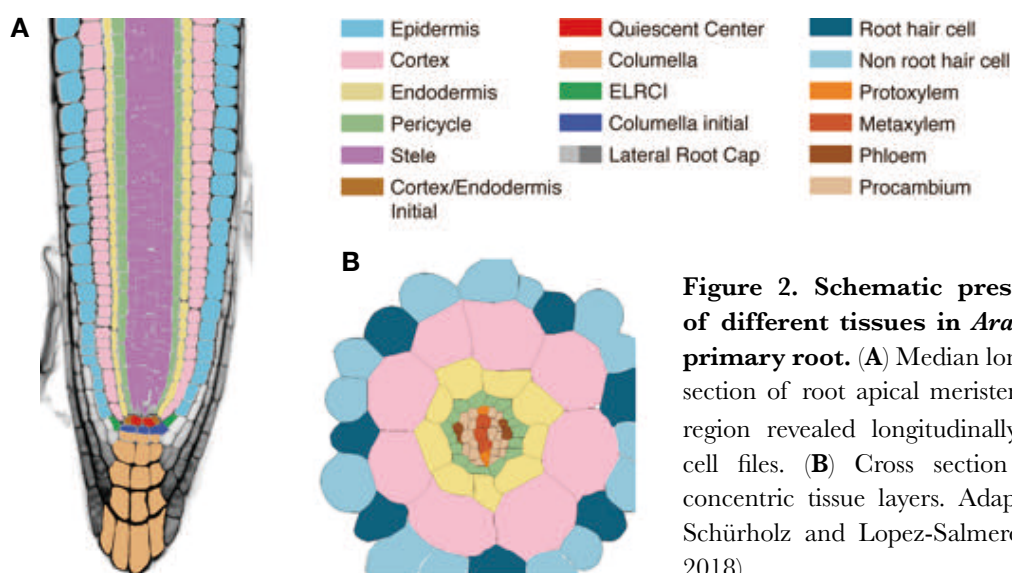


**Figure 2. Schematic presentation of different tissues in *Arabidopsis* primary root. (A) Median longitudinal section of root apical meristem (RAM) region revealed longitudinally parallel cell files. (B) Cross section showing concentric tissue layers. Adapted from Schürholz and Lopez-Salmeron et al., 2018).**

### 2.3.2. Cell wall in tissue/cell identity specification and plant development.

There are about 35 types of cells in plants that are formed through cell-type-specific differentiation programs, which lead to a wide variety of cell sizes, shapes, positions and cell wall characteristics (Cosgrove, 2005; Harholt et al., 2010; Braidwood et al., 2014). Plants can form very elaborate and complex structures through accurate co-ordination of asymmetric cell divisions, cell identity specification and cell-to-cell communication via positional signalling. In the root, most of the stem cells have been first specified and major tissues acquired their identities during globular stage of embryogenesis (Hove et al., 2015; Crawford et al., 2015). Later, a robust positional patterning system maintains a regular root architecture and a shift in the position of a given cell is sufficient to cause a cell fate change (von den Berg et al., 1995; Kinder et al., 2000). As different cell types fulfill distinct functions throughout the plant's life cycle, ranging from elongation to reproduction, as well as mediating responses to abiotic stresses (Dinneny et al., 2008; Gifford et al., 2008). Maintaining cell identities is crucial for normal plant growth, development, and physiology. Clonal analysis has revealed that in shoot apical meristem (SAM), meristematic cells have no pre-determined fate and the position is more likely to be the determinant factor for the acquisition of cell identity (Furner et al., 1995; Fletcher, 2002; Dodsworth, 2009). Stem cell progenitors in the SAM are displaced outward from the central zone to the periphery zone and contribute to lateral organ initiation (Reddy and Meyerowitz, 2005; Shi et al., 2018). This position change is accompanied by modifications of pectic cell wall polysaccharides (Peaucelle et al., 2008, 2011a, b). It has been reported that, mRNA localization of a subset of 152 genes encoding cell wall glycosyltransferases revealed their enrichment in or specificity to restricted sub-domains of the SAM during its development, suggesting distinctive wall properties of meristem cells and their relations to different cell identities (Yang et al., 2016).

In plants, different cell types are organized in ordered spatial patterns, which is achieved through strictly regulated cell division rate and plane (Cui and Benfey, 2009). Pattern formation initiates during embryogenesis and is elaborated in the meristems, which dictates the tissue/organ shape and size (Steeves and Sussex, 1989; Petricka et al., 2012; Cederholm et al., 2012). In *Arabidopsis*, it has also been described that cell wall structure and composition in cells of one specific tissue are different depending on plant's developmental stage and conditions (Keegstra, 2010). More evidence connecting the role of cell wall properties with tissue-related developmental processes has been provided by Hyodo et al., 2013, as during tomato fruit ripening, differential regulation of pectin methylesterification occurs in each tissue. This regulation is achieved by either differential expression of *PMEs* or post-translational control by *PMEI* activity, which have also been shown in other developmental processes than fruit ripening (Di Matteo et al., 2005). All these knowledge suggest a potential role of cell wall in the post-embryonic regulation of cell fate specification and tissue/organ development. This regulation is possibly mediated by cell wall signalling and mechanical sensing, given the signal molecule nature of cell wall-derived OGs and the influence of cell wall properties on mechanical strength of the cells. However, the underlying

mechanisms connecting cell wall and cell identity specification as well as tissue patterning still need to be more thoroughly studied.

### **3. Plant development according to its surrounding environment - the role of cell wall signalling (CWS) and its mechanisms.**

As sessile organisms, plants need to perceive various signals from both interior and exterior and adjust their growth in order to correctly allocate different resources between growth and defense (van Hulst et al., 2006; Yang et al., 2012; Lozano-Durán et al., 2013). As aforementioned, almost all the aspects of plant cell growth inevitably rely on cell wall biosynthesis and remodelling. To date, cell wall is not only considered as a cellular structure but rather as complex system of sensing, processing and responding to constant internal and external cues perceived by plants (Somerville et al., 2004). Cell wall integrity (hereafter referred to as CWI) is constantly challenged not only by growth itself but also the extrinsic cues evoked upon biotic or abiotic stresses. Therefore, surveillance of the cell wall's physical properties and its regulation are essential for plant growth control and survival. Indeed, studies focused on mutants affected in cell wall biosynthesis or modification did reveal secondary compensatory responses that are not directly related to the mutation in question (Ellis and Turner, 2001; Ana Caño-Delgado et al., 2003; Hernández-Blanco et al., 2007; Wolf et al., 2012b), which further support the existence of the cell wall surveillance system and its role in plant growth regulation. However, the current knowledge about the mechanisms by which cell wall state is monitored and the growth is adjusted accordingly, is limited.

Generally, all cell wall signalling (hereafter referred to as CWS) mechanisms require the transduction of the signal from the outside to the inside of the cell across the plasma membrane (Wolf, 2017). In different scenarios, signals can be transmitted through ionic channels formed by for example the plasma membrane protein Mca1 that correlates  $\text{Ca}^{2+}$  influx with mechanosensing in *Arabidopsis* (Nakagawa et al., 2006); arabinogalactan proteins, a ubiquitous cell surface proteoglycans that are thought to form crosslinks with cell wall components (Tan et al., 2012); mechanosensor MscS-Like (MSL) proteins that are found in the plasma membrane of *Arabidopsis* root cells and are relatives of the well-characterized mechanosensitive channel involved in protection against osmotic shock in *E. coli* (Haswell et al., 2008); and osmosensors that might coordinate the cellulose and carbohydrate metabolism (Wormit et al., 2012; Seifert and Blaukopf, 2010; Wolf, 2017). So far, most identified CWS signalling components or the likely candidates are classified as receptor-like kinase (RLK), a large family with more than 600 genes in *Arabidopsis* (Shiu et al., 2001, 2003; Tor et al., 2009; Wolf, 2017). Nevertheless, the upstream cell wall binding or sensing mechanisms, the nature of the ligand and the downstream signal transduction route remain largely unknown. The biggest subgroup of RLKs comprises proteins with leucine-rich repeats (LRR-RLKs), which have been intensively studied and assigned with different ligands. Upon ligand binding to the extracellular domain (ECD), LRR-RLKs usually form heteromers with

SOMATIC EMBRYOGENESIS RECEPTOR-LIKE KINASE (SERK) and, after activation through auto- and *trans*-phosphorylation, initiate the signal transduction cascade via phosphorylation of the downstream targets (Han et al., 2014; Ma et al., 2016). Some RLKs contain putative carbohydrate-binding motifs, making them promising candidates for cell wall sensors and signalling component (Wolf, 2017). Members of the *Catharanthus roseus* receptor-like kinase 1-like (CrRLK1L) group comprises the *Xenopus laevis* malectin homologous domains, which are speculated to bind to cell wall motifs (Hématy and Höfte, 2008; Lindner et al., 2012; Wolf and Höfte, 2014; Nissen et al., 2016). THESUS1 (THE1) has been identified in the suppressor screen of the CESA mutant *cesa6<sup>prc1-1</sup>* that was affected in cellulose biosynthesis (Hématy et al., 2007). While THE1 loss-of-function rescued the *cesa6<sup>prc1-1</sup>* growth phenotypes, the low cellulose level stayed unchanged, which strongly suggested THE1-mediated compensatory responses upon loss of CWI. FERONIA has been formerly described as indispensable for fertilization and as receptor for the secreted peptide RAPID ALKALINIZATION FACTOR 1 (RALF1). It is able to sense either a pollen tube- or cell wall-derived ligand and trigger a signalling cascade that ensures the fertilization of the female gametophyte. It can also interact with several other hormone pathways including BR, auxin, ethylene signalling as well as defense and mechanical signalling (Deslauriers and Larsen, 2010; Haruta et al., 2014; Yeats et al., 2016). ANXUR1 and ANXUR2, the close homologues of FER, have been reported to function redundantly in maintaining pollen tube integrity as a male counterpart to FER (Boisson-Dernier et al., 2009; Miyazaki et al., 2009). Another family of proteins, the wall-associated kinases (WAKs), have been demonstrated to bind to de-methylesterified HG, polygalacturonic acid and oligogalacturonides via its N-terminal part of the extracellular domain (Decreux et al., 2005, 2006; Kohorn et al., 2009; Brutus et al., 2010; Kohorn, 2016).

#### 4. Phytohormones and hormone signalling.

##### 4.1. Phytohormones in plant development.

Phytohormones (plant hormones) are families of structurally unrelated small chemicals produced in the secondary metabolism of the plants. They can act at very low concentrations and in a dose-dependent way (Mandava et al., 1988; Khan, 2005). This action takes place either locally in cells where phytohormones are produced or in more distant locations through different means of transport or movement into target cells (Machácková and Romanov, 2002). Over the past century, continuous studies of biosynthetic and signalling mutants, together with exogenous applications of different hormones and pharmacological interferences, have revealed multiple roles of phytohormones that are indispensable in virtually every aspect of plant growth and development by regulating numerous cellular mechanisms (Jaillais and Chory, 2010). As one of the first phytohormones to be discovered, auxin modulates such diverse developmental processes as gametogenesis, embryogenesis, organ patterning, vascular development, flowering,

tropic responses to light and gravity (Davies, 1995; Woodwar and Bartel, 2005; Y. Zhao, 2010). Ethylene is mainly involved in cell expansion along transverse axis, release of dormancy, leaf development and senescence as well as fruit ripening (Burg, 1973; Iqbal et al., 2017). Cytokinins affect plant growth and development by influencing cell division, shoot initiation and growth, leaf senescence, apical dominance, vascular development and photomorphogenesis (Kieber and Schaller, 2014). Gibberellins (GAs)-regulated plant growth responses are found to be involved in seed germination, stem elongation, leaf expansion, trichome development and pollen maturation (Davies, 1995; Davière and Achard, 2013). Abscisic acid (ABA) was discovered as a key regulator of seed dormancy, germination, cell division and elongation, induction of flowering, responses to environmental stresses such as drought, salinity, cold, UV radiation and pathogen attack (Finkelstein, 2013). Salicylic acid (SA) and jasmonic acid (JA), although antagonistic at mechanistic level, both play essential roles in activation of defense systems against pathogen attack (Tamaoki et al., 2013). Strigolactones (SLs), formerly known as germination stimulants for parasitic plants, have been recently discovered as a branching factor that shape the plant architecture (Zwanenburg et al., 2016). Last but not least, brassinosteroids (BRs) are indispensable for plant growth because of their regulatory role in cell proliferation and expansion (Clouse and Sasse et al., 1998).

#### 4.2. Brassinosteroids and brassinosteroid signalling pathway.

Although diverged more than 1 billion years ago, plants and animals, as well as algae and fungi, use hydroxylated steroidal molecules as hormones to control numerous developmental and physiological processes including gene expression, cell division and elongation, differentiation, etc. (Thummel et al., 2002). While biochemical characteristics and biological functions of steroids have been described in a large amount of studies in animals, their hormonal activity was first discovered in plant only about 40 years ago, when brassinolide (BL) (Figure 3) was isolated from pollen extracts of *Brassica napus* L. (rapeseed), and reported as a plant growth promoter (Grove et al., 1979). Steroids found in different plant species that share structural and functional similarities were then collectively called brassinosteroids (BR) (Clouse and Sasse et al., 1998).

In animals it is generally known that steroids act as chemical messengers to produce slow genomic responses by passing freely through plasma membrane and binding to members of the nuclear hormone receptors superfamily thus regulating transcription of target genes (Mangelsdorf et al., 1995; Ribeiro et al., 1995). In plant genomes, the encoding of such nuclear receptors has not been discovered (Koo et al., 2000), but steroids also act through gene expressions to trigger rapid

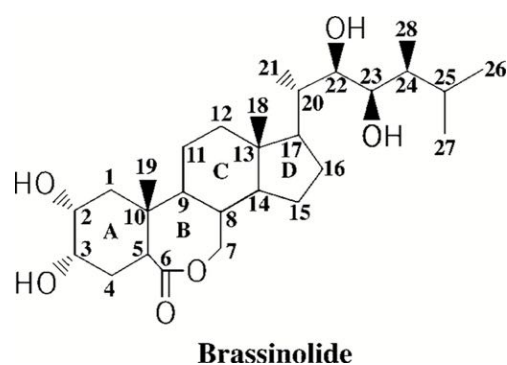


**Figure 3. Structure of brassinolide, the first isolated and the most active form of brassinosteroid** (Clouse and Sasse, 1998).

responses by binding directly to a wide range of plasma membrane-associated receptors (Norman et al., 2004).

In *Arabidopsis*, the BR signalling pathway has been intensively studied and is one of the most well-characterized pathways (Kim and Z-Y. Wang, 2010; Belkhadir and Jaillais, 2015; Singh and Savaldi-Goldstein, 2015; Wolf, 2017). BRs are perceived at the cell surface and bind to the ECD of its receptor – the plasma membrane-localized BRASSINOSTEROID INSENSITIVE 1 (BRI1) (Clouse et al., 1996; Kauschmann et al., 1996; Li and Chory, 1997; Fridrichesen et al., 2000; Z-Y. Wang et al., 2001), which encodes one of over 200 members of the leucine-rich repeat-receptor-like kinase (LRR-RLK) family in *Arabidopsis* (Shiu et al., 2001). BRI1 has an extracellular domain containing 25 leucine-rich repeats (LRRs) interrupted by a 70-amino-acid island domain between the twenty-first and twenty-second LLR, a transmembrane domain and a cytoplasmic serine/threonine kinase domain (Li and Chory, 1997; Fridrichesen et al., 2000; **Figure 4**). Ligand binding to BRI1 induces its heterodimerization with a shape-complementary co-receptor BRI1-ASSOCIATED RECEPTOR KINASE 1 (BAK1) (Jaillais et al., 2011a; Sun et al., 2013; Santiago et al., 2013). BAK1 is also known as SOMATIC EMBRYOGENESIS RECEPTOR-LIKE KINASE 1 belonging to a 5-member-family of LRR-RLKs with a small extracellular domain containing 5 LRRs (**Figure 4**). This stable association triggers the BRI1-mediated phosphorylation of BRI1 KINASE INHIBITOR 1 (BKI1), which associates with BRI1's kinase domain thereby inhibiting BRI1-BAK1 interaction. Phosphorylated BKI1 dissociates from the plasma membrane (Wang and Chory, 2006; Jaillais et al., 2011b; Wang et al., 2014) and allows the kinase domains of BRI1 and BAK1 to auto-phosphorylate and sequentially *trans*-phosphorylate each other, leading to full activation of the receptor complex (Wang et al., 2008; Bojar et al., 2014; Oh et al., 2009). To transduce the extracellular signal to the downstream components, the activated BRI1 receptor complex phosphorylates several receptor-like cytoplasmic kinases (RLCKs), including the BRI1 SUBSTRATE KINASEs (BSKs), the CONSTITUTIVE DIFFERENTIAL GROWTH 1 (CDG1) and its homologue CDG-LIKE (CDL). BSKs and CDG1 then activate the nucleocytoplasmic phosphatase called BRI1 SUPPRESSOR 1/BSU1-LIKE (BSU1/BSL) by phosphorylating the latter (Tang et al., 2008; Kim et al., 2009, 2011). Phosphorylated BSU1/BSL, in turn, dephosphorylates the negative regulator BRASSINOSTEROID-INSENSITIVE 2 (BIN2), a cytoplasmic glycogen synthase kinase-3 (GSK3)-like kinase, inactivates its kinase activity and directs the BIN2 protein to the subsequent degradation in a proteasome-dependent manner (Li et al., 2001, 2002; Kim et al., 2009; Tang et al., 2011). Inactivation of BIN2, together with PROTEIN PHOSPHATASE 2A (PP2A), allows the dephosphorylation of the downstream plant-specific transcription factors BRASSINAZOLE-RESISTANT 1 (BZR1) and BRI1-EMS-SUPPRESSOR 1 (BES1)/BZR2 (hereafter referred to as BES1), which are released from cytosolic retention by 14-3-3 phosphopeptide-binding proteins and can therefore translocate to the nucleus to regulate BR-responsive transcriptional program (Wang et al., 2002; Yin et al., 2002, 2005; He et al., 2005; Gampala et al., 2007; Tang et al., 2011).

### **4.3. Brassinosteroids and BR signalling in plant growth and development.**

Brassinosteroids (BRs) have been discovered as plant growth promoting hormones (Grove et al., 1979) and their effect of BRs have been revealed in both above-ground and below-ground tissues by a large body of evidence pointing to important roles in cell proliferation and expansion (Singh and Savaldi-Goldstein, 2015). BR-deficient plants show a typical dwarf phenotype on soil (Clouse et al., 1996; Kauschmann et al., 1996; Li and Chory, 1999, 2001; Z-Y. Wang et al., 2001). Intensive genetic studies brought to light key components that fully connect the BR signal transduction chain and established one of the most well-characterized plant hormone signalling pathways (see above §4.2). Hence, BR-dependent regulatory functions in different aspects of growth have been assigned to or shared by its downstream signalling factors and act through either linear BR signalling pathway or crosstalks with additional phytohormone pathways (Lipka et al., 2013; Zhu et al., 2013; Singh and Savaldi-Goldstein, 2015; see below §4.4). In spite of the complex interdependent regulation by BRs and other phytohormones, BRs also have effects on growth mostly through BZR1/BES1-mediated regulation of developmental factors (Zhu et al., 2013). For example, BR-deficient and BR-insensitive mutants showed delay in flowering due to increased expression of the floral repressor *FLOWERING LOCUS C* (*FLC*), which is negatively regulated by REF6 through interaction with BES1 (Domagalska et al., 2013; Yu et al., 2008). BR may also shorten circadian rhythms indirectly as demonstrated by Hanano et al., 2006. Mutants affected in BR biosynthesis or signalling exhibited reduced male fertility and defective sex determination, the regulation of which correlates with BES1 target gene expression (Ye et al., 2010; Hartwig et al., 2011). In RAM, a balanced BR signalling on cell proliferation and differentiation has important impact on meristem growth, quiescent center cell division and columella cell differentiation (González-García et al., 2010; Hacham et al., 2011; Fridman et al., 2014; Vilarrasa-Blasi et al., 2014). Besides, BRs are thought to regulate epidermal cell patterning by interfering with *WERWOLF* and *GLABRA 2*, two master regulators in position-dependent cell fate specification in root epidermis (Kuppusamy et al., 2009). The growth promoting effect of BRs was known to be concentration-dependent (Mandava et al., 1988; Müssig et al., 2003). Recent studies provide increasing amount of evidences showing that differential regulation of BRs and BR signalling level in different cell types/tissues fine-tune the growth (Zhu et al., 2013; Singh and Savaldi-Goldstein, 2015). Except the aforementioned context- and tissue-dependent effect of BRs on plant growth and development, BRs have also been reported to both promote and restrict shoot growth (Savaldi-Goldstein et al., 2007). Therefore, BR- and BR signalling-related responses need to be delicately modulated at tissue level to ensure normal plant growth.

### **4.4. Crosstalks between BR and other signalling pathways.**

As described in §4.1, different hormone signalling pathways can converge at certain point and regulate common mechanisms. The same is true for BRs. Although described as linear, BR signalling pathway is intensively connected to other hormone and/or developmental signalling pathways. Studies from the last decade revealed that crosstalks between BR and other signalling

pathways happen mostly at the level of the GSK3 kinase BIN2 and the BZR1/BES1 transcription factors (Belkhadir and Jaillais et al., 2015; Wolf et al., 2014; Wolf, 2017). The BIN2 kinase phosphorylates different components of the ERECTA-MAPK-SPCH pathway to inhibit (W. Wang, Bai and Z-Y. Wang, 2014b; Khan et al., 2013) or promote stomata development (Gudesblat et al., 2012). BR signalling is known to regulate vascular tissue development by promoting xylem differentiation (Cano-Delgado et al., 2004), which is inhibited by binding of the TRACHEARY ELEMENT DIFFERENTIATION INHIBITORY FACTOR (TDIF) to the TDIF RECEPTOR (TDR) kinase (Kondo et al., 2013). TDR kinase can directly phosphorylate BIN2 thus inactivate BES1 and inhibit xylem formation (Kondo et al., 2014). Interestingly, phosphorylation of BIN2 upon TDR activation can phosphorylate and activate AUXIN RESPONSE FACTOR 7 (ARF7) to promote lateral root development independent of BR signalling (Cho et al., 2014). Furthermore, BIN2-mediated phosphorylation of the ENHANCER OF GLABRA 3 (EGL3) regulates the balance between phosphorylated and non-phosphorylated forms of this transcription factor and their accumulation in the cytosol or nucleus of root hair cell and non-root hair cell (Cheng et al., 2014). Another crosstalk has been described to occur between BR and ABA signalling pathways, with the latter involved in the responses to abiotic stress (Nakashima et al., 2013). BIN2 can interact with and phosphorylate Snf1-RELATED KINASE 2s (SnRK2s) to positively regulate ABA signalling (Cai et al., 2014) while ABA receptors can promote BIN2 phosphorylation and thus inhibit BR signalling (Wang et al., 2018). Additionally, BIN2 phosphorylates many other transcription factors, such as PHYTOCHROME INTERACTING FACTOR 4 (PIF4) (Bernado-Garcia et al., 2014), homeo-domain-leucine zipper protein 1 (HAT1) (Zhang et al., 2013), and the bHLH transcription factor CESTA (CES), which directly regulate the expression of the BR biosynthetic gene *CPD* (Poppenberger et al., 2011). These BIN2-regulated transcription factors are known to interact with BZR1/BES1 in either synergistic or independent way.

At the level of BZR1/BES1 transcription factors, numerous results have shed light on their interactions with key components of signalling pathways of GA, glucose, SL, auxin and environmental cues including biotic and abiotic stress (W. Wang, Bai and Z-Y. Wang, 2014b; Belkhadir and Jaillais et al., 2015). Upon GA accumulation and perception, DELLA-mediated repression of BZR1 is released and BZR1 can bind to its target gene promoter sequence to regulate cell elongation (Gallego-Bartolomé et al., 2012; Bai et al., 2012b). BZR1 can also regulate light response either by forming heterodimers with phytochrome-interacting factor 4 (PIF4) that bind to the promoter of their common target genes and negatively regulate photomorphogenesis (Oh et al., 2012), or by transcriptionally controlling the expression level of light-signalling components (Z-Y. Wang et al., 2012). Interestingly, DELLA has been previously shown to inhibit PIF transcription factors (de Lucas et al., 2008). Therefore, DELLA-BZR1-PIF4 forms a core transcriptional module that regulates plant growth by integrating hormonal and environmental signalling pathways (Jaillais et al., 2015; Belkhadir and Jaillais et al., 2015). Besides, auxin-mediated co-regulation of shoot cell elongation together with BR and phytochrome has been recently revealed as through direct interaction between BZR1, PIF4 and ARF6 (Oh et al., 2014),

adding a new element to this transcription network. Another example of convergence between hormone and environmental signalling is illustrated by glucose and target of rapamycin (TOR) kinase-regulated accumulation of BZR1 that allows the plant to balance carbon supply and demand under resource-limiting growth conditions (Zhang et al., 2016). Another class of phytohormones, strigolactones, control shoot and lateral root branching and promote photomorphogenesis through mediation of ubiquitination and degradation of BES1 by the F-box ubiquitin E3 ligase MORE AXILLARY GROWTH 2 (MAX2), known as a SL signalling component (Wang et al., 2013). Since plants need to maintain the balance between growth and defense, the regulatory mechanisms shared by growth promotion and immune system have always attracted a lot of attention. In the context of BR signalling, BRI1 shares its co-receptor BAK1 and its substrates BSK1 and BIK1 with the flagellin receptor kinase FLS2 (Chinchilla et al., 2007; Shi et al., 2013; Fan & Bai et al., 2014). However, it has been suggested that the major crosstalk between BR and flagellin signalling pathways happens downstream of the membrane-bound kinases or even further downstream of transcriptional level probably due to the absence of PAMP-induced effect on BZR1 accumulation and activity (Albrecht et al., 2012). Consistent with this, BZR1 has been shown to associate with WRKY40 transcription factor and negatively regulation the expression of defense genes (Lozano-Duran et al., 2013). Another basic helix-loop-helix (bHLH) transcription factor HOMOLOG OF BRASSINOSTEROID ENHANCED EXPRESSION2 INTERACTING WITH IBH1 (HBI1) has been identified as a positive regulator of BR-related responses and has inhibitory effect on PAMP-triggered immune responses (Malinovsky et al., 2014; Fan and Bai et al., 2014), which further indicates the importance of BZR1 as a major node of the crosstalks integrating hormonal and environmental signals and mediating the trade-off between plant growth and defense.

## **5. RLP44- & BRI1-mediated cell wall signalling ensures cell wall homeostasis.**

### **5.1. RLP44- & BRI-mediated cell wall signalling.**

Previous studies in our group allowed the discovery of a novel CWS pathway in *Arabidopsis thaliana* that ensures cell wall homeostasis by monitoring the state of pectin in the cell wall and regulating plant growth through activation of BR signalling pathway (Wolf et al., 2012b; **Figure 4**). It has been reported that interfering with PME activity by over-expressing *PMEI5* (AT2G31430), which encodes a PME inhibitor, inhibits the removal of methyl groups from HG (the major form of pectins) and thus caused a significant increase of ester bonds in the cell wall. The loss of CWI and altered cell wall extensibility were suggested as primary effect of a reduced PME activity and were manifested as cell swelling, detachment and rupture (Wolf et al., 2012b). Changes in the cell wall or signals derived from the wall components could be sensed by the receptor-like protein (RLP)44. RLP44 recruits BR signalling module at the level of BRI1 receptor complex, downstream of its ligand binding, through direct interaction with BRI1 and its co-receptor BAK1 (Wolf et al., 2014; Holzwart et al., 2018). BR signalling could then be activated and

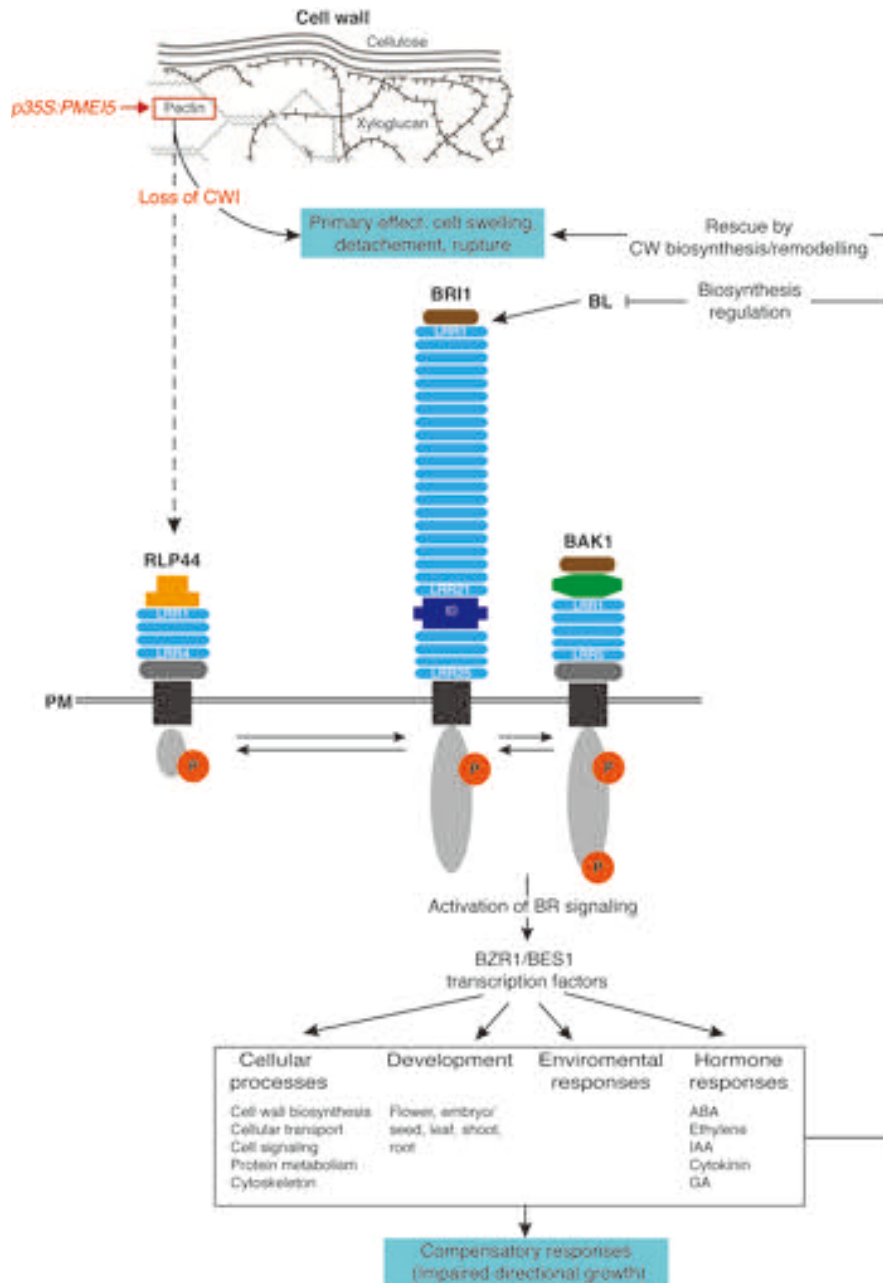


**Figure 4. RLP44- and BRI1-mediated CWS.** Upon loss of cell wall integrity (CWI) due to over-expression of *PME15* (*p35S:PME15*), RLP44 perceived the signal from the wall and activated the BR signalling pathway through interaction with BRI1 and BAK1. BR-mediated regulatory responses compensated the primary effects caused by *PME15* over-expression at the cost of impaired directional growth. Adapted from Cosgrove, 1997; Kim and Z-Y. Wang, 2010; Sun et al., 2010; Wolf et al., 2012b, 2014; Wolf, 2017).

act as a compensatory mechanism that allows the survival of the plant by regulating expression of its downstream target genes among which cell wall biosynthesis and remodelling genes are over-represented. This rescue is achieved at the cost of an impaired directional growth, manifested as waving seedling roots, curled leaves, convoluted shoots, and misshapen siliques in adult plant (Wolf et al., 2012b).

### **5.2. The receptor-like protein 44 (RLP44) and its role in cell wall signalling.**

RLP44 is a receptor-like protein with a predicted signal peptide, an extracellular domain containing 4 LRRs, a single pass transmembrane domain, and a short cytosolic tail (Wolf et al., 2014; **Figure 4**). Analysis of a GFP-tagged version of RLP44 (RLP44:GFP) by using confocal laser scanning microscope showed its localization in both the plasma membrane as well as intracellular compartments (Wolf et al., 2014). In the RAM, RLP44:GFP has been described to be expressed in most tissues except columella cells, with an clear enriched expression in epidermis, lateral root cap and xylem precursor cells. In the stele of the distal RAM, the signal is further enhanced, while in the differentiated part of the root it is predominantly observed in procambial cells with a weaker presence in phloem and xylem (Holzwardt et al., 2018). As described above, RLP44-mediated cell wall signalling regulates plant development by monitoring cell wall especially pectin status and integrating BR signalling pathway. Loss of RLP44 function impairs plant growth and responses in stress conditions. The *rlp44<sup>cnu2</sup>* mutant, isolated in the suppressor screen of PMElox (Wolf et al., 2014), contains a premature stop codon in *RLP44* gene (AT3G49750) and showed hampered growth phenotype on soil including shorter petioles and reduced rosette surface. In addition, *rlp44<sup>cnu2</sup>* mutants were hypersensitive to certain stress conditions such as high concentrations of sucrose or NaCl in the growth medium, which has been illustrated by reduced dark-grown hypocotyl length (Wolf et al., 2014). Besides the activation of BRI1-mediated signalling pathway upon loss of CWI, RLP44 also contributes to the crosstalk between BR and PHYTOSULFOKINE (PSK) signalling at the level of plasma membrane by directly interacting with PHYTOSULFOKINE RECEPTOR (PSKR) 1 and 2 (Holzwardt et al., 2018). PSKs are small secreted peptide growth factors implicated in many developmental processes and their receptors PSKR1 and 2 are close relatives of BRI1 (Matsubayashi et al., 2006; Sauter, 2015). The interaction between RLP44 and PSKR integrates BR signalling and is believed to involve in xylem differentiation control (Holzwardt et al., 2018). Alternatively, it is possible that RLP44 is directly or indirectly connected to other signalling pathways, as it interacts with BAK1, a LRR-RLK involved in various regulatory mechanisms especially those related to immune system (Jaillais et al., 2013).

### **6. Aim of the study: role of RLP44-mediated cell wall signalling in cell type/tissue-specific context.**

As discussed above, BRs and BR signalling are shown to mediate growth responses in a tissue-specific manner (see §4.3), and cell wall properties are involved in cell division, cell expansion and cell fate specification, which in turn influence on tissue patterning and development (see §2.3). Moreover, it has been shown that cell wall status is constantly monitored and the derived signal is transduced into the cell via RLP44-BRI1-mediated CWS (Wolf et al., 2012b; Wolf et al., 2014; see §5.1). However, little is known about the role of a such cell wall surveillance and growth regulation mechanism at tissue level. The aim of this project is to gather more insight into the spatio-temporal relevance of cell wall properties to the downstream

signalling pathways, as well as the role of the key regulator RLP44 in plant growth coordination. By using *Arabidopsis thaliana* primary root as model and triggering the loss of CWI in cell type/tissue-specific way, we expect to answer the following questions: How does cell wall properties contribute to cell identity and tissue patterning ? Which tissues are responsive to the triggering of the loss of CWI ? Is the response cell-autonomous or non cell-autonomous ? Is RLP44 and BR signalling involved in the compensatory responses to the cell type/tissue-specific challenge of CWI ? Are there any other mechanisms in play? Besides, we further analyzed the pleiotropic phenotype caused by ubiquitous perturbation of cell wall with the aim of better understanding how do cell wall homeostasis and RLP44/BRI1-mediated CWS influence on root growth.

## Results

### 1. Loss of cell wall integrity by *PMEI5* over-expression activates cell wall signalling and results in compensatory regulation of root growth.

#### 1.1. Cell wall signalling-mediated compensatory responses resulted in pleiotropic phenotypes in root.

Previous studies showed that *PMEI5* over-expression (*p35S:PMEI5*) inhibited the modification of the pectic polysaccharide homogalacturonan (HG) and resulted in the loss of cell wall integrity (CWI). This loss of CWI is sensed by the plasma membrane-localized RLP44, which activates the BR signalling pathway through interaction with the brassinosteroid (BR) receptor BRI1. Thus, the cell wall defects are rescued by compensatory mechanisms at the cost of altered directional growth (Wolf et al., 2012b; Wolf et al., 2014; **Figure 4**). As described in Wolf et al., 2012b, disturbing the cell wall by over-expressing *PMEI5* under control of 35S promoter (*p35S:PMEI5*, termed *PMElox*) did result in an irregular root waving phenotype at 5 day after germination (DAG) when grown on plate (**Figure 5A**). Compared to the wild type (WT) Columbia 0 (Col-0), adult plant showed an overall stunted growth phenotype on soil with impaired directional growth manifested as curled leaves and convoluted shoots (**Figure 5B**), as well as delayed maturation and reduced fertility.

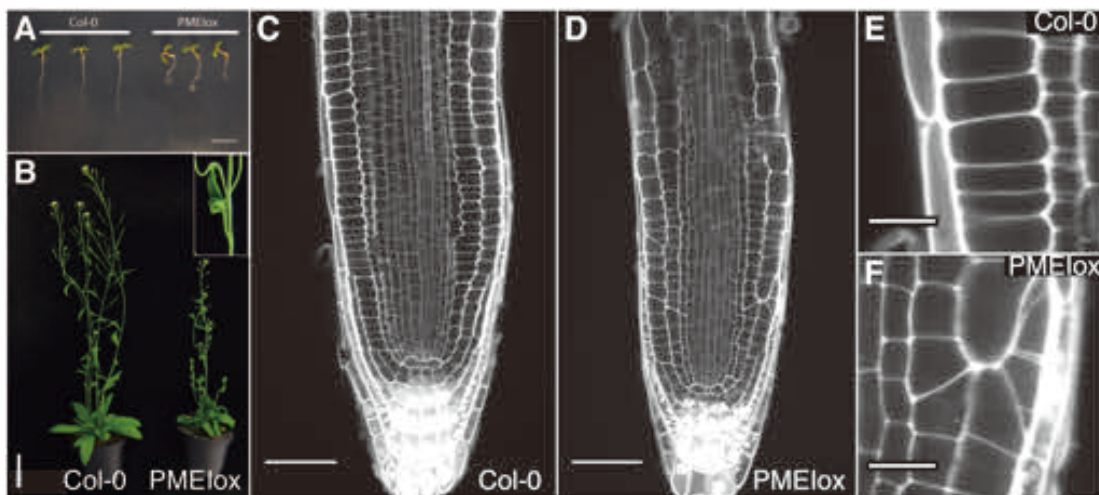


**Figure 5. Pleiotropic phenotype in *PMElox*.** (A) 5 DAG-old seedlings showed root waving when grown on plate. (B) On soil, *PMElox* was dwarfed and showed impaired directional growth compared to Col-0. (C) The root apical meristem (RAM) of Col-0 and (D) of *PMElox* with oblique cell walls in the latter. (E) and (F) Zoom in of the RAM. Cells are counter-stained with propidium iodide (PI). Bars = 1 cm in (A), 5 cm in (B), 50  $\mu$ m in (C) and (D), 10  $\mu$ m in (E) and (F).

**1.2. The pleiotropic phenotype in *PMElox* roots is a consequence of impaired cell division, expansion, and differentiation in the root apical meristem.**

As regular morphology and normal growth of a given organ requires coordinated cell division, expansion, and differentiation in all tissues (Dupuy et al., 2010), examination of such processes in the root, especially in the root apical meristem (RAM) which harbors the stem cell niche (SCN), would bring more information about the causation of observed phenotype. In line with our expectation, the root growth of *PMElox* has been affected in those aspects: **1)** oblique transverse cell walls relative to each cell's longitudinal axis (**Figure 5D, F**), which might result from a perturbed cell division plane determination during mitosis (**Figure 7F-H**); **2)** a decrease in RAM size, accompanied by a reduction in root growth with more pronounced effect on RAM size (meristematic cell number and RAM length) (**Figure 10A-C**) possibly due to an early transition of meristematic cells from division to elongation (**Figure 10F**); **3)** an over-differentiation of columella stem cells (CSCs). These defects are characterized in details in the following sections.

**1.2.1. The oblique cell walls observed in *PMElox* were caused by an altered cell division plane during mitosis.**

**1.2.1.(1) The oblique cell walls resulted from an oblique cell division plane in mitosis.**

To visualize the cellular organization in the RAM, we stained the seedling root, after fixation, with a modified pseudo-Schiff propidium iodide staining (mPS-PI) method (Truernit et al., 2008). The mPS-PI staining marks the cell outline by labelling the cell wall material with fluorescent propidium iodide and allows imaging of all root tissues with high resolution. Subsequent analysis of the mPS-PI stained primary root tip under laser scanning confocal microscope revealed neatly organized RAM in *Col-0* with different tissues represented as longitudinal cell files. Each cell file was composed of non-elongated cells that are vertically stacked one on the other (**Figure 5C, E**). In contrast, *PMElox* showed a substantial amount of obliquely orientated transverse cell walls that were easily spotted in epidermis, cortex and endodermis (**Figure 5D, F**), which caused an irregular tissue organization and, in some severe cases, almost indiscernible tissue boundaries (**Figure 5F**). An oblique transverse cell wall (and the oblique cell division plane in subsequent analyses) was scored when orientation differed with more than a  $10^\circ$  angle from the transverse orientation perpendicular to the

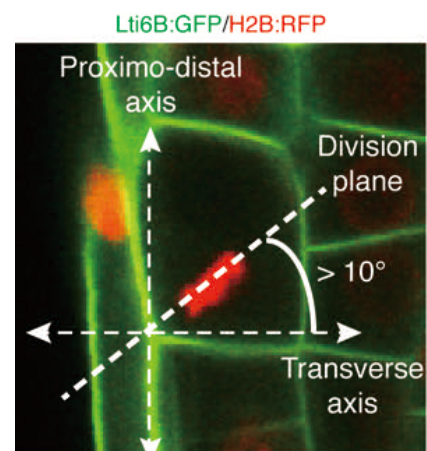


**Figure 6 The determination of the oblique division plane.** The oblique division plane or cell wall is defined as having an angle  $> 10^\circ$  between the plane of the division/cell wall and the transverse axis, which is perpendicular to the proximo-distal axis of the meristem. Shown here is a dividing cell at metaphase. Chromosomes are revealed by H2B:RFP (red), cell outline is represented with plasma membrane by Lti6B:GFP (green).

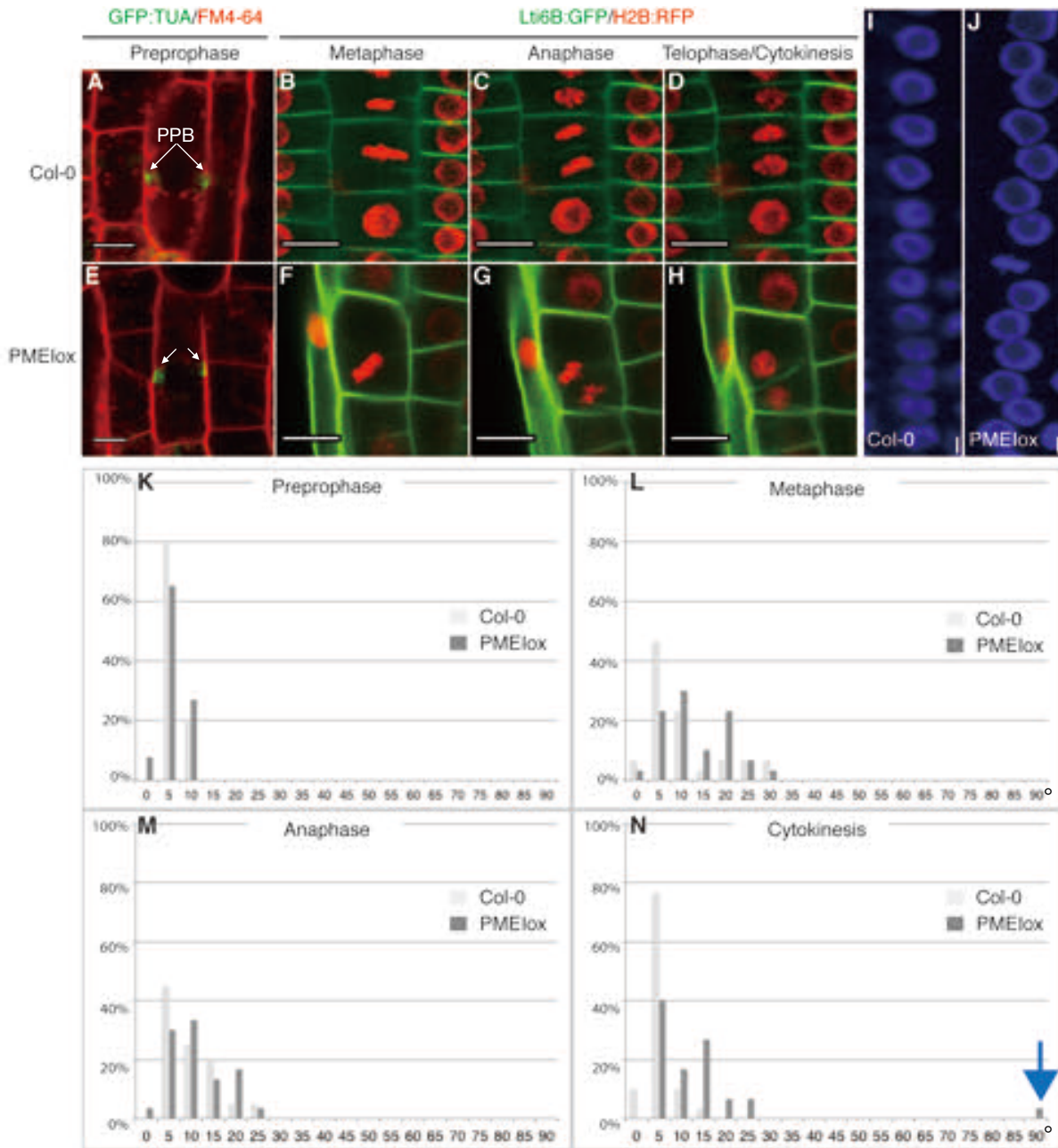


**Figure 7 Division angle analysis during mitosis.** In Col-0, the division plane remained transverse during (A) preprophase and (B) metaphase as defined by the PPB position and the axis of metaphase plate. (C) The division plane shifted to an oblique position during anaphase and (D) has been ‘corrected’ during telophase/cytokinesis. In PMElox, this division plane orientation was similar to Col-0 in preprophase (E) but became oblique already at (F) metaphase stage and remained oblique through (G) anaphase and (H) until the end of the mitotic cycle. The longitudinal organization of nuclei in one cell file showed (I) a straight alignment in Col-0 and (J) was zigzagged in PMElox. (K-N): Quantification of oblique division plane during mitosis as illustrated in Fig. R1-1, blue arrow indicates an extreme case of a shift of division angle to almost 90° in PMElox. X axis = degree of division angle, Y axis = percentage of cells. In (I) and (J): nuclei are stained with DAPI. n = 30 - 50. Bars = 20 μm in (A-H), = 10 μm in (I,J).

proximo-distal axis of the primary root growth (Figure 6; Zhang et al., 2016). As transverse cell walls are formed through phragmoplast-guided cell plate fusion with the vertical parental wall at

the stage of cytokinesis during mitotic cell division, it is plausible that an altered plane of cell plate or cell division is the origin of the formation of such an oblique transverse wall. To investigate the cell division plane orientation, we used transgenic lines expressing GFP- $\alpha$  tubulin or Lti6B-GFP/H2B-RFP together with FM4-64 and DAPI fluorescent dyes, as well as immunolabelling of microtubules to study the position and the orientation of microtubule-derived preprophase band (PPB), mitotic spindle, cell plate and chromosomes throughout the division cycle (**Figure 7**). In almost all cells of Col-0, a transverse division plane was observed in preprophase as defined by the position of the PPB (**Figure 7A**). This division plane, represented by the metaphase plate orientation, remained transverse until early metaphase, and then shifted to a slightly oblique orientation in late metaphase till anaphase/early telophase-cytokinesis (**Figure 7B, C**). However, this oblique division plane shifted back to the initial transverse orientation as the cell plate formation progressed (**Figure 7D**). Interestingly, in PMElox, although the position of PPB showed a regular transverse orientation (**Figure 7E**), a shift of the division plane orientation was observed earlier than in Col-0, occurring mostly during metaphase (**Figure 7F**) and remained oblique through entire anaphase (**Figure 7G**) till cytokinesis, where an obliquely orientated cell plate was formed and gave rise to a new oblique transverse wall (**Figure 7H**). Quantification of the division angle has been carried out in approximately 50 cells for each cell division phase and further confirmed the previous observation. In Col-0, the division plane was established transversely by PPB in all cells analyzed (**Figure 7K**) and in most of metaphase cells it remained its position with a slight trend of shifting to the oblique orientation in about 23.33% of the cells (**Figure 7L**). This shift reached its peak frequency of 30% at anaphase (**Figure 7M**) and was 'corrected' and brought back to the initial transverse position during cytokinesis, with only 3.33% of the cells still showing a division angle  $> 10^\circ$  (**Figure 7N**). Contrarily, in PMElox the shift of transverse division plane to an oblique orientation occurred in 43.33% of the cells already in metaphase (**Figure 7L**), this frequency remained at 33.33% in anaphase and 43.33% during cytokinesis, meaning that the oblique division plane did not shift back to the initial transverse orientation (**Figure 7N**). The persisting oblique division plane in PMElox caused in extreme cases a shift of division angle to almost  $90^\circ$  (**Figure 7N, blue arrow**). In addition, PMElox showed zigzagged nuclei alignment along one longitudinal cell file (**Figure 7J**) whereas in Col-0 they aligned rather straightly (**Figure 7I**). Given the observation that the oblique cell walls did not occur as regular as the zigzagged nuclei alignment, they might not be directly causative for the latter.

1.2.1.(2) The oblique division plane in PMElox seemed to be related to the failure in maintaining a proper cortical division site position.

It is widely accepted that the future division plane is predicted by PPB (Smith, 2001; Rasmussen et al., 2013), the position of which defines the cortical division site (CDS). The CDS is constantly present during cell division and represented by complex of cortical MT-derived

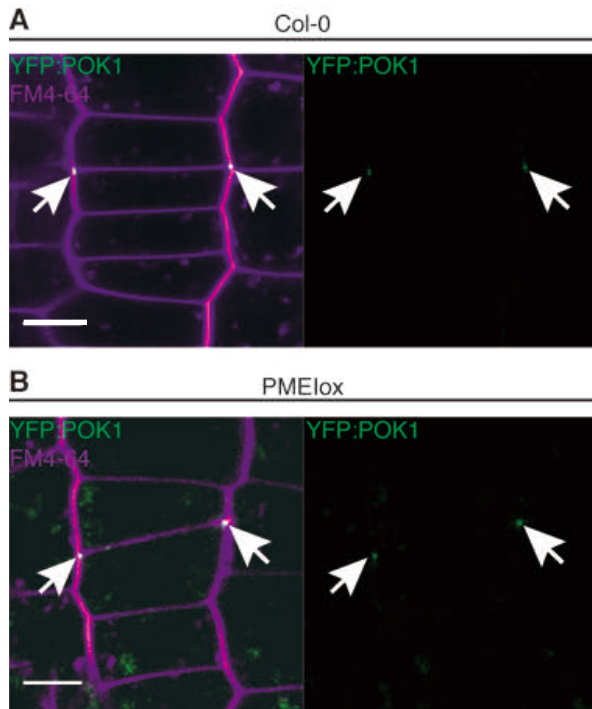


**Figure 8. Analysis of cortical division site (CDS) position by following YFP:POK1 localization at the end of cytokinesis. (A)** In Col-0 the POK1-marked CDS remained at the transverse axis and guided the fusion of cell plate to the vertical parental wall thus forming a transverse cell wall. **(B)** In PMElox, the CDS appeared to be shifted and the cell plate still fused to the parental wall at the CDS, which resulted in an obliquely positioned transverse wall. White arrow heads indicated YFP-POK1-marked CDS. Bars = 20  $\mu$ m.

structures accompanied by MT-associated proteins, signalling proteins, and actin filaments, and serves as guide for the future fusion point between the newly synthesized cell plate and the vertical parental wall (Smith, 2001; Müller et al., 2006, 2010; Panteris, 2008; Rasmussen et al., 2013). The PPB is known as a faithful but transient predictor of and pre-establishes the division plane by setting up the CDS only during preprophase and disassembles in later stages (Rasmussen et al., 2013; Lipka et al., 2014). After PPB disassembly, the CDS positional information is preserved by factors that are continuously localized to the cell cortex throughout mitosis. Among those factors, the PHRAGMOPLAST-ORIENTING KINESIN 1 and 2 (POK1 and POK2), are retained to the CDS during prophase and their retention on the CDS appears to be static in the absence of microtubules after PPB disassembly (Müller et al., 2006; Lipka et al., 2014). The function of POK1 and POK2 is also strictly required to maintain the CDS identity marker TANGLED (TAN) (Walker et al., 2007; Rasmussen et al., 2010). Our observation did not show any abnormal position of PPB during preprophase in both Col-0 and PMElox as revealed by the microtubule marker GFP- $\alpha$  tubulin (Figure 7A, E). There are two possible scenarios in which the observed oblique cell walls could be formed: either the CDS stayed at the predicted sites after PPB disassembly and the cell plate fused to a random point in the vertical wall during cytokinesis; or the CDS moved within the plasma membrane during the mitosis and the fusion of cell plate to the parental wall at the shifted CDS resulted in an oblique orientation of the newly synthesized wall. To gather more information about these possibilities, we used POK1 as CDS marker to track its position through out the division cycle. Due to the weak and easily-bleached signal of the YFP-tagged POK1 protein, the observation was concentrated on the cytokinesis stage of the mitotic division cycle. In Col-0 the CDS remained its transverse position during cytokinesis as indicated

by the CDS-residing protein POK1 (**Figure 8A, white arrow head**). This is consistent with the previously observed regular cell plate orientation (**Figure 7D**). Interestingly, in *PMEIox* the POK1-marked CDS appeared at a shifted position (**Figure 8B, white arrow head**) and the cell plate faithfully fused to the vertical parental wall at the mis-positioned CDS and resulted in an oblique transverse cell wall (**Figure 8B, magenta channel**). Therefore, such a failure in maintaining the proper CDS position is possibly the reason why the oblique cell division plane has been established.

### 1.2.1.(3) The seedling root waving was unrelated to oblique cell walls in the RAM.

Under constitutive expression of *PMEI5*, the seedling root waving and the oblique cell wall in the RAM were both observed at the same time. One might wonder whether these two

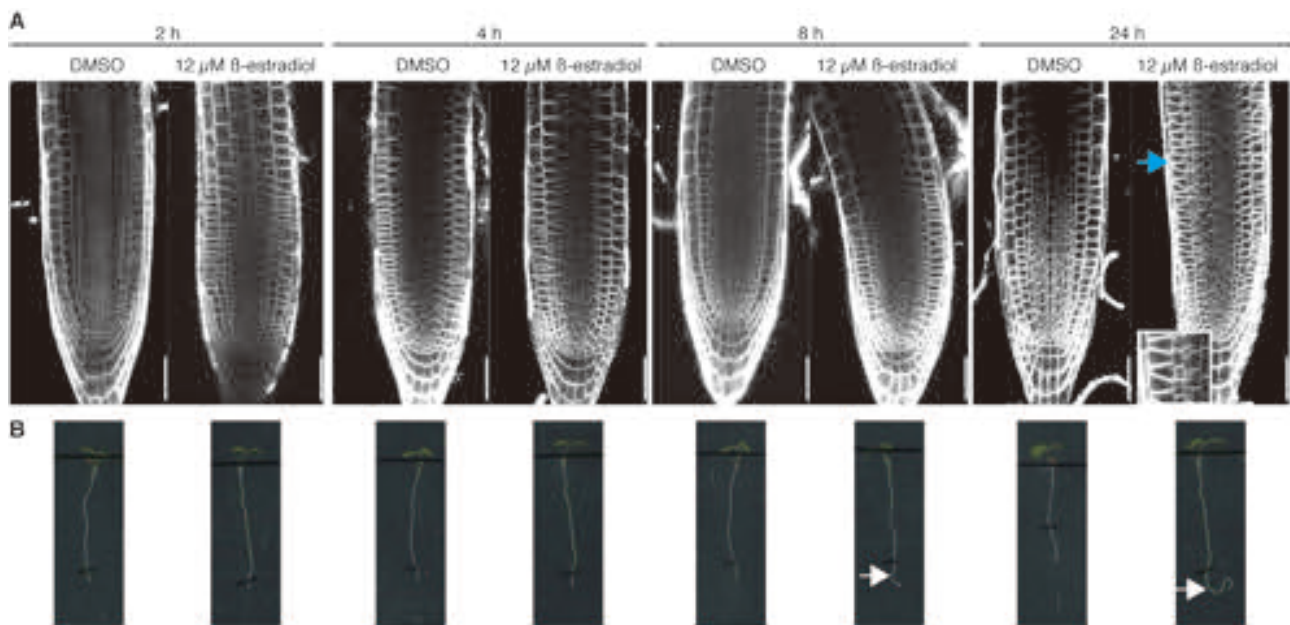


**Figure 9. Uncoupling root waving and oblique cell wall caused by *PMEI5* over-expression through time-course induction of inducible *PMEIOx* line (*iPMEIOx*).** (A) PI-stained RAM of *iPMEIOx* showed oblique cell walls only at 24 hours after induction while (B) root waving appeared already at 8 hours after induction. Blue arrow indicates oblique cell walls and white arrows indicate root waving. Bars = 50 μm.

phenotypes are related as irregular orientation of transverse cell wall might have an influence on cell shape and thus tissue organization. In order to unravel this connection, we made use of transgenic plants with inducible *PMEI5* expression (*iPMEIOx*) established in previous studies of our group (Wolf et al., 2012b). Until 4 hours after transfer to induction medium, the seedling root and RAM showed normal morphology and regular tissue organization, respectively (**Figure 9**). At 8 hours after induction, a clear waving was observed above the tip region of the root (**Figure 9B, white arrow**) while no oblique cell walls had yet appeared in the RAM (**Figure 9A**). At 24 hours post-induction, the root waving was even more pronounced and successive oblique cell walls

were clearly visible mainly in epidermis and cortex (**Figure 9A, blue arrow**). These results hence suggested that the root waving might not be related to the oblique cell wall in the RAM since it appeared before the emergence of any observable oblique transverse wall.

*1.2.2. The reduced primary root growth in PMElox is caused by a premature transition of meristem cells from division to transition.*

Besides the root waving, PMElox showed reduced vertical growth in the primary root with 23.8% of decrease compared to Col-0 (**Figure 10A**). Primary root growth largely depends on the

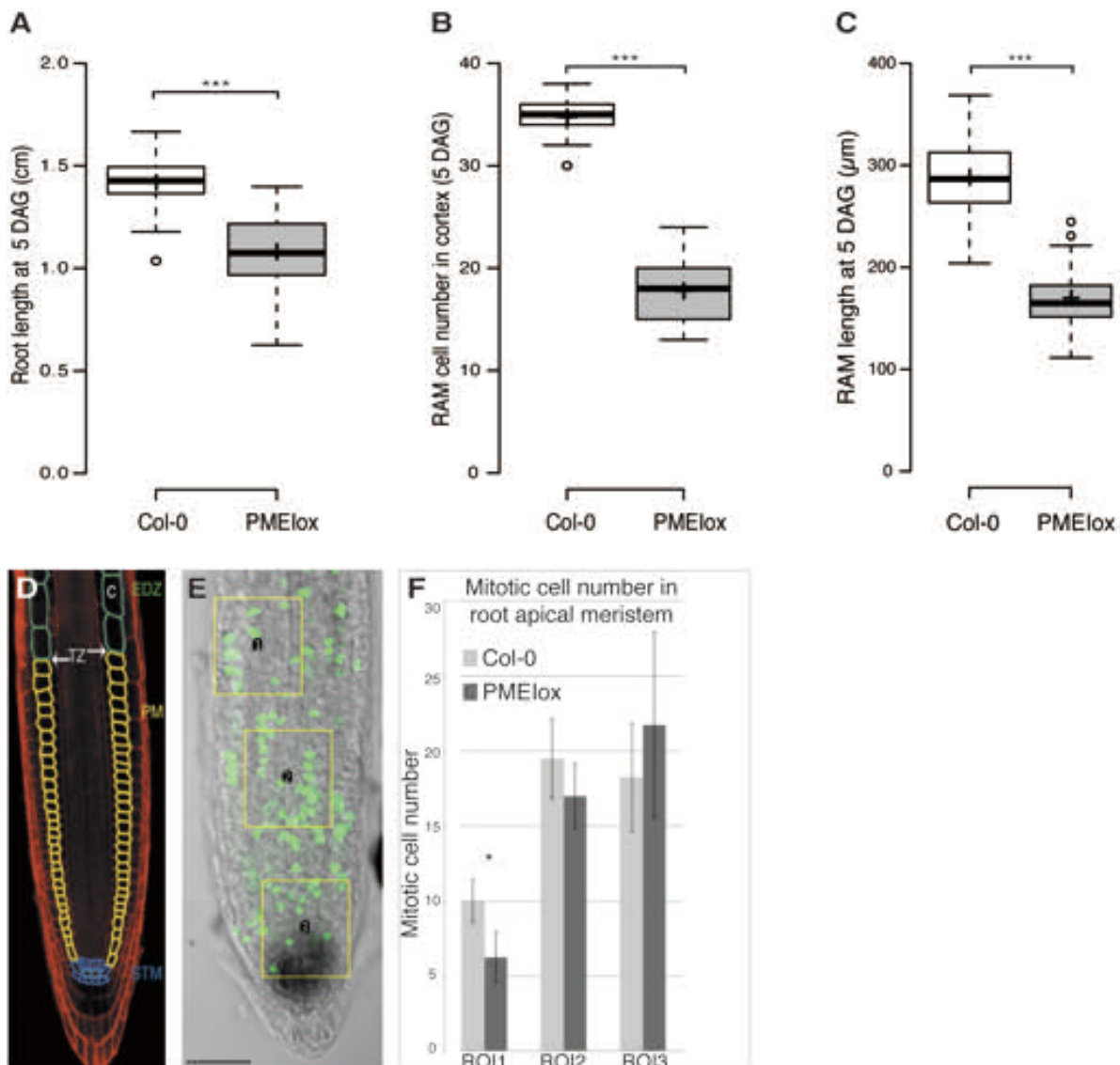


**Figure 10. Reduced root growth and RAM size in PMElox were due to a premature transition from cell division to elongation in the meristem.** (A) Vertical primary root growth was reduced at 5 DAG, which was the consequence of (B) a decrease in RAM cell number and (C) the RAM length. (D) RAM size is expressed as cortex cell numbers between the CEI and the first elongated cell (cells outlined in yellow), STM (stem cell), TZ (transition zone), PM (proximal meristem)meristem), EDZ (elongation/differentiation zone), adapted from Dello Ioio et al., 2007. (E) Quantification of mitotically active cells after EdU staining in three different regions of interest (ROIs): ① transition zone, ② middle meristem zone, ③ proximal meristem including QC and SCN. (F) PMElox only showed a decrease of mitotically active cells in ① transition zone. Asterik indicates a statistically significant difference in mitotic cell numbers by a two-tail t-test with  $p < 0.05$ . Bar = 50 µm in (E).  $n = 34 - 46$  in (A-C), = 16 in (F).

rate of cell proliferation in the apical meristem and cell elongation in the upper elongation zone. In case of *PMElox*, the RAM cell number dramatically dropped off by 48.9% (**Figure 10B**). Meristematic cell number was expressed as the number of cortex cells in a file that expands from the first cell after the CEI to the first elongated cell (**Figure 10D**; [Dello Iorio et al., 2007](#)). Interestingly, the RAM size expressed as absolute length (in  $\mu\text{m}$ ) showed 41.1% of decrease (**Figure 10C**). This slightly less pronounced abatement of RAM length indicated a possible compensation of reduced RAM cell number by increased meristematic cell expansion resulting in a bigger cell size. Cells in the meristem zone are active in division and latent for expansion/elongation. They start to increase in size along the longitudinal axis once they exit the meristem zone and enter the elongation phase. To find out whether the reduced cell number and the bigger cell size are due to a reduced cell division activity or an early transition from the meristem zone to the elongation zone, we analyzed cell proliferation by using the Click-iT® EdU staining method. The 5-ethynyl-2'-deoxyuridine (EdU) is a thymidine analogue incorporated into the DNA during its replication. Thanks to its detectable tag, cells that are actively dividing can be visualized and quantified ([Zeng et al., 2010](#)). Dividing meristematic cells within three different regions of interest (ROIs) are quantified: ROI1 — end of meristem zone with transition into elongation zone; ROI2 — middle meristem zone; ROI3 — proximal meristem zone surrounding the QC and SCN (**Figure 10E**). In ROI2 and 3 no significant difference was found between *Col-0* and *PMElox*. In ROI1, *PMElox* showed a slight but significant decrease of mitotically active cells (**Figure 10F**). This observation indicated that the reduced RAM cell number and the increased cell size could result from a premature transition of meristematic cells from division to elongation.

### 1.2.3. Over-expression of *PMEI5* promoted columella stem cell differentiation.

To further analyze the effect of *PMEI5* over-expression of cell differentiation, we quantified the rate of columella stem cell (CSC) differentiation as previous studies reported that BRs and BR signalling pathways play a role in the control of distal CSCs differentiation ([González-García et al., 2011](#); [Lee et al., 2015](#)). 80% of the WT plants had a single layer of CSCs, while nearly 20% had two layers and very few had 0 layer. This frequency reached 100% in *bri1-116* ([González-García et al., 2011](#)), a null allele of *bri1* ([Li and Chory, 1997](#)). *bes1-1D*, a mutant with constitutively active version of BR signalling-responsive transcriptional factor *BES1*, showed 0 layer of CSCs in more than 60% of the plants and almost no plant had more than 1 layer. This observation was further supported by a hugely increased number of plants with 0 layer of CSCs after treatment with 4 nM brassinolide (BL) ([González-García et al., 2011](#)). On the contrary, *BZR1*, known as a *BES1* homologue, was demonstrated to suppress CSC differentiation, opposite to the *BES1* effect ([Lee et al., 2015](#)). In view of the above-mentioned claims, *PMElox* might also be affected in CSC differentiation as it showed enhanced BR signalling ([Wolf et al., 2012b](#)). Therefore, we quantified the number of CSC layers in mPS-PI stained root tip and used the starch granule accumulation as indicator for differentiated CSCs (**Figure 11A, B**). Indeed, *PMElox* had 0 layer of CSCs in 48.68%,

1 layer in 46.05%, and 2 layers in only 5.26% of the plants, compared to Col-0 with 0, 1 and 2 CSC layers observed in 12.16%, 70.27% and 17.57% of the plants, respectively (**Figure 11C**). This observation pointed to a promoting role of RLP44- and BRI1-mediated signalling pathway in CSCs differentiation regulation.

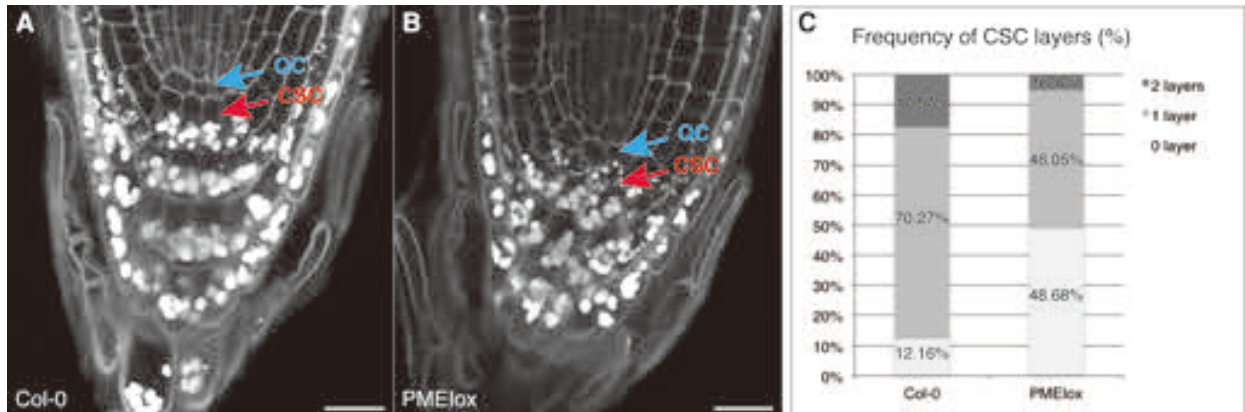


**Figure 11. Columella stem cell (CSC) over-differentiation in PMElox.** (A) Most of Col-0 plants had 1 layer of CSCs (red arrow) below the QC (blue arrow). (B) Some of PMElox plants had even zero layer of CSCs. (C) Proportion of Col-0 and PMElox plants that had 0, 1 and 2 layers of CSCs. Cells are counter-stained with PI. n = 74 for Col-0 and 76 for PMElox. Bars = 20  $\mu$ m.

### 1.3. The pleiotropic phenotype in PMElox is a result of enhanced BR-signalling, altered cytokinin and auxin signalling, and altered cell identity specification.

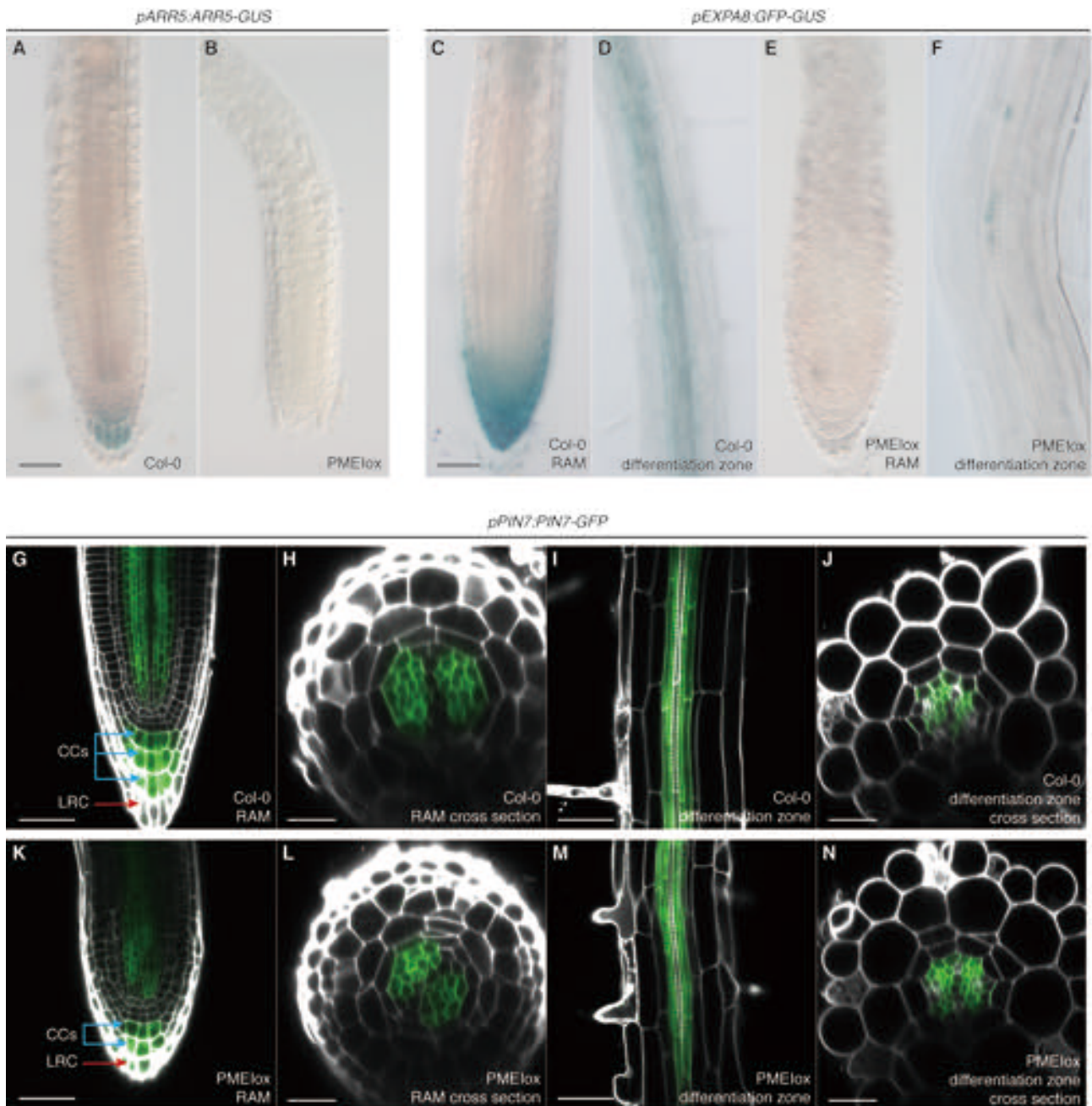
#### 1.3.1. The premature transition of meristematic cells into elongation and CSC over-differentiation in PMElox might result from crosstalk with cytokinin and auxin signalling pathways.

BRs are generally known to both promote and restrict shoot growth from the epidermis (Savaldi-Goldstein et al., 2007). It has been formerly demonstrated that the small root meristem of *bri1* mutants that are defective in BR perception and signaling is a result of altered cell cycle progression and cell expansion, which are crucial for maintaining the meristem cell number and cell size. In root epidermis, both processes require BR signalling (Hacham et al., 2011). However, PMElox showed an enhanced BR signalling (Wolf et al., 2012b) indicating that its smaller meristem might result from another regulatory mechanism(s). The maintenance of the RAM requires a balance between the generation of new stem cells through regular progression through cell cycle and the differentiation of daughter cells. Besides BRs, other phytohormones that have been shown to crosstalk with the BR signalling pathway were also revealed to play important roles in controlling RAM cell proliferation and differentiation. For example, GA controls RAM size by targeting DELLA degradation in dividing endodermal cells to regulate their expansion rate, which in turn dictates the rate of division and elongation of the cells in other root tissues (Ubeda-Tomás et al., 2009). It has also been reported that cytokinins control RAM size by regulating cell differentiation in the transition zone of the stele and antagonizing the auxin-mediated cell division (Blilou et al., 2005; Dello Iorio et al., 2007, 2008; Di Mambro et al., 2017).

Downstream of cytokinin perception, type-B ARRs are transcription factors that positively mediate cytokinin responses while type-A ARRs are thought to negatively regulate cytokinin responses by interfering with type-B ARR activity (D'Agostino et al., 2000; Hwang and Sheen, 2001; To et al., 2004, 2007; To and Kieber, 2008). Reduced expression of ARR5, a type-A ARR, in the stele of the PMElox root (**Figure 12B**) compared to Col-0 (**Figure 12A**) would suggest a decrease in ARR5-related negative regulation of ARR1 activity. This interference might lead to ARR1-mediated auxin degradation and negative regulation of *PIN* genes, which in turn resulted in a promoted cell differentiation over cell division in the transition zone, resulting in a reduced RAM size (Dello Iorio et al., 2007, 2008; Di Mambro et al., 2017). In line with this, PIN7 distribution seemed to be reduced in the stele of PMElox RAM (**Figure 12G, K**), suggesting a decrease of auxin level in this zone, but without any change in the radial distribution (**Figure 12H, L**). However, PIN7 distribution in the vasculature of the mature part of the root showed a slightly expanded distribution in the XPP and protoxylem cells in PMElox (**Figure 12I, J, M, N**). This extended expression domain of *PIN7* resembles the redistribution of PIN7 to the protoxylem cells caused by a too high cytokinin level in the procambial cells (Bishopp et al., 2011). Whether this gently altered cytokinin and auxin distribution in the mature vascular tissue interfere with the RAM size has not been reported. Hence, these observations collectively corroborates the previous result of EdU staining showing that the decreased RAM size and meristematic cell number in PMElox primary root is probably due to a premature transition of cells from division to elongation/differentiation.

The SCN position is determined by formation of an auxin maximum around the QC, allowing the establishment of a gradient of the AP2-domain transcription factors PLETHORA (PLTs), which in turn maintains the expression of auxin-efflux carriers PIN-FORMED proteins (PINs) forming a feed-forward loop to position the SCN (Sabatini et al., 1999; Blilou et al., 2005; Křeček et al., 2009; Bennett and Scheres, 2010; Petricka et al., 2013; Liu et al., 2017). In Col-0, auxin maxima have been described to locate in the SCN surrounding the QC, consistent with PIN7 localization above and below this region (**Figure 12G**; Bielach et al., 2012). In Col-0, PIN7 was mainly localized in procambial vascular cells and 3 layers of differentiated columella cells (**Figure 12G**), while in PMElox this expression pattern was still present in 3 cell layers in the proximal meristem but with only 2 layers that are supposed to be differentiated columella cells and the outermost one as LRC (**Figure 12K**). Expansins are cell wall-loosening proteins that are involved in cell division and expansion (Cosgrove, 2000a, b). In rice (*Oryza sativa*), *OsEXPA8* has been shown to improve root system architecture by increasing cell length in root vascular bundles (Ma et al., 2013). In the *Arabidopsis* root, *AtEXPA8* is primarily expressed in the distal cells of the root tip including LRC, columella and SCN as well as vascular tissue in the differentiation zone (**Figure 12C, D**). This expression was largely depleted in PMElox (**Figure 12C, D**) pointing to an altered cell division and proliferation in those tissues. Interestingly, the domain with decreased *AtEXPA8* expression overlaps with that of *ARR5* expression depletion, suggesting that the altered cell division and proliferation might be a consequence of cytokine and auxin-mediated regulation

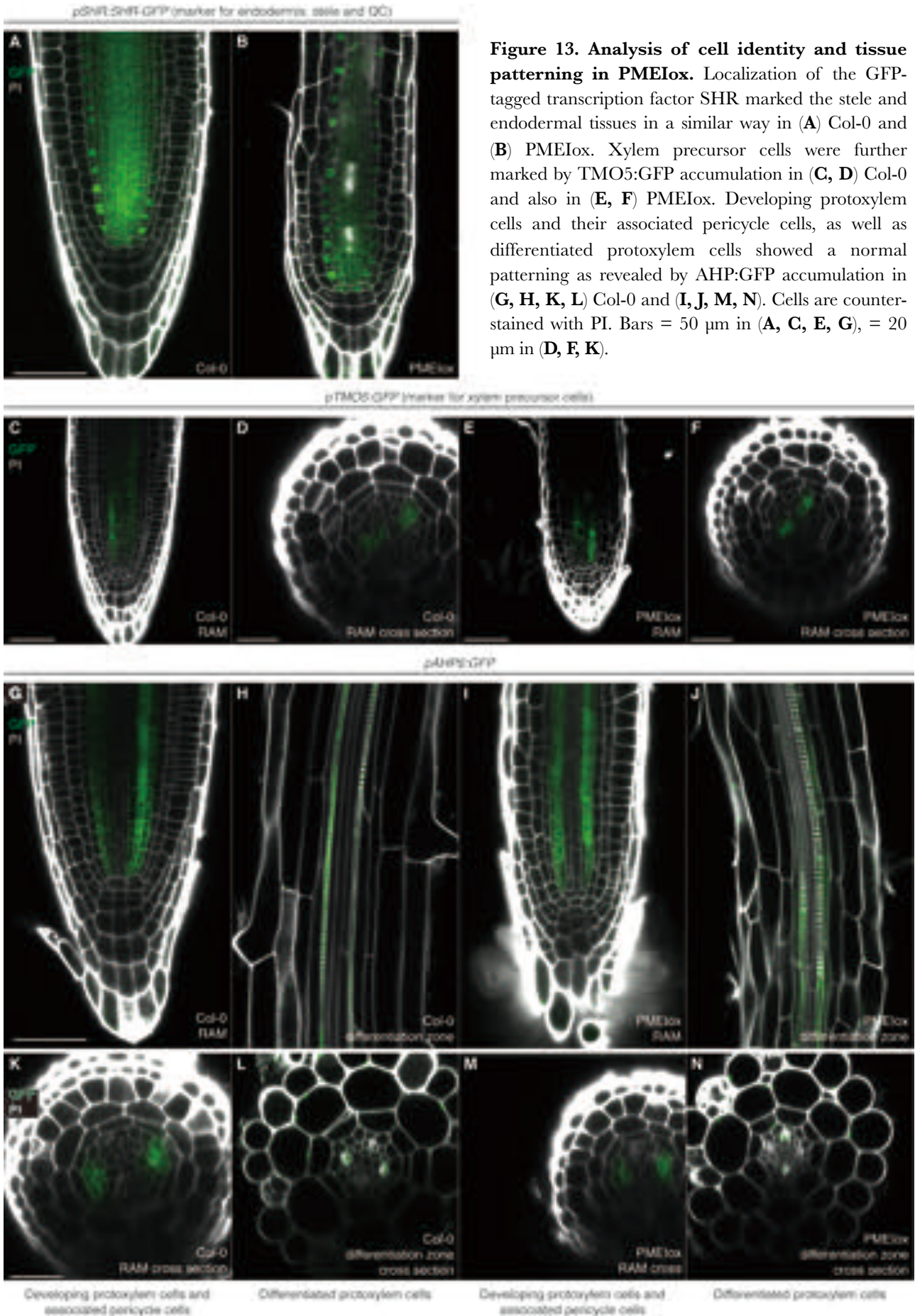
of root growth and tissue patterning, and contribute to the observed phenotypes of RAM size and columella stem cell differentiation.



**Figure 12. Other hormonal signalling pathways might influence on RAM growth and patterning in PME1ox.** (A) In Col-0, ARR5 was mainly expressed in the SCN, the columella cells and the stele, which (B) was largely in PME1ox. (C, D) EXPA8 expression was in the proximal meristem and the differentiated vascular tissue, which (E, F) almost completely disappeared in PME1ox. PIN7 localization seemed to be similar in the vascular tissue in both Col-0 (G-J) and PME1ox (K-N) except for the columella cells: in Col-0 PIN7 was observed to be present in all three layers of columella cells (G) while in PME1ox it was present in only two layers of columella cells and conquered also the LRC cells (K). Cells are counter-stained with PI in (G)-(N). Bars = 50  $\mu$ m in (A-F, G, I, K, M); = 20  $\mu$ m in (H, J, L, N).

1.3.2. *Altered cell identity specification might contribute to altered tissue organization and overall impaired plant morphology.*

In the light of distinct cell wall properties regarding cell and/or tissue types (Fridman et al., 2016), as well as the role of cell wall in positional signalling (Dolan, 2006; Liang et al., 2015), it would be interesting to know whether challenging the wall in PMElox altered the positional information in at least a subset of cells and/or provoked a switch in cell identity thus led to an impaired tissue organization and overall plant morphology. To do so, cell identity markers are the tool of choice. In Col-0 the GRAS transcription factor SHORT-ROOT (SHR) is synthesized in the stele cells and localized in the cytosol, it moves outward to the endodermis to execute the transcriptional regulation of target genes in the nucleus of endodermal cells and specify endodermal identity (Figure 13A; Gallagher et al., 2004; Kim et al., 2017). A similar expression pattern of *SHR:GFP* has been observed in the stele, endodermis and the QC of PMElox when compared to Col-0 (Figure 13B). The TARGET OF MONOPTEROS 5 (TMO5) is involved in the establishment of the vascular tissue and marks specifically the xylem precursor cells in the stele (Figure 13C, D; Rybel et al., 2013). Again, a Col-0 comparable expression pattern has been observed in PMElox (Figure 13E, F). The *Arabidopsis* Phosphotransfer Protein 6 (AHP6), an inhibitor of cytokinin signalling, is specifically expressed in the developing protoxylem cells and its associated pericycle cells (Figure 13G, K). This vascular expression domain becomes even more restricted in the differentiated zone with signal only seen in the lignified protoxylem cells (Figure 13H, L). As before, no ectopic expression was detected in PMElox (Figure 13J, N) suggesting a globally regular vascular development. The enhancer-trap line E3745 drives GFP expression only in pericycle cells that are opposite to the protoxylem cells observed as two groups of 2 or 3 xylem pole pericycle (XPP) cells along the root and opposing each other at an angle of 180° (Figure 14A, B; A', B' for illustration). Surprisingly, PMElox only showed one group of GFP-marked XPP cells that seemed to comprise more than 3 XPP cells (Figure 14C, D; C', D' for illustration). XPP cells are considered as meristem cells or cells with pluripotency as they still exhibit mitotic division potential and are at the origin of lateral root and callus formation (Dubrovsky et al., 2000; Atta et al., 2008; Beeckman and Smet, 2014). Furthermore, they seem to be recruited into cambial zone to establish the radial symmetry and are tightly connected to its neighbouring vascular tissue (Miyashima et al., 2013; Parizot et al., 2011). Thus, it should not be surprising to observe the severe growth phenotype in PMElox as it had perturbation in XPP cell specification. Nevertheless, how this perturbation influence on plant growth without affecting vascular tissue development remains obscure. Additionally, the enhancer-trap line Q0990 revealed a rather normal cell specification and patterning in procambial cells and the QC in both Col-0 and PMElox (Figure 14E-H), which again demonstrated a regular vascular development and stem cell maintenance.



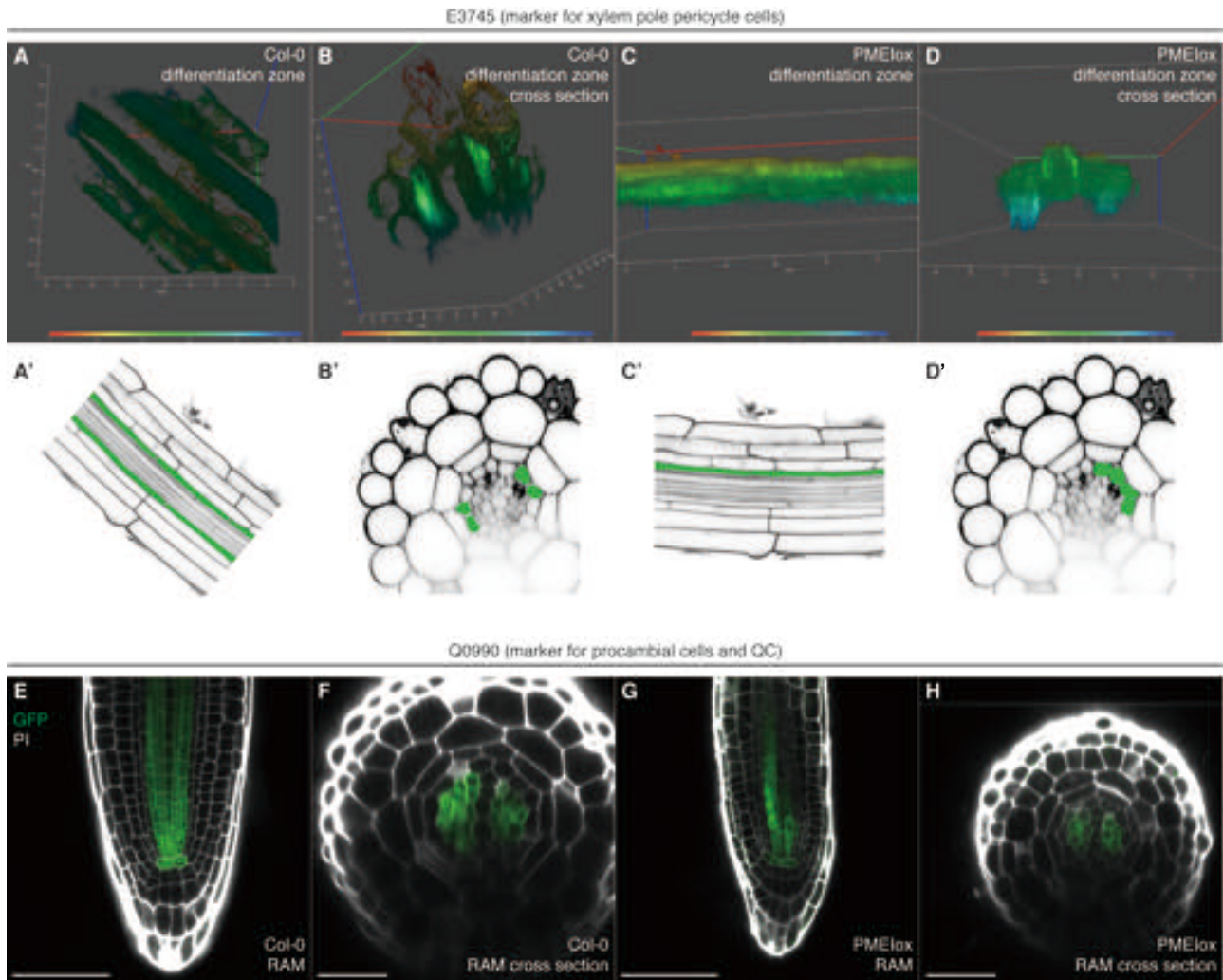


**Figure 14. Analysis of cell identity and tissue patterning in PME1ox (follow-up).** The enhancer-trap line E3745 showed GFP signal in xylem pole pericycle cells (XPP) (**A, B**) in Col-0 as two longitudinal groups of cells as illustrated in (**A', B'**), with each group containing 2 or 3 XPP cells. (**C, D**) In PME1ox, only one group of such GFP signal-enriched cells were observed with seemingly more than 3 cells, illustration in (**C', D'**). Another enhancer-trap line Q0990 marked the QC and non-xylem stele cells in (**E, F**) Col-0 and showed similar pattern in (**G, H**) PME1ox. Cells are counter-stained with PI. Bars = 50  $\mu\text{m}$  in (**E, G**); = 20  $\mu\text{m}$  in (**F, H**).

## **2. RLP44- and BRI1-mediated CWS is partially involved in regulation of root growth and development in the responses to cell type/tissue-specific perturbation of cell wall properties.**

### **2.1. A case study about the effect of cell type specific cell wall properties on plant growth and development – disrupting the wall only in XPP cells was sufficient to cause pleiotropic phenotype.**

Regarding the intriguing observation of an altered XPP cell identity acquisition when the cell wall integrity is ubiquitously challenged in the plant (PMElox), triggering the same disruption specifically in XPP cells would be conducive to understanding the role of RLP44-mediated CWS in a cell type-specific context. We made use of transgenic plants expressing the same *PMEI5* gene (AT2G31430) as in [Wolf et al., 2012b](#) under a XPP cell-specific promoter (*pXPP:PMEI5*, kindly provided by Maizel lab, COS, University of Heidelberg) to study the role of CWS in root growth regulation at tissue level.

Very much to our surprise, *pXPP:PMEI5* seedlings clearly exhibited a PMElox-like root waving at 5 DAG, although weaker compared to ubiquitous over-expression (**Figure 15A, B**). Confocal microscopy analysis of mPS-PI stained RAM showed some irregular cell file organization in the stele, which seemed to result from abnormal cell divisions in the procambial cells (**Figure 15C**). It is noteworthy that *PMEI5* expression driven by *XPP* promoter only started in XPP cells in the elongation/differentiation zone of the root (**Figure 15O-Q**). Examination of vascular tissue, especially xylem, in the more differentiated part of the root did not reveal any obvious defect in root architecture. When grown on soil, *pXPP:PMEI5* showed a rather normal rosette with slightly narrower leaves (**Figure 15E, F**). Surprisingly, plant belonging to 3 independent T3 stable homozygous lines of *pXPP:PMEI5* were all severely delayed in shoot bolting, with the first shoot appearing around 3 weeks later than Col-0 (**Figure 15D, F**). In addition, different individuals within each T3 homozygous line showed a gradient of delay in shoot bolting: while the initiation of shoot bolting occurred in some of the *pXPP:PMEI5* plants with a delay of 3 to 5 weeks, there were extreme cases in which the shoot was never formed, indicating a failure of transition from vegetative growth to reproductive growth. Despite the different degree of shoot bolting delay, all *pXPP:PMEI5* plants had massive rosettes formed with 2 to 3 times more leaves than in Col-0 (**Figure 15E, F**). During late developmental stages, some plants reached a final size that almost doubled the size of Col-0 (**Figure 15I**) and their rosette leaves and shoot turned purple, suggesting an over-accumulation of stress-related metabolites (**Figure 15G-I**). In addition, there was ectopic leaf formation along the shoots as well as defective phyllotaxis (**Figure 15J, K**). Such a severe phenotype regarding shoot formation led us to examine vascular tissue development in the shoot. Cross sections of the basal part of the first shoot formed in Col-0 and *pXPP:PMEI5* showed similar xylem tissue organization with slightly more vascular bundles and pith cells

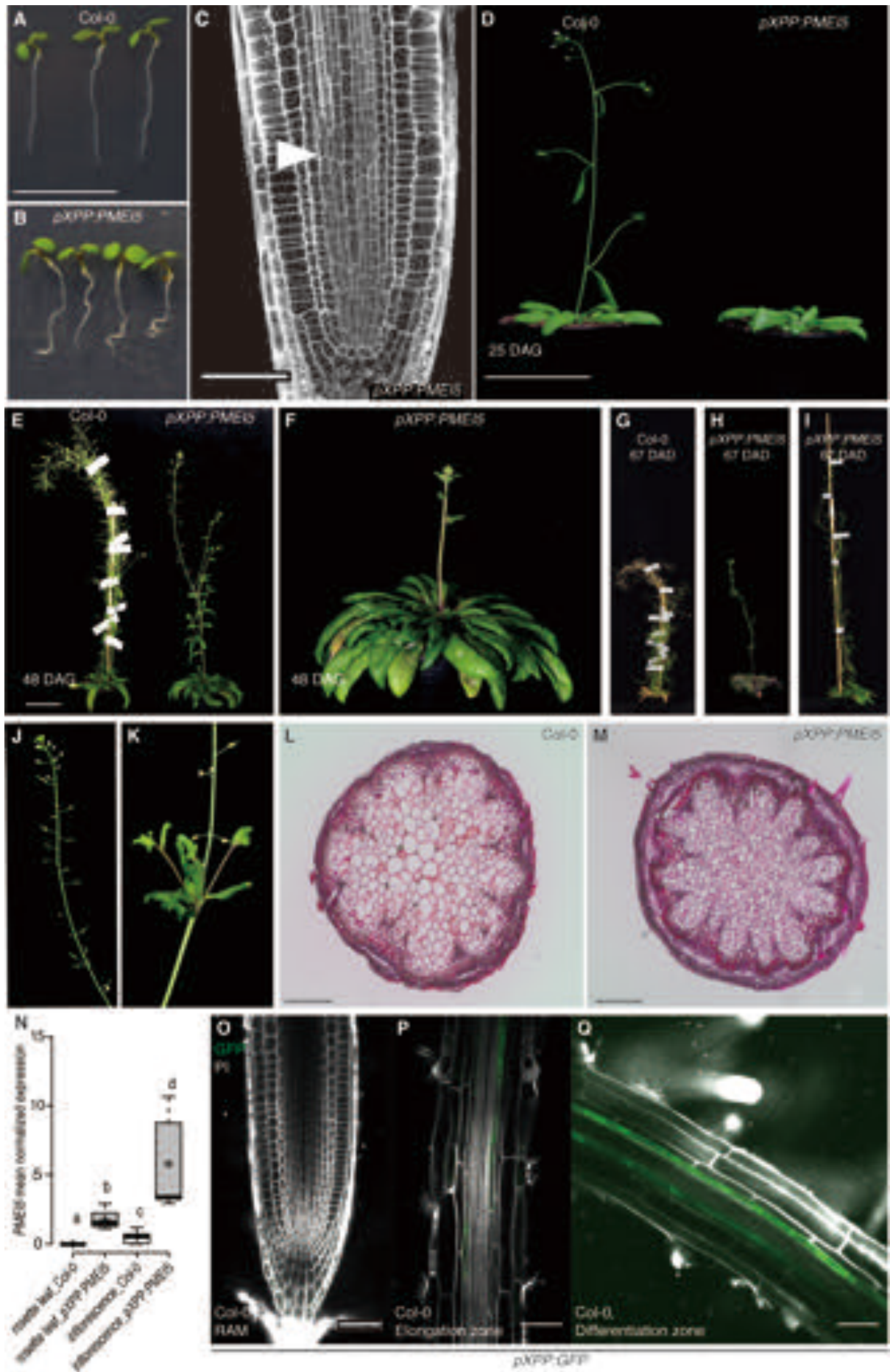


**Figure 15. Constitutive ectopic expression of *PMEI5* only in XPP cells (*pXPP:PMEI5*) triggered pleiotropic phenotypes.** (A, B) seedling root waving. (C) occasional random cell divisions in the stele. (D-I) delayed shoot bolting and over-grown rosette with (J, K) impaired phyllotaxis and lateral organ formation. (L, M) increased number of parenchyma cells in the shoot with reduced cell size as well as increased number of vascular bundles. (N) qRT-PCR analysis revealed over-expression of *PMEI5* in rosette leaves and at a higher level in the inflorescence. (O-Q) *pXPP:GFP* showing GFP expression in XPP cells starting only from elongation zone. Cells are counter-stained with PI in (C, O-Q). Bars = 1 cm in (A, B), =50  $\mu\text{m}$  in (C, O-Q), = 5 cm in (D, E), =100  $\mu\text{m}$  in (L, M). Statistically significant difference in *PMEI5* transcript level in (N) is revealed by ANOVA with n=3.

(parenchyma) observed in the latter (**Figure 15L, M**). qRT-PCR analysis of *PMEI5* expression in rosette leaves and inflorescence (tip of the inflorescence including flower buds and SAM) confirmed an over-expression of *PMEI5* in the transgenic line with the highest level in the reproductive organs (**Figure 15N**). Taken together, these results showed a clear responsiveness to cell wall perturbation in one specific cell type. The resulted phenotypes are pleiotropic, as in *PMElox*, but with distinguishable appearance suggesting a divergent regulatory mechanism of cell wall homeostasis maintenance in cell type-specific context. This intriguing observation led us to further investigate the responses to the loss of CWI in other cell types/tissues.

## 2.2. Triggering the loss of CWI in specific cell types/tissues with Dex-inducible system.

### 2.2.1. The cell type/tissue-specific dexamethasone-dependent cis-inducible system.

In order to express our gene of interest (*PMEI5*) in both spatial and temporal manner, we made use of the widely applied *pOp/LhG4* transcription activation system (Moore et al., 1997) in combination with different cell type/tissue-specific promoters (*promTS*). Moreover, besides the spatial characteristic of the system, we also introduced the temporal control by using a dexamethasone (Dex)-inducible derivative named *pOp6/GR-LhG4* (**Figure 16A**), which comprises the ligand-binding domain (LBD) of the rat glucocorticoid receptor (GR) in addition to LhG4, as well as an improved *pOp6* promoter with six copies of the lac operator sequence (Samalova et al., 2004). The induction system has been created in *cis* meaning that the activation element *GR-LhG4* transcription factor, the reporter element carrying the *pOp6* promoter and the gene of interest are in the same T-DNA cassette (**Figure 16A**). Thus, the inducible tissue-specific expression of our gene of interest can be triggered in the plant without the need of external intervention. In the absence of Dex, the GR-LhG4 is constantly produced in those cell types or tissues defined by the *promTS*. Upon Dex treatment, the corticosteroid binds to the GR ligand binding domain in the cytosol and the formed Dex-GR-LhGR complex translocates into the nucleus and binds in turn to the *pOp6* promoter, which initiates the transcription of *PMEI5* in the desired cell types/tissue (**Figure 16B**). However, it is always possible to add other *trans* reporter element simply by crossing with another reporter line. The constructs have been designed by

using the GreenGate cloning technique that has been developed within our institute (Lampropoulos et al., 2004).

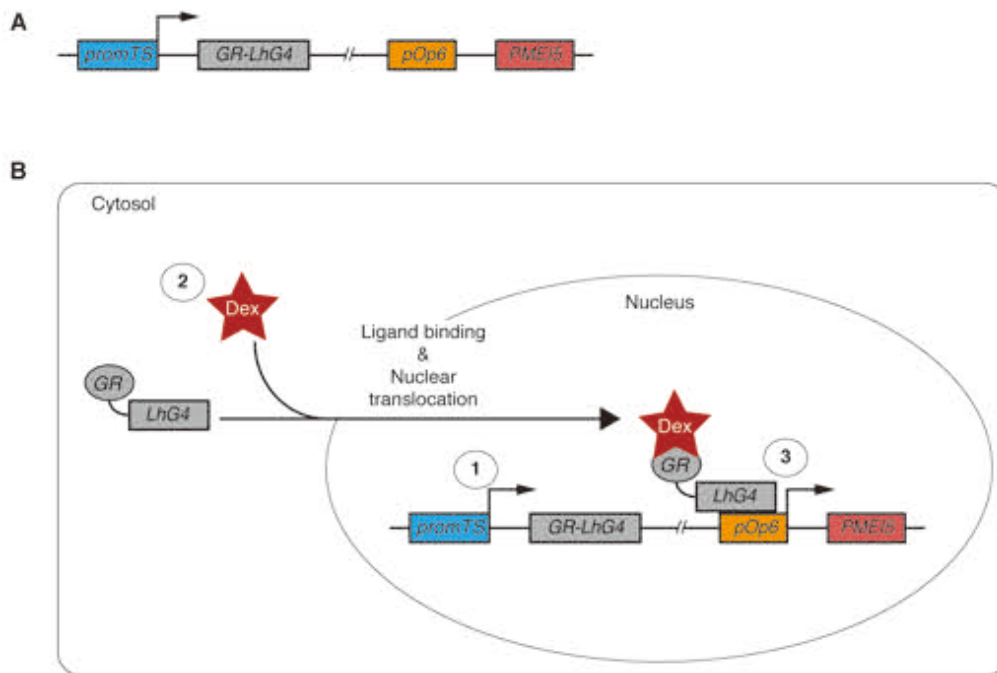


**Figure 16. Scheme of dexamethasone (Dex)-inducible system.** (A) The *cis* induction system: on the same T-DNA sequence are carried two expression cassettes. The first one comprises the cell type/tissue-specific promoter (*promTS*) and the chimeric transcription factor LhG4 fused to the ligand binding domain of the rat glucocorticoid receptor (GR); the second one consists of the *pOp6* promoter and the gene of interest (here illustrated as *PMEI5*). (B) The induction mechanism: ① the *promTS* constitutively drives expression of the *GR-LhG4*, which ② is located in the cytosol in the absence of Dex; upon Dex treatment, it binds to the GR ligand bind domain and together ③ translocates into the nucleus and binds to the *pOp6* promoter, which is activated and drives expression of the gene of interest (*PMEI5*).

### 2.2.2. Functional test of the cell type/tissue-specific Dex-inducible system (dose- and time-dependent induction).

It has been shown earlier in this study that constitutive cell type-specific and ubiquitous perturbation of cell wall in *pXPP:PMEI5* and *p35S:PMEI5*, respectively, resulted in dramatic growth phenotypes. We then sought to discover the responsiveness of other cell types/tissues upon loss of CWI. To do so, we established a dexamethasone (Dex)-inducible system to trigger the loss of CWI by expressing *PMEI5* ectopically under control of different cell type/tissue-specific promoters (Figure 16). This system allows expression of the gene of interest in desired tissues at different time points by simply introducing Dex into the growth condition. In order to confirm the functionality of our cell type/tissue-specific Dex-inducible system, we tested the induction efficiency and the specificity of expression domain in both dose- and time-dependent manner by using *pSCR>GR>mTurquoise2* line (Schürholz and Lopez-Salmeron et al., 2018), which is

supposed to show mTurquoise2 signal only in endodermal cells and QC. Indeed, induction with 0.1, 1, 10 and 100  $\mu\text{M}$  Dex in growth medium triggered clear expression of *mTurquoise2* in the QC, CEI and endodermis (**Figure 17A**). Quantification of fluorescence intensity indicated a constant strong expression level in the QC and CEI (**Figure 17C**) while in the endodermal cell file the expression level became stable when Dex concentration was higher than 1  $\mu\text{M}$  (**Figure 17D**). When induced on plate with 10  $\mu\text{M}$  for different duration, the mTurquoise2 signal was clearly visible only after 24 hours of induction, suggesting a minimum induction time frame (**Figure 17B, E**).

### 2.2.3. The promoters drove expression specifically to the expected cell types/tissues.

A groups of cell type/tissue-specific promoters have been used to drive *PMEI5* expression (**Table 1**). Reporter lines have been constructed with the same promoters driving expression of *mVenus* (*pTS>GR>SP-mVenus-HDEL*) or *3xGFP* (*pTS>GR>3xGFP-NLS*) to reveal the exact expression domain of selected promoters, since *PMEI5* protein activity is altered by commonly used tags. As shown in **Figure 18**, expression of mVenus or 3xGFP under *pTS* was as we expected. *pUBQ10*, used as control for ubiquitous expression of *PMEI5* as in *PMEIox* (*p35S:PMEI5*), showed GFP signal in all tissues of the root. Expression under *pML1* showed signal in epidermal cells in the RAM. *pCOBL9* and *pGL2* drove expression in trichoblasts and atrichoblasts respectively and the signal was observed in the early elongation/differentiation zone. Notably, *pCO2*-driven expression was found not in the entire cortex cell file as we expected but rather in the CEI and the few following cortex cells. *pCASP1* was specific to endodermal tissue also in the more differentiated part of the root. *pXPP* drove expression in XPP cells, which were found next to protoxylem cells that started to get lignified and form the typical ring structure. And *pRLP44* drove expression was found in the differentiated vascular tissue and in most of the tissues of the RAM with the highest level in the epidermis, LRC, and the vasculature in the mature part of the root, as described in [Holzwardt et al., 2018](#).

**Table 1. Cell type/tissue-specific promoters used for driving specific expression of *PMEI5*.**

Tissue-specific promoter	Locus	Expression domain in RAM
<i>pUBQ10</i>	AT4G05320	Ubiquitous
<i>pCOBL9</i>	AT5G49270	Trichoblast (root hair cell)
<i>pGL2</i>	AT1G79840	Atrichoblast (non root hair cell)
<i>pML1</i>	AT5G61960	Epidermis
<i>pCO2</i>	AT1G62500	Cortex
<i>pCASP1</i>	AT2G36100	Differentiating and mature endodermis
<i>pXPP</i>	AT4G30450	Xylem pole pericycle (XPP)
<i>pRLP44</i>	AT3G49750	Epidermis, LRC and vasculature

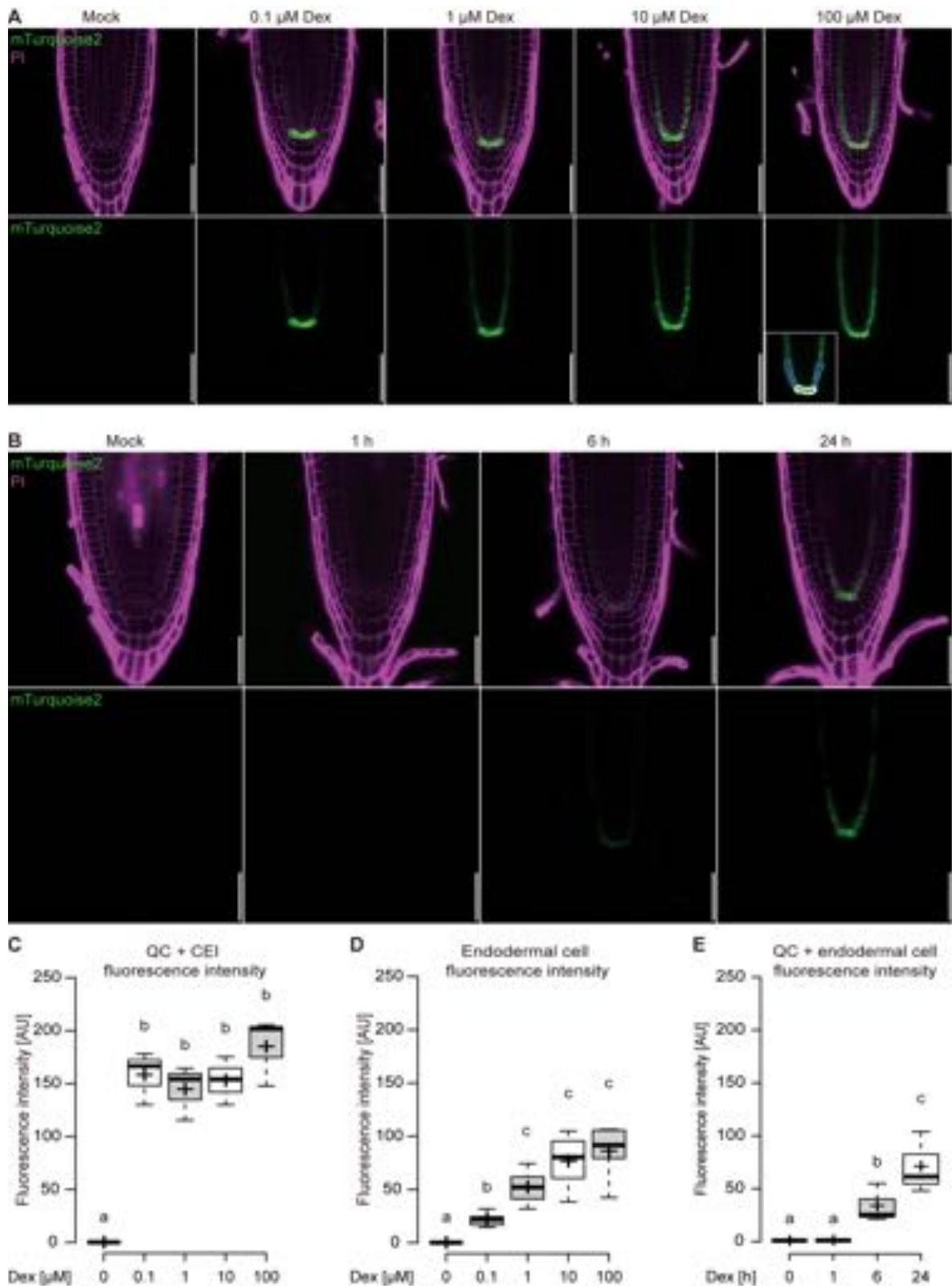


**Figure 17. Dose-dependent and time-course induction test of Dex-inducible system** (Schürholz and Lopez-Salmeron et al., 2018). **(A)** Transgenic line  $pSCR>GR>mTurquoise2$  was induced on plate with Dex concentrations at 0.1, 1, 10 and 100  $\mu\text{M}$  for dose-dependent expression and **(B)** with 10  $\mu\text{M}$  Dex for 1, 6 and 24 hours for time-course analysis. Cells are counter-stained with PI. Cells in which fluorescence signal has been quantified are shown in panel **(A)**, 2nd row right most image: cells marked in white = QC+CEI, in blue = endodermal cells. PI channel is false-coloured in magenta and mTurquoise2 in green. Bars = 50  $\mu\text{m}$ . **(C-E)** Quantification of fluorescence intensity after dose- and time-dependent induction. Statistically significant difference is revealed by ANOVA test with  $n = 3$ .

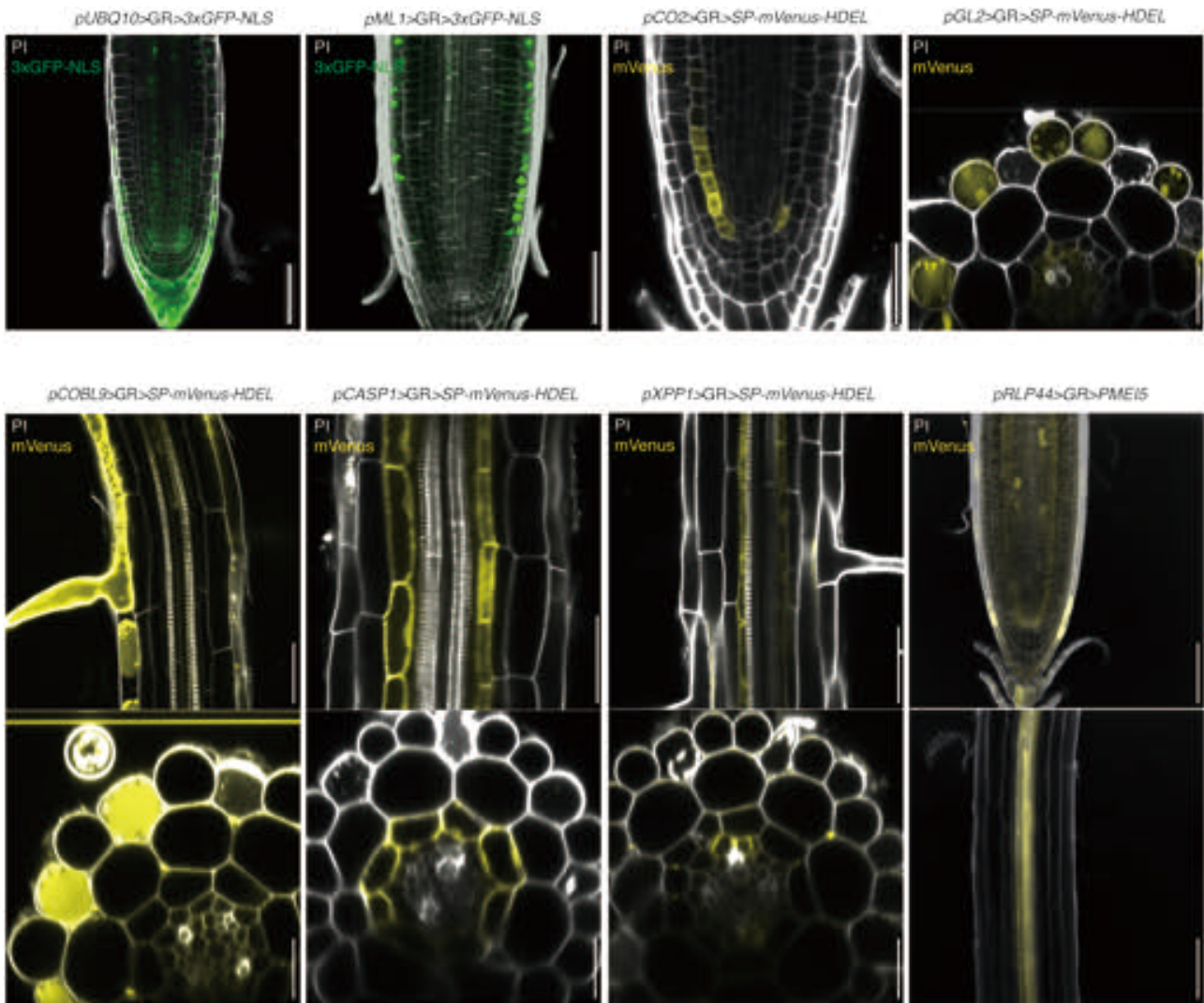


**Figure 18. Reporter lines showing expression domains mediated by different cell type/tissue-specific promoters.** Expression in epidermis under *pML1*, in the first few cortex cells following the CEI under *pCO2*, in trichoblast (root hair) cells under *pCOBL9* and atrichoblast (non root hair) cells under *pGL2*, in differentiating and mature endodermis under *pCASP1*, in xylem pole pericycle (XPP) cells under *pXPP*, and in most RAM tissues with highest expression in the vascular tissue under *pRLP44*. Cells are counter-stained with PI. Bars = 50  $\mu\text{m}$  in longitudinal images and = 20  $\mu\text{m}$  in cross sections.

#### 2.2.4. The cell type/tissue-specific Dex-inducible system triggered an increase of *PMEI5* expression.

To further confirm the induced expression driven by cell type/tissue-specific promoters, we determined the level of *PMEI5* transcript in different transgenic lines. qRT-PCR analysis revealed an increase of *PMEI5* expression in seedling roots when grown on plate containing 30  $\mu\text{M}$  Dex from germination to 5 DAG (**Figure 19**). *PMElox* showed a clearly higher expression of the transgene compared to Col-0 but the Dex treatment seemed to repress this over-expression yet it was still two orders of magnitude higher than Col-0. Although the expression was a bit leaky under *pUBQ10*, it had an increase of 22.6 folds compared to its control. Another highly induced *PMEI5* expression was found for *pCOBL9* with 153.3-fold increase relative to non-induced plants.

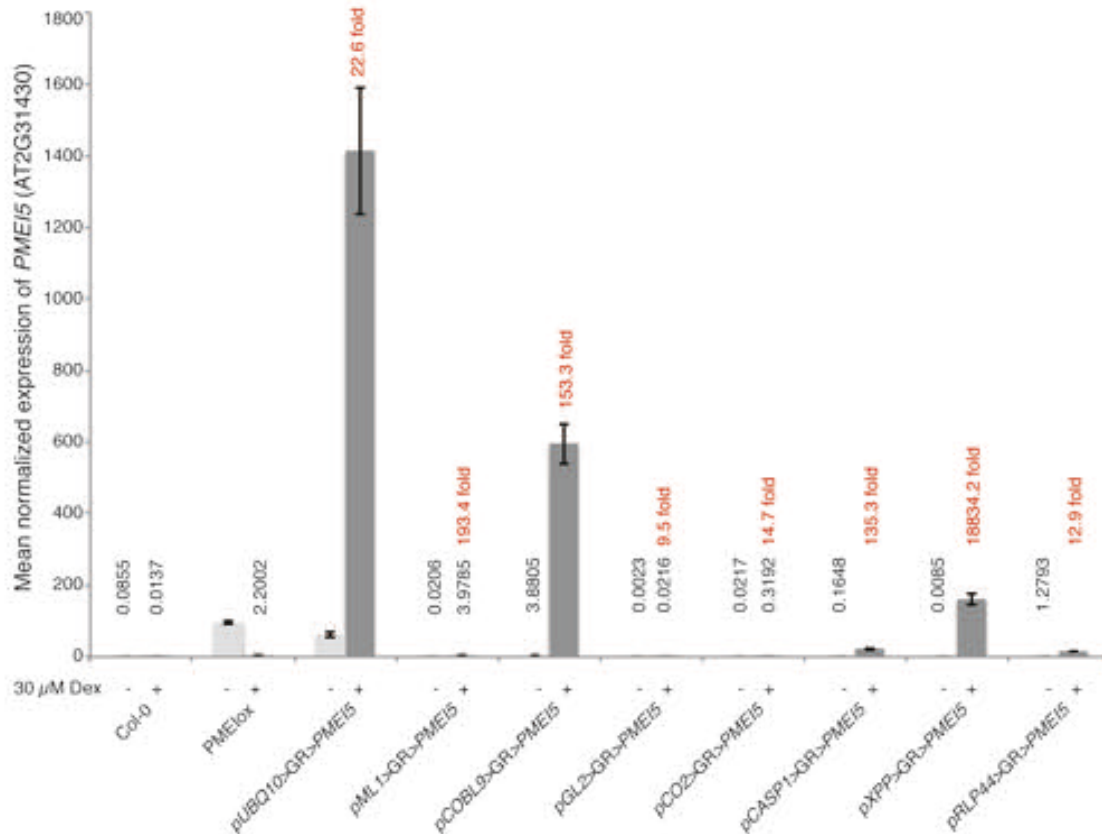


**Figure 19.** qRT-PCR analysis of *PME15* expression in 5 DAG seedling root of cell type/tissue-specific lines -/+ induction with 30  $\mu$ M Dex. Numbers in red indicate fold change between - Dex and + Dex within each line.

*pXPP* with expression in only a small subgroup of pericycle cells triggered the highest fold change (188342.2 folds) among all the lines. *pCASP1*- and *pRLP44*-driven expression of the transgene had a significant higher level compared to the non-induced one and Col-0 but still remained lower than the untreated PMElox. Even though the expression under *pCO2* was relatively low, which might be due to its restricted expression domain only in the first few cortex cells but nowhere else in the root (**Figure 18**), it still showed a 14.7-fold increase. To our surprise, *pML1* covering the entire epidermal tissue in the root showed limited expression level after induction and *pGL2*-driven expression was at a Col-0 comparable expression level. In summary, most lines showed a very low level of *PME15* expression when grown on plate without Dex, which was similar to Col-0, except for those under *pUBQ10* and *pCOBL9* that had some leaky expression from the promoter in the absence of Dex. When grown on plate supplied with 30  $\mu$ M Dex, most of the lines showed a significant increase in *PME15* transcript level. The surprising Dex-repressive effect on transgene effect observed in PMElox did not seem to interfere with cell type/tissue-specific expression.

### 2.3. Loss of CWI in specific cell types/tissues triggered diverse responses.

#### 2.3.1. Seedling root waving was triggered independently by expression of *PMEI5* in root hair cells, epidermis, or XPP cells.

As shown in **Figure 20**, root waving of *pUBQ10>GR>PMEI5* resembled that of *PMEIox* (**Figure 5A**). The similar root waving has also been seen in plants expressing *PMEI5* in the epidermis (*pML1>GR>PMEI5*) and trichoblast (*pCOBL9>GR>PMEI5*) but not in atrichoblast (*pGL2>GR>PMEI5*), which suggested a role of trichoblasts in maintaining root morphology. Similarly to *pXPP:PMEI5* that expressed *PMEI5* constitutively in XPP cells, *pXPP>GR>PMEI5* also exhibited root waving, which further corroborated an effective induction of the transgene and a potential influence of XPP cells on root growth regulation.

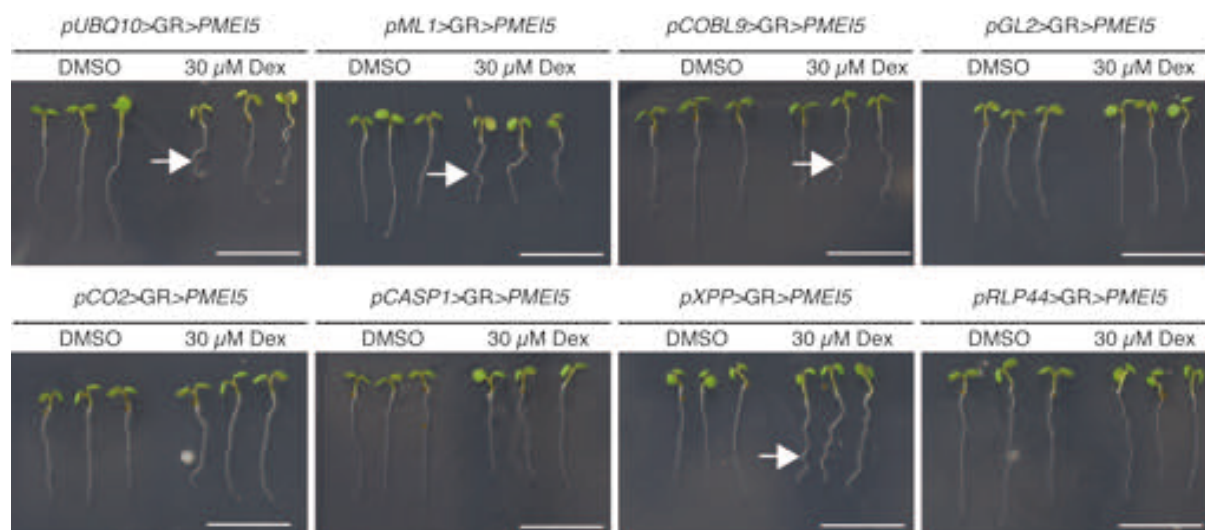


**Figure 20. Seedling root phenotype of cell type/tissue-specific lines at 5 DAG.** The root waving has been observed in *pUBQ10>GR>PMEI5*, *pML1>GR>PMEI5*, *pCOBL9>GR>PMEI5* and *pXPP>GR>PMEI5* lines (white arrows) when grown on plate containing 30  $\mu$ M Dex from germination to 5 DAG. Bars = 1 cm.

#### 2.3.2. Specific expression of *PMEI5* in different cell types/tissues triggered similar yet diverse directional growth phenotypes on soil.

When induced on soil, only *pCO2>GR>PMEI5* and *pXPP>GR>PMEI5* showed altered morphology already at rosette stage with long and narrow leaves for the former and a bit curled leaf shape for the latter (**Figure 21A**). At later stages, except for *pCASP1>GR>PMEI5*, which showed a Col-0 comparable overall plant morphology, all other lines showed impaired growth and/or malformation of certain organs (**Figure 21B**). *pUBQ10>GR>PMEI5* and *pML1>GR>PMEI5* were dwarfed on soil but the directional growth phenotype was impaired to a lesser degree when compared to *PMEIox* (**Figure 5B**). *pCOBL9>GR>PMEI5* and *pGL2>GR>PMEI5* both had a slight decrease in the root vertical growth and a more severe defect in lateral development. In addition, *pGL2>GR>PMEI5* showed organ fusion in leaves and silique petiole (**Figure 21E**).

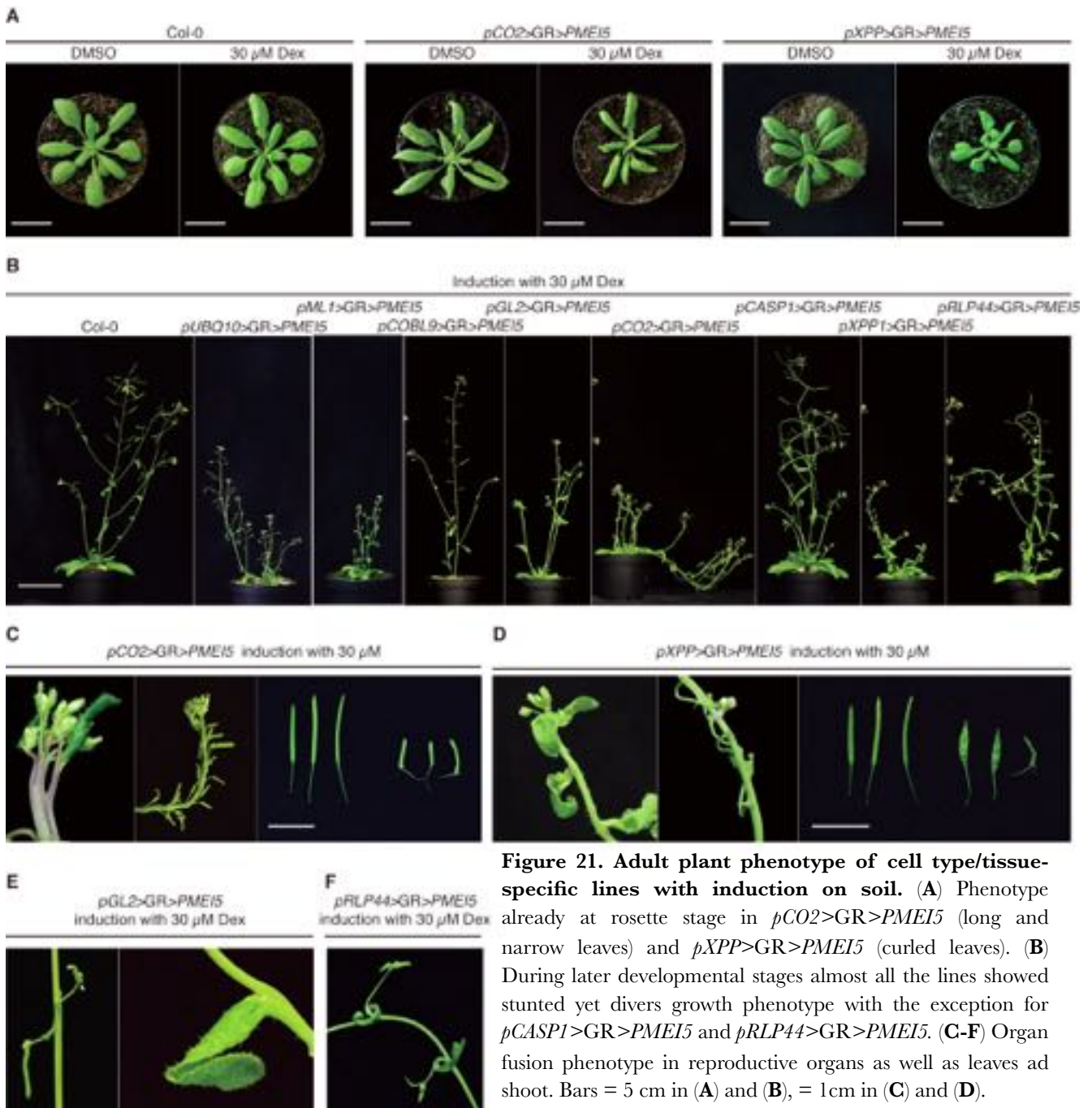


**Figure 21. Adult plant phenotype of cell type/tissue-specific lines with induction on soil. (A)** Phenotype already at rosette stage in  $pCO_2>GR>PMEI5$  (long and narrow leaves) and  $pXPP>GR>PMEI5$  (curled leaves). **(B)** During later developmental stages almost all the lines showed stunted yet divers growth phenotype with the exception for  $pCASPI1>GR>PMEI5$  and  $pRPL44>GR>PMEI5$ . **(C-F)** Organ fusion phenotype in reproductive organs as well as leaves ad shoot. Bars = 5 cm in **(A)** and **(B)**, = 1cm in **(C)** and **(D)**.

$pCO_2>GR>PMEI5$  plants seemed to be weakened in mechanical properties as shoots could not stay upright, and the reproductive organs showed fusion between flower buds and also between silique petiole and the shoot. Furthermore, siliques of  $pCO_2>GR>PMEI5$  were reduced to only half of WT size and had a flattened shape (**Figure 21C**).  $pXPP>GR>PMEI5$  had the most similar on-soil phenotype compared to  $PMEIox$  (**Figure 21B**) in terms of plant body size, leaf and floral organ fusion, shoot convolusion and silique morphology (**Figure 21D**). This observation strongly differed from that of  $pXPP:PMEI5$  plant on soil (**Figure 15D-K**), pointing to a potential influence of  $PMEI5$  expression level (or intensity) and duration on plant growth during distinct developmental stages.

The plants of *pRLP44>GR>PMEI5*, although looked normal in plant body size and morphology, still showed mild organ fusion in leaves and shoot (**Figure 21B, F**).

*2.3.3. Specific expression of PMEI5 in the beginning of cortex cell file was sufficient to provoke abnormal cell division and disrupted tissue patterning.*

At the tissue level, PMElox-like oblique cell walls have been observed in *pUBQ10>GR>PMEI5* and *pCO2>GR>PMEI5* primarily in outer tissues as epidermis, cortex and endodermis. Oblique cell walls also appeared in inner vascular tissues in *pCO2>GR>PMEI5* (**Figure 22A, B, I, J**, red arrow). In addition, *pCO2>GR>PMEI5* had a disrupted organization in the region of QC/SCN, where different cell types were hard to define based on standard RAM anatomy (**Figure 22J**, blue arrow). Besides, *pRLP44>GR>PMEI5* showed a slightly enlarged stele in the RAM with massive procambial cells (**Figure 22P**, white arrow head). The expression domain of the transgene under the promoter of *pUBQ10* and *pRLP44* correlated with the location of observed phenotypes in the RAM. In *pCO2>GR>PMEI5*, this connection was not as tight as in the other two lines but RAM cells with impaired organization or oblique cell walls have been either located very closely to the expression domain of *PMEI5* (**Figure 18**) or born through divisions of the cells located in this domain, respectively. These observations raised the possibility of both cell-autonomous and non cell-autonomous responses upon triggering of cell wall disruption.

*2.3.4. Expression of PMEI5 in the beginning of cortex cell file showed mild effect on root growth and RAM size.*

As described in **Figure 20**, *pCO2>GR>PMEI5* plants did not show any morphological defect in seedling root. In addition, primary root length measurement only revealed a slight decrease in root length with *PMEI5* expression in cortex cells (**Figure 23A**). Similarly, quantification of RAM cell number and RAM length only showed a very mild but opposite effect of *PMEI5* expression: there was a slight trend of decrease in cell number (**Figure 23B**) and an increase in RAM length (**Figure 23C**).

*2.3.5. Ectopic expression of PMEI5 triggered PMElox-comparable yet distinctive growth phenotypes.*

In light of diverse phenotypes observed in different transgenic lines, ectopic expression of *PMEI5* in distinct cell types/tissues did cause growth responses resembling those of PMElox such as root waving, oblique cell wall, reduced RAM and defective directional growth on soil (Overview of different phenotypes in **Table 2**). While the ubiquitous expression control *pUBQ10>GR>PMEI5* nicely phenocopied PMElox in all aspects, each of the cell type/tissue-specific lines shared only some phenotypes with PMElox, apart from *pCASP1>GR>PMEI5*, which drove expression of

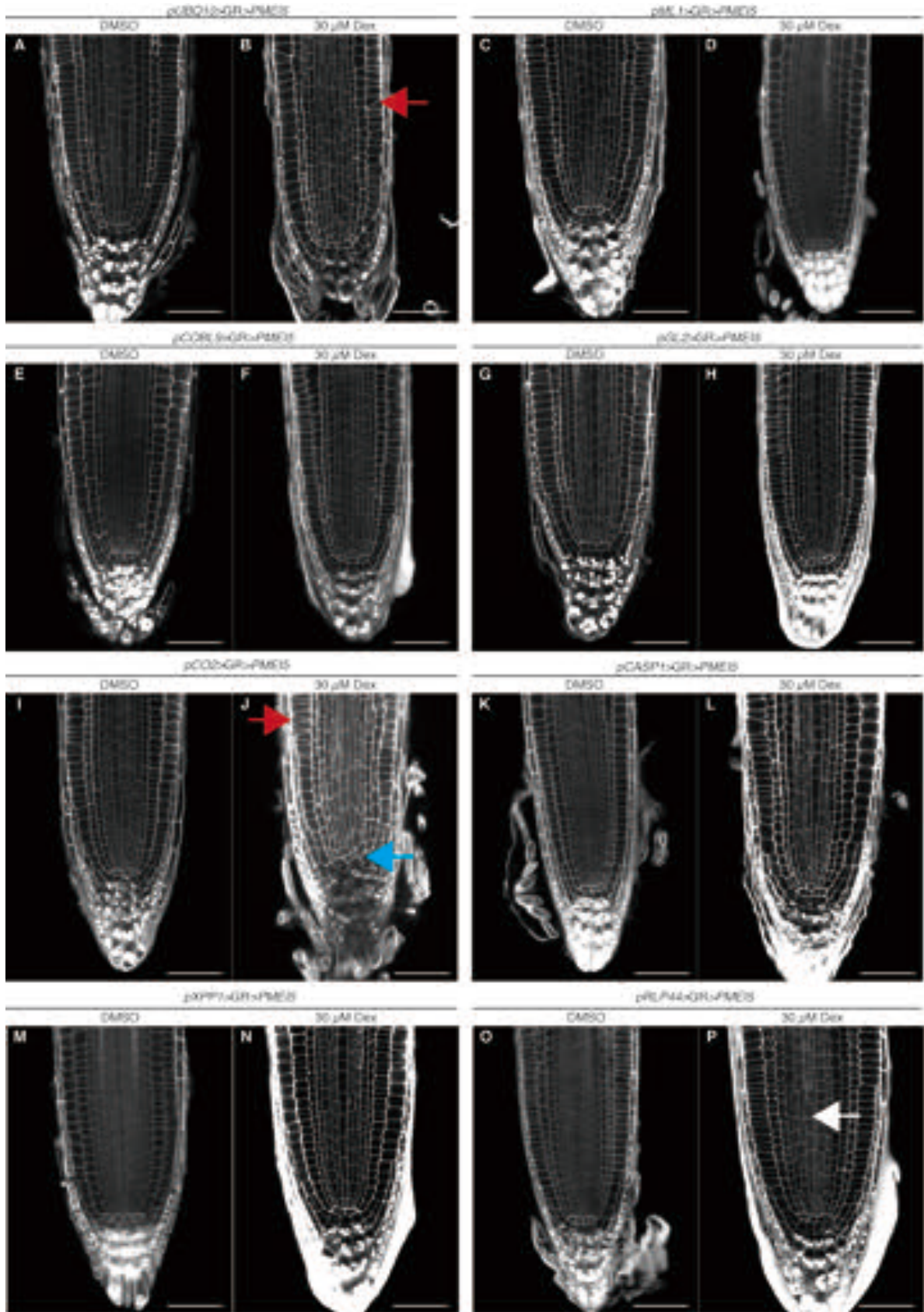


**Figure 22.** RAM tissue organization of cell type/tissue-specific lines in 5 DAG root grown on plate with 30  $\mu\text{M}$  Dex since germination (A-P). Oblique cell walls were observed in *pUBQ10>GR>PMEI5* (B) and *pCO2>GR>PMEI5* (J) plants (red arrows). The latter showed additionally a new phenotype as disruption in the QC/SCN region (J, blue arrow). The RAM of *pR1P44>GR>PMEI5* showed some slight enlargement of stele cell files (P, white arrow). Cells are counter-stained with PI. Bars = 50  $\mu\text{m}$ .

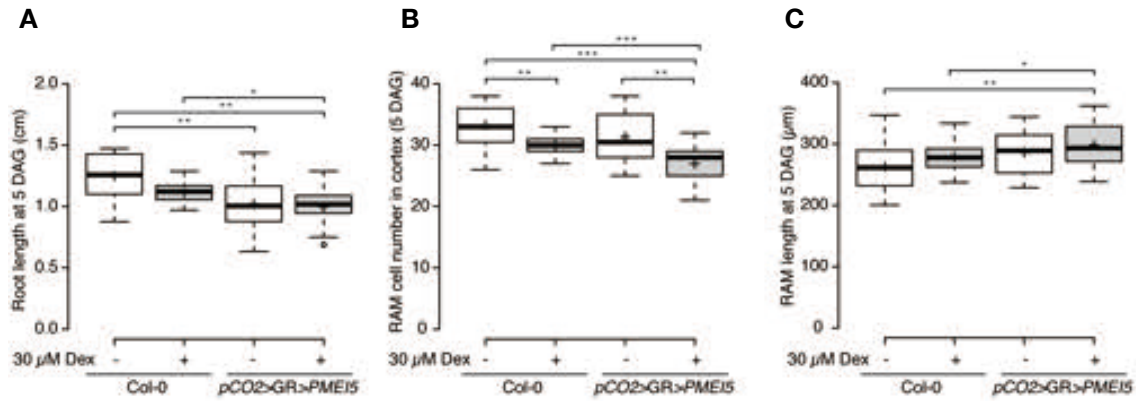


**Figure 23.** *PMEI5* expression in the beginning of cortex cell file (*pCO2>GR>PMEI5*) had mild effect on primary root and RAM growth. (A) Primary root length at 5 DAG. (B) Quantification of RAM cell number in the cortex cell file. (C) RAM length. n = 40 - 50. Asterisks indicate statistically significant difference revealed by a two-tail t-test with  $p < 0.05$  (\*),  $p < 0.01$  (\*\*), and  $p < 0.001$  (\*\*\*) .

**Table 2. Summary of morphological and tissue-level phenotypes observed in cell type/tissue-specific lines.** The row in red shows phenotypes observed in *PMEIox* and cells in blue shows the newly discovered phenotype that has not been observed in *PMEIox*.

Transgenic line	Expression domain	5 DAG seedling root phenotype				Adult plant phenotype
		Seedling root waving	Oblique cell wall	Reduced RAM	QC/SCN disruption	Organ fusion
<i>PMEIox (p35S:PMEI5)</i>	Ubiquitous	x	x	x		x
<i>pUBQ10&gt;GR&gt;PMEI5</i>	Ubiquitous	x	x	n/a		x (less severe than <i>PMEIox</i> )
<i>pCOBL9&gt;GR&gt;PMEI5</i>	Trichoblast	x		n/a		
<i>pGL2&gt;GR&gt;PMEI5</i>	Atrichoblast			n/a		x
<i>pML1&gt;GR&gt;PMEI5</i>	Epidermis	x		n/a		x
<i>pCO2&gt;GR&gt;PMEI5</i>	Beginning of cortex		x	x	x	x
<i>pCASP1&gt;GR&gt;PMEI5</i>	Differentiating and mature endodermis			n/a		
<i>pXPP1&gt;GR&gt;PMEI5</i>	Xylem pole pericycle	x		n/a		x ( <i>PMEIox</i> -like)
<i>pRPL44&gt;GR&gt;PMEI5</i>	Stele, epidermis, LRC			n/a		mild

*PMEI5* in endodermal cells starting from elongation/differentiation zone, did not show any impaired growth phenotype and thus can serve as negative control. It is noteworthy that expression under control of *pCASP1* starts late in the differentiation zone of the primary root. Very

interestingly, with a very restricted expression domain (**Figure 18**) and only a slight increase in *PMEI5* expression (**Figure 19**), *pCO2>GR>PMEI5* shared 3 out of 4 major phenotypes of *PMEIox* and showed an additional phenotype with a severe tissue organization defect in the QC/SCN region. These results strongly suggested that different cell types/tissues do respond to cell wall perturbation distinctively and the cell wall homeostasis as well as CWS might have essential functions in root growth and development at the tissue level.

**2.4. The oblique cell walls and QC/SCN disruption in *pCO2>GR>PMEI5* seemed to originate from abnormal cell divisions in cortex cells harbouring ectopic *PMEI5* expression.**

With *PMEI5* expression only in the beginning of the cortex cell file following the CEI, *pCO2>GR>PMEI5* not only showed *PMEIox*-like phenotypes but also the tissue patterning defect that has not been observed in any other lines. To confirm that the observed phenotypes in

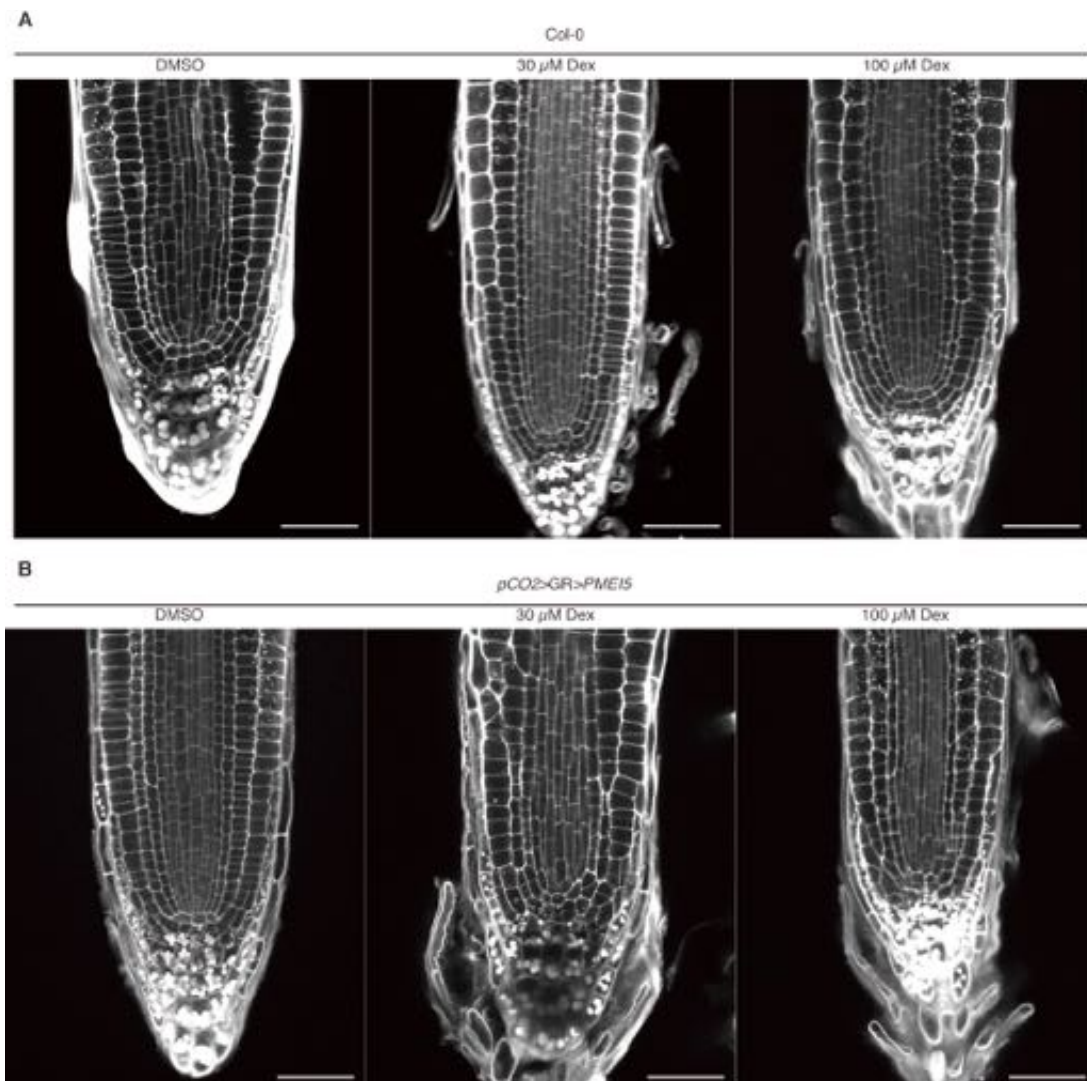


**Figure 24. Effect of dose-dependent induction on *pCO2>GR>PMEI5* RAM morphology.** Seedling grew on plates with DMSO, 30 μM and 100 μM Dex from germination to 5 DAG and were stained with PI. Higher concentration of Dex did not trigger more severe RAM phenotype in both (A) Col-0 and (B) *PMEIox*. Scale bar = 50 μm.

*pCO2>GR>PMEI5* root were constant with different induction conditions, and that we did not overlook any phenotype due to insufficient induction strength, we carried out dose-dependent induction test. The results suggested that Dex concentration at 30  $\mu$ M on plate was sufficient to trigger clear phenotypes and a concentration of Dex at 100  $\mu$ M did not provoke any further effect in either Col-0 roots (**Figure 24A**) or *pCO2>GR>PMEI5* (**Figure 24B**).

To investigate when, where and possibly how the oblique cell walls and the QC/SCN disruption happened in *pCO2>GR>PMEI5* root meristem, we performed time-course induction by transferring plants from control plate to induction plate containing 30  $\mu$ M Dex at 2, 3 and 4 DAG, which allowed an induction for 3, 2 and 1 day(s) respectively. All plants were stained and observed at 5 DAG. Induction starting at 2 and 3 DAG, meaning a duration of 3 and 2 days, provoked the previously described tissue organization disruption phenotype with irregular cell divisions that perturbed the predicted tissue patterning. This area of disruption included almost all

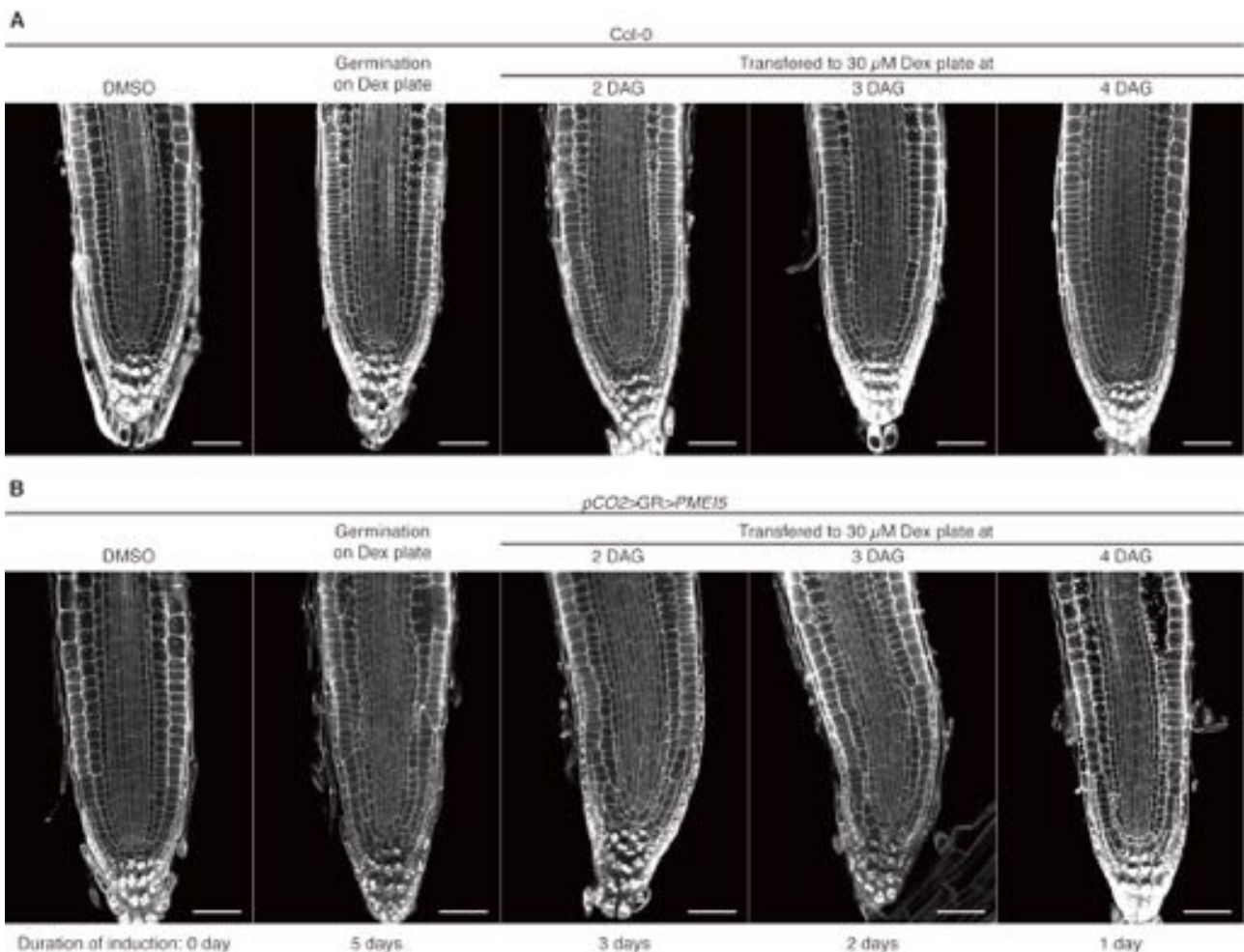


**Figure 25. Effect of time-dependent induction on *pCO2>GR>PMEI5* RAM morphology.** Seedlings germinated on plate without Dex and were then transferred to plate with 30  $\mu$ M Dex at 2, 3 and 4 DAG. All roots were stained with PI at 5 DAG. (A) Different induction conditions did not cause any phenotype in Col-0. (B) Induction starting from 2 and 3 DAG resulted in a rather local disruption of cells around the expression domain of *pCO2* and did not provoke any clear oblique cell wall in the upper part of the RAM; induction at 4 DAG was not sufficient to cause the above-mentioned RAM phenotypes. Bars = 50  $\mu$ m.

types of cells (QC, initial cells and the first few cells of epidermis, cortex, endodermis and stele) that were surrounding the expression domain of *pCO2* (**Figure 25B**). These results indicated that loosening CWI post-embryonically in mitotically active meristem cells could affect local tissue organization probably via ectopic cell divisions. Whether the ectopic cell division and the resulting disruption in tissue organization were the consequences of an imbalanced mechanical strength caused by cell wall perturbation or due to the loss of positional information remained mysterious. The oblique cell walls observed in epidermis and ground tissue of the upper meristem zone when induced for 5 days were much less present when induced for 3 and 2 days. When induction lasted for only 1 day, neither phenotype was observed.

## ***2.5. Mechanical imbalance between different tissues was not likely to be responsible for the defective root morphology, cell division and tissue patterning.***

### *2.5.1. Re-establishing the balance of cell wall mechanical properties between neighbouring tissues did not rescue the root waving phenotype.*

Previously (§2.3.2, **Figure 20**), seedling root waving has been observed in *pCOBL9>GR>PMEI5* (expression in trichoblast) and *pML1>GR>PMEI5* (expression in the entire epidermis), but not in *pGL2>GR>PMEI5* (expression in atrichoblast). This suggested a role of trichoblasts specifically but not the imbalanced in mechanical properties of the two adjacent epidermal cell layers in root morphology, as *PMEI5* expression in *pML1>GR>PMEI5* triggered the loss of CWI in both trichoblasts and atrichoblasts and thus should provide a balanced mechanical strength between these two cell types in epidermis. To further test this hypothesis, we re-established such a balance by crossing *pCOBL9>GR>PMEI5* with *pGL2>GR>PMEI5*. Since all the transgenic lines carried the resistance cassette to the same antibiotic, we could only observe the F1 plants of the cross (**Figure 26**). In order to make sure that one single copy of transgene was enough to provoke the phenotype, we crossed *pUBQ10>GR>PMEI5*, *pCOBL9>GR>PMEI5* and *pXPP>GR>PMEI5* with Col-0. Both F1 of *pUBQ10>GR>PMEI5* Col-0 and *pCOBL9>GR>PMEI5* Col-0 showed similar root waving on plate as seen in its relative stable homozygous lines, whereas F1 plants of *pXPP>GR>PMEI5* Col-0 were not able to reproduce the same phenotype (**Figure 26A**). Re-establishing the balance of cell wall mechanical properties in the epidermis by crossing *pCOBL9>GR>PMEI5* with *pGL2>GR>PMEI5* mimicks the epidermal expression pattern of *pML1>GR>PMEI5* line but only in the differentiated part of the root, and the F1 plants were not able to suppress the root waving (**Figure 26B, left panel**), suggesting again a role of trichoblasts but not the mechanical balance within epidermis in maintenance of root morphology. The ‘negative control’ *pCASP1>GR>PMEI5*, when crossed with *pCOBL9>GR>PMEI5*, did not suppress the root waving (**Figure 26B, middle and right panel**). F1 plants from the cross between *pUBQ10>GR>PMEI5* and *pCASP1>GR>PMEI5* also showed root waving, ruling out the possibility that the incapability of *pCASP1>GR>PMEI5* to suppress the root waving is due its non-

overlapping *PMEI5* expression domain with *pCOBL9>GR>PMEI5*. In addition, the PMElox-like

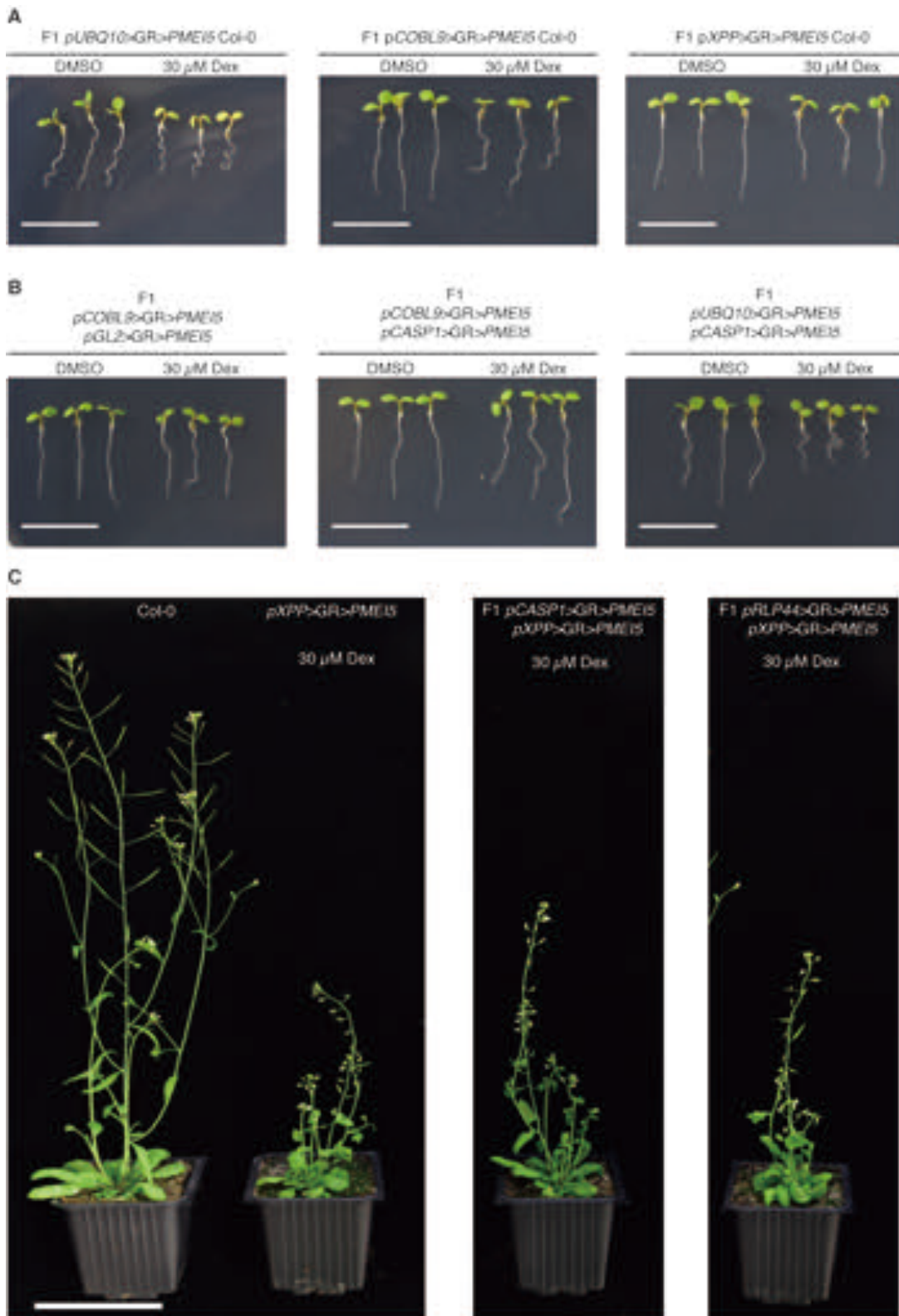


**Figure 26. Crosses between different cell type/tissue-specific lines.** (A) A single copy of *PMEI5* transgene expressed either ubiquitously or in trichoblasts was sufficient to induce the root waving, which was not the case when expressed in XPP cells. (B) F1 plants of crosses between different cell type/tissue-specific lines grown on plate with 30  $\mu$ M Dex from germination to 5 DAG. (C) F1 plants of the same crosses induced on soil. Bars = 1 cm in (A, B), = 7 cm in (C).

phenotype of  $pXPP>GR>PMEI5$  on soil was, unlike on plate, largely maintained even with only one copy of the transgene (**Figure 26C**). Introduction of  $PMEI5$  expression into differentiating and mature endodermis ( $pCASP1>GR>PMEI5$ ) or vascular tissue ( $pRLP44>GR>PMEI5$ ) did not alleviate the directional growth defect (**Figure 26C, middle and right panel**), indicating a differential regulation in above-ground tissue growth.

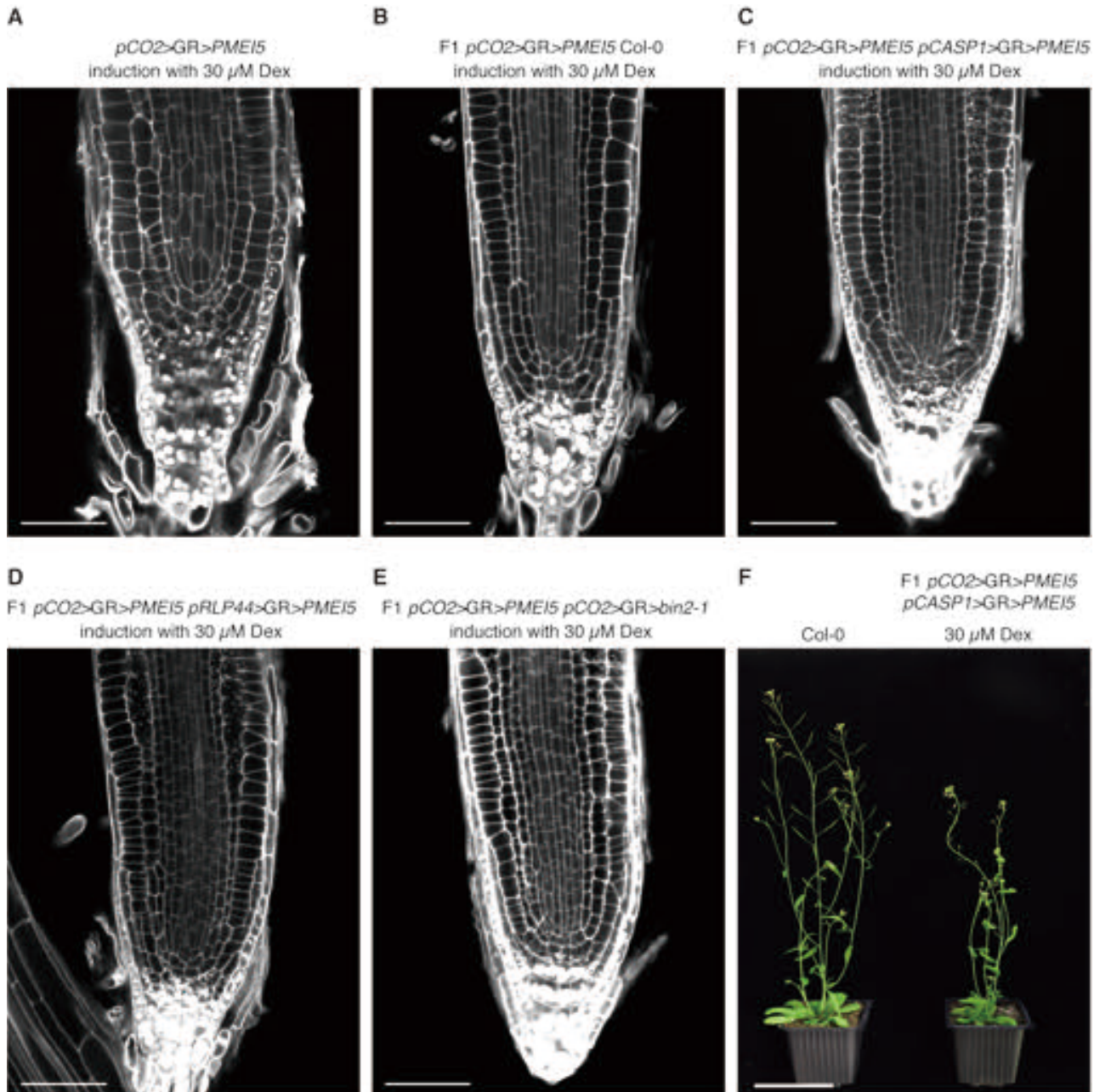


**Figure 27. Re-establishing the mechanical balance around the beginning of cortex did not rescue the tissue patterning defect.** (A) The oblique cell walls and the QC/SCN disruption in  $pCO2>GR>PMEI5$  were also present in (B) plant containing only one copy of  $PMEI5$  transgene. (C) Complementary expression of  $PMEI5$  introduced into differentiating and mature endodermis by crossing with  $pCASP1>GR>PMEI5$  and (D) into cells surrounding the beginning of cortex cell file by crossing with  $pRLP44>GR>PMEI5$  did not ameliorate the phenotype. (E) Expression of  $bin2-1$  under the  $pCO2$  however partially alleviated the QC/SNC disruption. (F) When grown on soil  $pCASP1>GR>PMEI5$  rescued to some extent the above-ground directional growth phenotype in  $pCO2>GR>PMEI5$ . Cells are counter-stained with PI. Bars = 50  $\mu$ m in (A-E), = 7 cm in (F).

### 2.5.2. Re-establishing the balance of cell wall mechanical properties in cells surrounding the beginning of the cortex file did not alleviate the QC/SCN disruption.

F1 plants of the cross between *pCO2>GR>PMEI5* and Col-0 still had oblique cell walls and the QC/SCN disruption in the RAM (**Figure 27A, B**), indicating that a single copy of *PMEI5* gene expressed under *pCO2* was sufficient to provoke the phenotypes. Again, the cross between *pCO2>GR>PMEI5* and *pCASP1>GR>PMEI5* could not suppress these phenotypes (**Figure 27C**), which was expected since the *PMEI5* expression domain under *pCASP1* was relatively far away from the proximal meristem (**Figure 18**). It is then plausible to re-establish the mechanical balance between the beginning of cortex and the neighbouring cells. To do so, we performed a cross between *pCO2>GR>PMEI5* and *pRLP44>GR>PMEI5*, the expression domain in the latter covers most of the cell types in the proximal meristem except the columella cells. Contrary to our expectations, the F1 plants did not show ameliorations of the oblique cell wall and the disruption in the SCN/QC (**Figure 27D**). On the other hand, the relatively low expression level of *PMEI5* under control of *RLP44* promoter, as revealed by qRT-PCR analysis, might suggest an insufficient activity of *PMEI5* leading to the failure in phenotype suppression. However, there was a partial suppression of *pCO2>GR>PMEI5* phenotype on soil by *pCASP1>GR>PMEI5*, which could be explained by their overlapping expression domain of *PMEI5* as well as a distinct regulatory mechanism in the above-ground tissues (**Figure 27F**). Interestingly, expressing a constitutively active version of BIN2 (AT4G18710), a negative regulator of BR signalling pathway, under *pCO2* and in the *pCO2>GR>PMEI5* background seemingly alleviated the QC/SCN disruption (**Figure 27E**), suggesting that *pCO2>GR>PMEI5* effects are at least partially BR signalling-dependent.

### 2.6. Cell identity specification in *pCO2>GR>PMEI5*.

As demonstrated in *PMElox* and *pXPP:PMEI5*, cell wall properties might directly or indirectly influence on cell identity specification and perturbing the wall in a given cell type or tissue gave rise to a severe phenotype in the whole plant (§1.4.2, **Figure 13A-D**; §2.1, **Figure 15**). Besides, it is likely that hormonal signalling pathways having crosstalks with BR, especially those of cytokinins and auxin, intervene in the regulation of tissue patterning in the root (§1.4.1, **Figure 12A**). Therefore, we investigated the cell identity specification and auxin response and signalling in the proximal meristem with the aim of gathering more insight into the disturbed tissue patterning phenotype observed in *pCO2>GR>PMEI5* (**Figure 21J**). Interestingly, two cell identity markers revealed changes in the QC. In the *pIAA19:4xYFP* line (Marquès-Bueno et al., 2016) the YFP signal marked specifically the developing protoxylem in the stele. In the meristem of *pCO2>GR>PMEI5* the signal was observed additionally in the QC cells (**Figure 28A**). Contrarily, the enhancer-trap line Q0990 that marked procambial cells in the stele and the QC lost GFP signal in the QC of *pCO2>GR>PMEI5* meristem (**Figure 28B**). Observation with these two marker

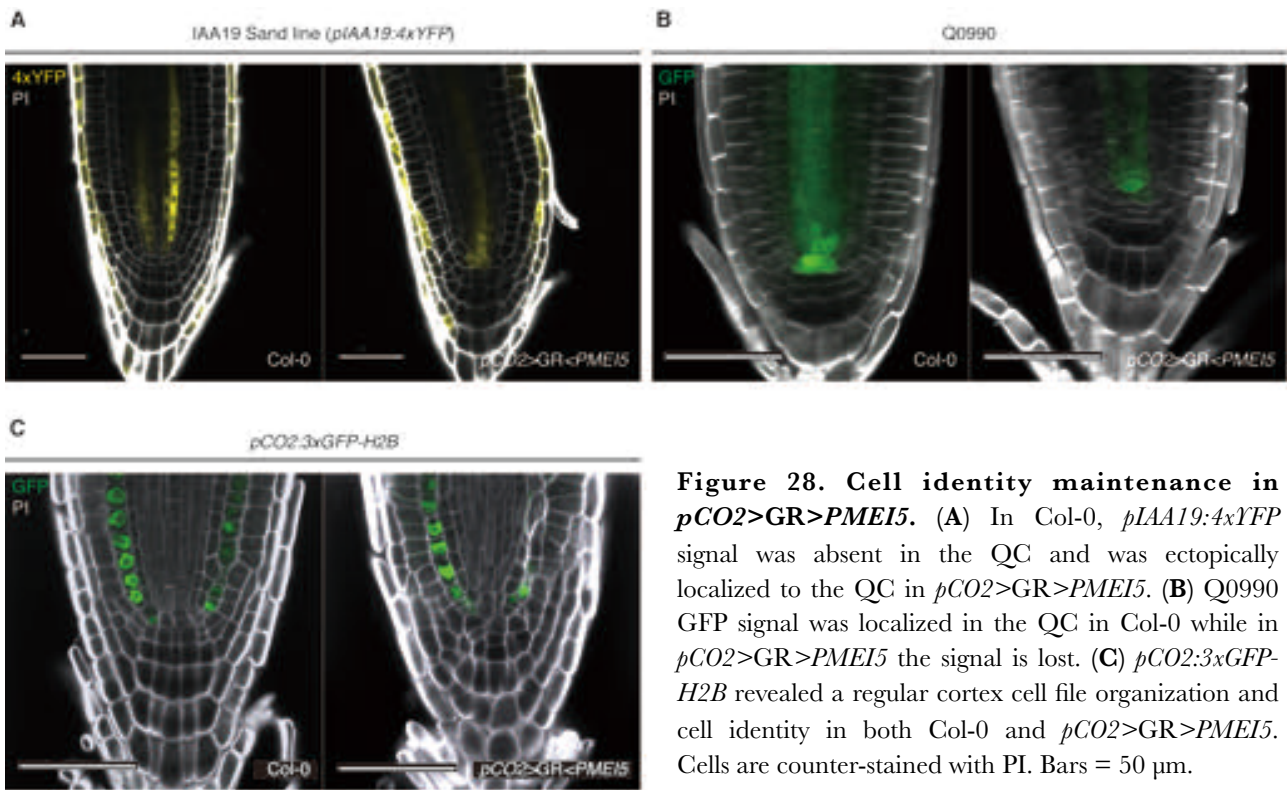


**Figure 28. Cell identity maintenance in  $pCO2>GR>PMEI5$ .** (A) In Col-0,  $pIAA19:4xYFP$  signal was absent in the QC and was ectopically localized to the QC in  $pCO2>GR>PMEI5$ . (B) Q0990 GFP signal was localized in the QC in Col-0 while in  $pCO2>GR>PMEI5$  the signal is lost. (C)  $pCO2:3xGFP-H2B$  revealed a regular cortex cell file organization and cell identity in both Col-0 and  $pCO2>GR>PMEI5$ . Cells are counter-stained with PI. Bars = 50 µm.

lines thus provided evidence for the loss of QC cell identity. Interestingly, the cortex cell identity was maintained without any ectopic cell division or cell file duplication in the cortex (**Figure 28C**).

As mentioned in §1.3.1, the formation of auxin gradient in the proximal meristem along the longitudinal axis is essential for the maintenance of cell differentiation and tissue patterning (Bielach et al., 2012). Around the QC are formed auxin maxima, which determine the SCN position. Auxin also regulates the gradual distribution of AP2-domain transcription factor PLTs that are required for maintaining SCN. In addition, PLTs regulate auxin efflux PINs, which forms a feed-forward loop for SCN position maintenance (Aida et al., 2004; Galinha et al., 2007; Vanneste and Friml, 2009; Liu et al., 2017). Thus, investigation of auxin distribution and auxin-dependent responses in the proximal meristem region could help to better understand the formation of a disrupted QC/SCN in  $pCO2>GR>PMEI5$  root. In this study, we used the recently developed auxin-input marker R2D2 (ratiometric version of 2 D2's, Liao et al., 2015) to assess the auxin response in the RAM. The R2D2 marker combines the Venus-tagged AUX/IAA degradation domain II (DII::n3xVenus) and the ntdTomato-tagged- mutated undegradable domain II (mDII::ntdTomato). The latter can not be degraded upon auxin accumulation (Liao et al., 2015), in comparison to which the sites of auxin promoted-AUX/IAA degradation can be revealed. In addition, the mDII::ntdTomato can also serve as reporter for auxin accumulation that does not lead to gene regulation. Both reporters are driven by RPS5A promoter allowing its expression in dividing cells. In brief, auxin accumulation is evidenced as a reduced DII::n3xVenus signal (in yellow) relative to the mDII::ntdTomato (in red) (Liao et al., 2015). In Col-0, auxin input had its peak in the SCN as shown by the absence of DII::n3xVenus signal (in yellow), in comparison to a stable level of mDII::ntdTomato (in red) signal in this area (**Figure 29A, white circle**). In  $pCO2>GR>PMEI5$ , the

DII::n3xVenus (in yellow) signal was also absent in the SCN/QC and was clearly reduced in the rest of the RAM relative to the mDII::ntdTomato signal (in red) (**Figure 28C**). These results indicate that in *pCO2>GR>PMEI5* root tip auxin was maintained at a similar level in the SCN/QC when compared to Col-0, but the overall auxin level was enriched in the RAM. As R2D2 reporter nicely revealed auxin levels in dividing cells, we exploited another widely used reporter *pDR5v2::n3xmTurquoise* (Liao et al., 2015). The synthetic promoter *DR5v2* contains AuxREs with high ARF-binding affinity and marks the sites of transcriptional auxin responses in the proximal meristem that are referred to as ‘auxin response maxima’ (Grieneisen et al., 2007; Liao et al., 2015; Liu et al., 2017). In line with the literature, auxin responses peaked in the QC and the SCN, and gradually fell down along the columella cell layers (**Figure 29B**). In *pCO2>GR>PMEI5* root, this gradient was altered: auxin responses still showed the peak in the SCN, but with a slight decrease, and the region harbouring this peak was broader along the proximo-distal axis than in Col-0 (**Figure 29D**). This more diffused pattern of auxin maximum in the QC also indicated a loss

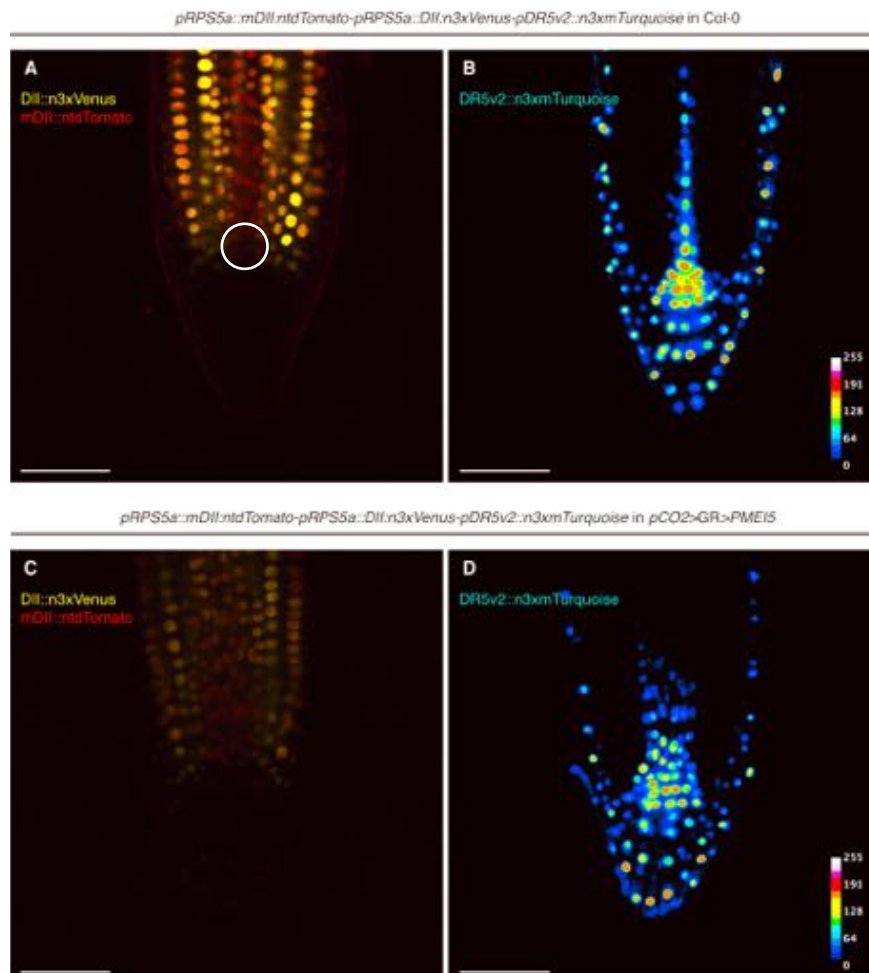


**Figure 29. Auxin level and responses are disrupted in *pCO2>GR>PMEI5*.** (A) R2D2 expression in Col-0 showed a high auxin level and (B) a gradient of auxin maxima in the QC/SCN illustrated by DR5v2 reporter. (C) In *pCO2>GR>PMEI5*, the decreased DII::n3xVenus signal revealed an enrichment of auxin in the meristem but (D) the auxin-dependent transcriptional responses seemed to be reduced suggesting a loss of stem cell quiescence. Bars = 50  $\mu$ m.

of quiescent center cell identity, as auxin maximin in the QC is thought to be involved in maintaining the quiescence of those cells (Bielach et al., 2012). Together with the evidence suggesting the loss of QC identity in *pCO2>GR>PMEI5*, the altered auxin maxima gradient in the QC/SCN region might be causative for the disrupted SCN position.

### ***2.7. RLP44- and BRI1-dependent but BRs-independent mechanisms seemed to be involved in the responses to loss of CWI in cell type/tissue-specific context.***

Upon loss of CWI in the whole plant, changes in the wall can be sensed by the membrane-residing RLP44 which through interaction with BRI1 activates the BR signalling pathway to trigger compensatory responses and allows the survival of the plants (Wolf et al., 2012b; **Figure 4**). However, whether the same compensatory regulation also the core mechanism in the responses to cell type/tissue-specific cell wall perturbation is the question awaiting its answer. To elucidate the involvement of RLP44 and the RLP44- and BR1-mediated CWS, we introduced separately *rlp44<sup>cnu2</sup>* and *bri1<sup>cnu4</sup>* mutations, both have been discovered as capable of PMElox phenotype suppression (Wolf et al., 2014; Holzward et al., unpublished), into different transgenic lines to turn of the signalling pathway at different levels.

#### ***2.7.1. RLP44- and BRI1-mediated signalling pathway had different effect on root and above-ground tissue growth in pXPP:PMEI5.***

In addition to *rlp44<sup>cnu2</sup>* and *bri1<sup>cnu4</sup>*, another suppressor of PMElox — *bri1<sup>cnu1</sup>* (Wolf et al., 2012b) has been crossed into *pXPP:PMEI5*. On plate, *bri1<sup>cnu1</sup>* suppressed the root waving, which was also much alleviated by *rlp44<sup>cnu2</sup>* (**Figure 30A, B, D**) but not by *bri1<sup>cnu4</sup>* (**Figure 30C**). When grown on soil, *bri1<sup>cnu1</sup>* not only suppressed the delayed shoot bolting and other growth phenotypes (**Figure 15D-K**), but also showed a typical BR-deficient phenotype as in *bri1<sup>cnu1</sup>* mutant alone (**Figure 30E**; Wolf et al., 2012b). In contrast, *pXPP:PMEI5* phenotypes have been rescued to a Col-0 comparable level by *bri1<sup>cnu4</sup>* and to a lesser extent by *rlp44<sup>cnu2</sup>* (**Figure 30F, G**). Although mutated in the same protein, the phenotypes of *bri1<sup>cnu1</sup>* and *bri1<sup>cnu4</sup>* were not in complete accord. While *bri1<sup>cnu1</sup>* carried a mutation in the kinase domain and behaved as a typical BR-deficient mutant, *bri1<sup>cnu4</sup>* with a mutation in the extracellular domain did not show strong BR signalling-related defects and its BL sensitivity as well as its protein accumulation and subcellular localization remained very similar to WT (Holzward et al., unpublished). Taken together, these results suggested that the responses to cell wall perturbation in XPP cells of *pXPP:PMEI5* are very likely to be mediated by RLP44-BRI1 signalling.

#### ***2.7.2. Cell type/tissue-specific expression of PMEI5 might not have altered BR signalling.***

To gather more information about the involvement of BR signalling in the responses to loss of CWI in cell type/tissue-specific context, we analyzed the transcript level of a standard BR

signalling target gene *IAA19* (AT3G15540) by qRT-PCR (Sun et al., 2010). In contrast to an elevated transcript level in *PME1ox*, all cell type/tissue-specific lines showed a similar level to

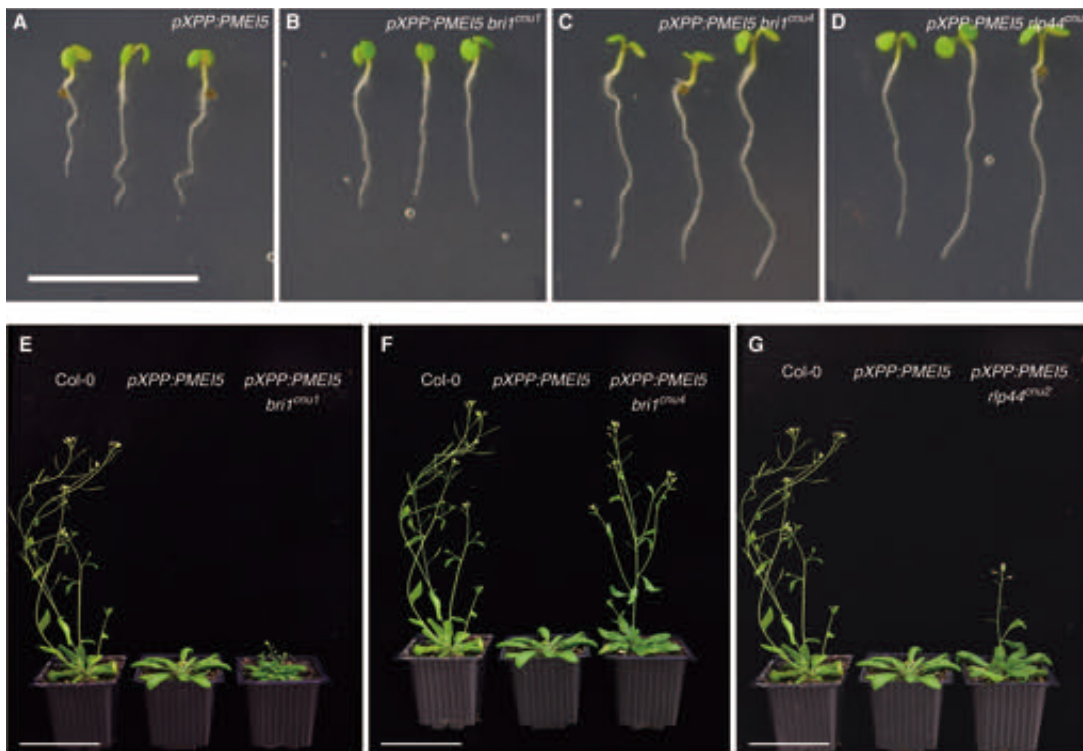


**Figure 30. Suppression of *pXPP:PMEI5* phenotypes by *bri1<sup>enu1</sup>*, *rlp44<sup>enu2</sup>* and *bri1<sup>enu4</sup>*.** (A-D) Seedling root waving was successfully suppressed by *bri1<sup>enu1</sup>*, alleviated by *rlp44<sup>enu2</sup>* and still persisted in the *bri1<sup>enu4</sup>* mutant background. (E) *bri1<sup>enu1</sup>* also suppressed the pleiotropic phenotype of *pXPP:PMEI5* adult plant and showed a typical BR-deficient phenotype. (F) *bri1<sup>enu4</sup>* also rescued *pXPP:PMEI5* adult plant phenotype to a Col-0 comparable level. (G) *rlp44<sup>enu2</sup>* rescued the massive rosette phenotype in *pXPP:PMEI5* but still showed a delay in shoot bolting. Bars = 1 cm in (A-D), = 7 cm in (E-G).

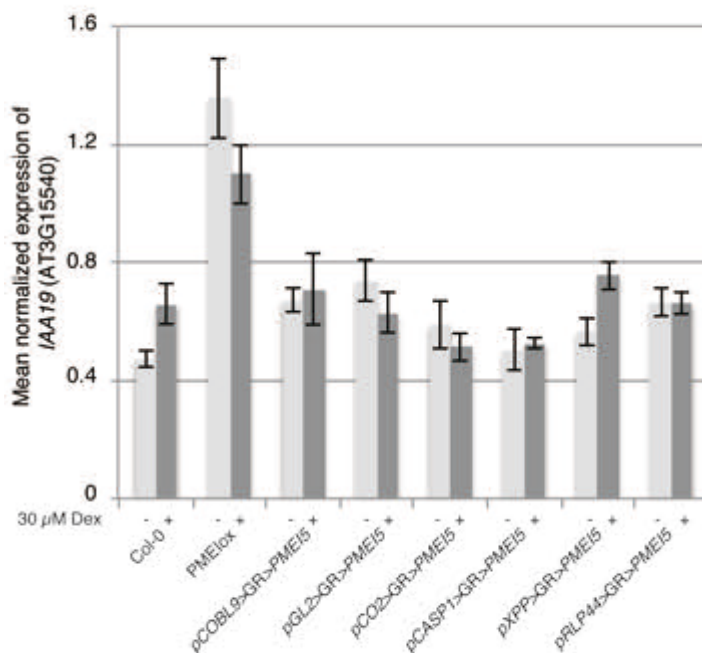


**Figure 31. qRT-PCR analysis of a standard BR signalling target gene *IAA19* (AT3G15540) in 5 DAG seedling roots of cell type/tissue-specific lines.**

Col-0 (**Figure 31**). Thus, it raised the possibility that other regulatory mechanisms than BR-mediated responses intervened but one should keep in mind that the unchanged transcript level of *IAA19* can only be representative of a constant BR signalling in a very narrow aspect such as BR and auxin co-regulated responses.

### 2.7.3. *rlp44<sup>cnu2</sup>* but not *bri1<sup>cnu4</sup>* rescued the root waving upon cell type/tissue-specific loss of CWI.

We then investigated whether *rlp44<sup>cnu2</sup>* and *bri1<sup>cnu4</sup>* could re-establish the WT-like phenotype in cell type/tissue-specific lines. Similarly to previous observation in *pXPP:PMEI5* (**Figure 30C, D**), *rlp44<sup>cnu2</sup>* largely rescued the root waving in *pUBQ10>GR>PMEI5*, *pML1>GR>PMEI5*, *pCOBL9>GR>PMEI5* and *pXPP>GR>PMEI5* (**Figure 32A**). The same phenotype, however, was not suppressed by *bri1<sup>cnu4</sup>* in all the lines mentioned above. For

**Table 3. Summary of root waving suppression in cell type/tissue-specific lines by *rlp44<sup>cnu2</sup>* and *bri1<sup>cnu4</sup>*.**

Transgenic line	Suppression of root waving by	
	<i>rlp44<sup>cnu2</sup></i>	<i>bri1<sup>cnu4</sup></i>
<i>pUBQ10&gt;GR&gt;PMEI5</i>	✓	X
<i>pML1&gt;GR&gt;PMEI5</i>	✓	✓
<i>pCOBL9&gt;GR&gt;PMEI5</i>	✓	X
<i>pXPP&gt;GR&gt;PMEI5</i>	✓	✓

*pUBQ10>GR>PMEI5* and *pCOBL9>GR>PMEI5*, in which *PMEI5* expression domain included

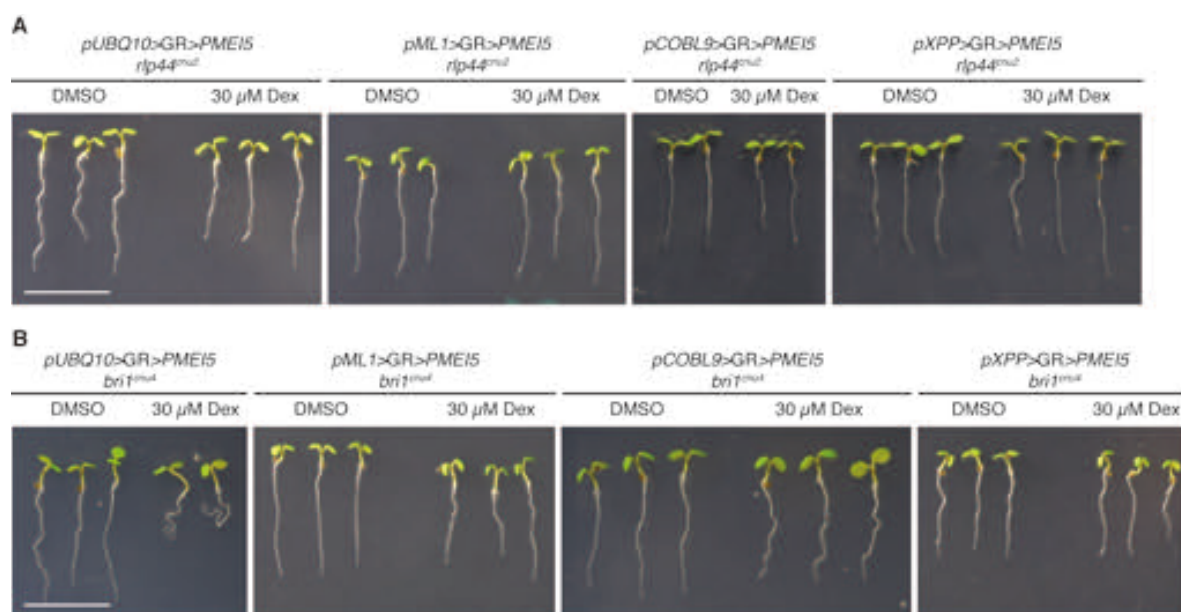


**Figure 32. Root waving suppression by *rlp44<sup>cnu2</sup>* and *bri1<sup>cnu4</sup>* in seedlings grown on 30 μM Dex-plate from germination to 5 DAG. (A) *rlp44<sup>cnu2</sup>* mutation was able to suppress root waving in all lines affected. (B) *bri1<sup>cnu4</sup>* could only suppress this phenotype in *pML1>GR>PMEI5* and *pXPP>GR>PMEI5*. Bars = 1 cm.**

trichoblasts, the root waving phenotype still persisted in *bri1<sup>cnu4</sup>* background (**Figure 32B; Table 3**). Such a persisting root waving phenotype reminded us of the preceding observation in which cell wall homeostasis in trichoblasts might play an important role in maintaining root morphology (§2.3.1, **Figure 20**; §2.5.1, **Figure 26B**).

*2.7.4. The oblique cell walls were possibly caused by RLP44- and BRI1-dependent mechanisms while unknown processes could play a role in QC/SCN organization.*

We next attempted to suppress the oblique cell walls and the QC/SCN disruption in *pCO2>GR>PMEI5* by *rlp44<sup>cnu2</sup>* and *bri1<sup>cnu4</sup>*. The oblique cell walls were partially suppressed by *rlp44<sup>cnu2</sup>* and almost rescued to a Col-0 comparable level by *bri1<sup>cnu4</sup>* (**Figure 33A, B, E, F**). Concerning the region of QC/SCN, it remained disrupted in *rlp44<sup>cnu2</sup>* background with clear disorganization not only in the QC/SCN but also in the beginning of cortex cell file, where the *pCO2*-driving expression of *PMEI5* was, as well as in its neighbouring tissues (**Figure 33D**). This result is in accordance with the formerly observed QC/SCN disruption (**Figure 21J, R17B, 18B and 20A**). In regard to *pCO2>GR>PMEI5* in *bri1<sup>cnu4</sup>* background, the tissue patterning defect also persisted but seemed to be restricted only to the QC and its surrounding initials. The cortex cells appeared with a more regular organization compared to *pCO2>GR>PMEI5* (**Figure 33H**). These observations suggested a role of BR signalling in cell division plane orientation and tissue patterning in the proximal meristem upon cell type/tissue-specific triggering of cell wall perturbation. However, the involvement of RLP44 seemed to be limited, indicating diverging regulatory roles between RLP44 and BRI1 in root growth.

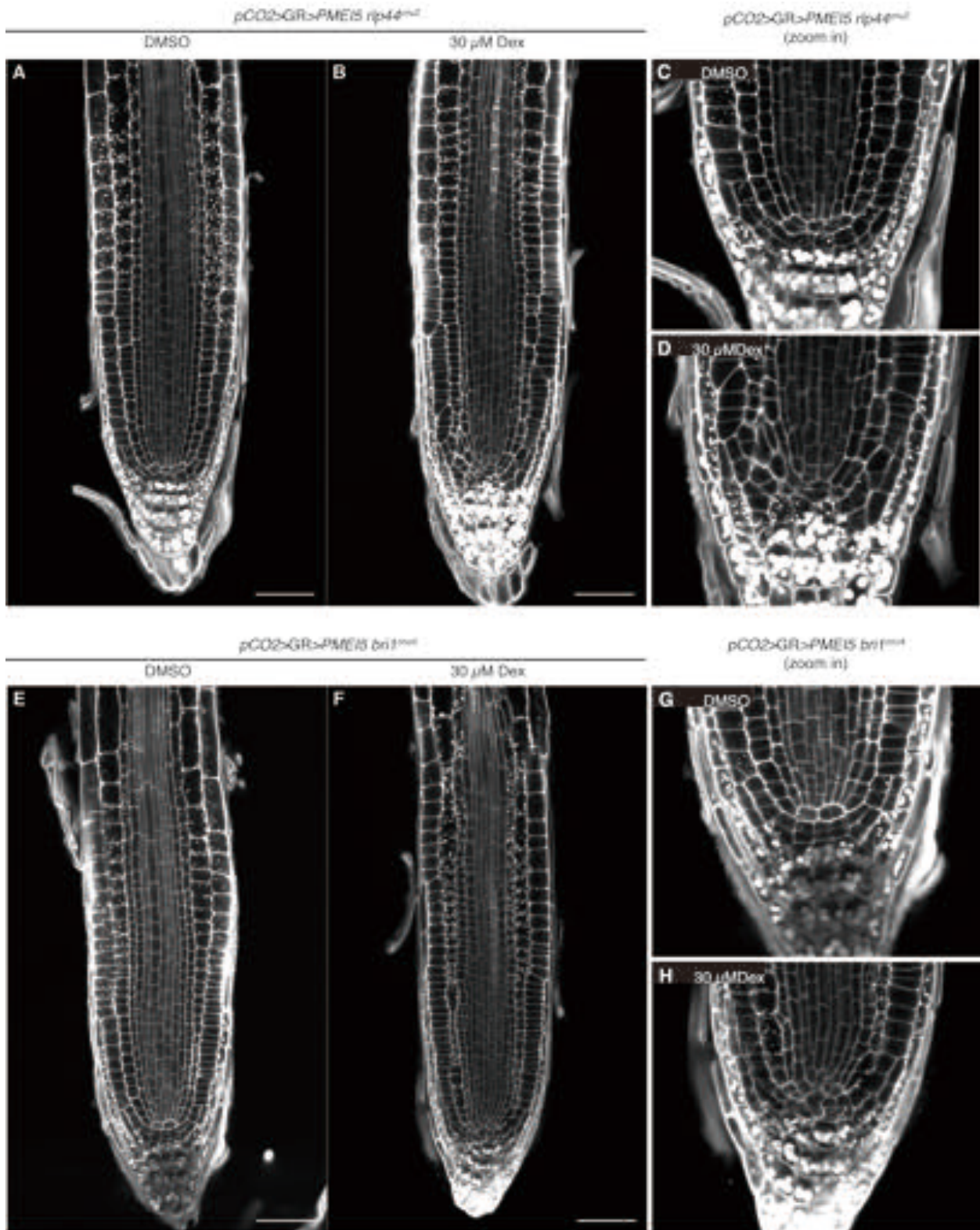


**Figure 33. Suppression of oblique cell walls and disruption of QC/SCN in *pCO2>GR>PME15* by *rlp44<sup>enu2</sup>* and *bri1<sup>enu4</sup>* in seedlings grown on 30 μM Dex-plate from germination to 5 DAG. (A-D) The oblique cell walls were partially suppressed by *rlp44<sup>enu2</sup>* and almost rescued to a Col-0 comparable level by *bri1<sup>enu4</sup>*. (E-F) The disrupted QC/SCN still persisted in *rlp44<sup>enu2</sup>* background and was ameliorated by *bri1<sup>enu4</sup>*. Cells are counter-stained with PI. Bars = 50 μm.**

## Discussion

### 1. Cell identity and tissue specificity might play an important role in RLP44/BRI1-mediated CWS in *PMElox*.

Ubiquitously challenging the cell wall in plants by over-expressing the pectin modification enzyme inhibitor *PMEI5* (*p35S:PMEI5*), affects the removal of the methyl group from HG and results in the loss of cell wall integrity (CWI). This loss of CWI has as primary consequences cell swelling, detachment and rupture in the entire seedling root (Wolf et al., 2012b). Changes in the cell wall are monitored by the RECEPTOR LIKE PROTEIN 44 (RLP44) and the derived signal is transduced through its interaction with BRASSINOSTEROID INSENSITIVE 1 (BRI1) and its co-receptor BRI1-ASSOCIATED RECEPTOR KINASE 1 (BAK1), which in turn activates the Brassinosteroid (BR) signalling pathway (Wolf et al., 2012b; Wolf et al., 2014; Holzwart et al., 2018). The activated BR signalling cascade regulates the expression of a wide range of genes via the downstream transcription factors BRASSINAZOLE-RESISTANT 1 (BZR1) and BRI1-EMS-SUPPRESSOR 1 (BES1), among which cell wall biosynthesis and remodelling genes are particularly over-represented (Wang et al., 2002; Yin et al., 2002; Sun et al., 2010; Wolf et al., 2014). Thus, this BR-mediated compensatory regulation allows the survival of the plant at the cost of impaired directional growth (Wolf et al., 2012b; Wolf et al., 2014; **Figure 4, R1A, B**). While *BRI1* is ubiquitously expressed in young tissues, especially in the meristem (Friedrichsen et al., 2000), the expression domain of *RLP44* is more restricted: it is expressed in most tissues of the root apical meristem (RAM) with highest level in the epidermis, lateral root cap (LRC) as well as in the stele/vasculature of the more mature part of the root, and to a lesser extent in the xylem precursor cells (Holzwart et al., 2018; **Figure 18**). As RLP44 is supposed to sense the changes in the cell wall, its partially overlapping expression domain with that of BRI1 suggests the involvement of both cell-autonomous and non cell-autonomous regulation. While the cell-autonomous regulation could act locally through RLP44/BRI1-mediated cell wall signalling (CWS), the non cell-autonomous one could activate regulatory mechanisms remotely through cell-to-cell communication. However, whether both types of regulation depend on RLP44/BRI1-mediated CWS remains a big question. In another scenario, the cell wall defects caused by *PMEI5* over-expression in regions other than *RLP44* expression domain might be caused by mechanical stress due to cell wall impairment in neighbouring cells. Thus, the compensatory responses in *PMElox* could result from the combinatorial effects of both RLP44/BRI1-mediated regulatory mechanism mainly in epidermis, LRC, stele/vasculature, and the persisting cell wall defects in other cell types/tissues. Arguing against this, the *comfortably numb 2* (*cnu2*), suppressor mutant of *PMElox* carrying a point mutation in *RLP44*, restored all phenotypes to a wild-type comparable level (Wolf et al., 2014). This insensitivity makes the plant 'blind' to the cell wall defects and suppresses the

BR-mediated compensatory responses. Thus, the impaired growth in *PMElox* might be predominantly caused by the enhanced RLP44/BR1-mediated growth regulation specifically in the RAM and the vascular tissue in the mature part of the root. This hypothesis points out the importance of cell identity and tissue specificity in RLP44-mediated responses to the loss of CWI. To gain more insight into the how these responses are regulated, through cell-autonomous and/or non cell-autonomous manner, we triggered the loss of CWI in different cell types/tissues and studies the resulted phenotypes.

## 2. Both cell-autonomous and non cell-autonomous regulations are implicated in the responses to cell wall perturbation.

Triggering the loss of CWI in different cell types/tissues independently did give more insight to the role of cell identity in plant growth control by RLP44-mediated CWS. Except for *pCASP1>GR>PMEI5*, resulting in expression in differentiating and mature endodermis, all lines with ectopic expression of *PMEI5* in distinctive cell types/tissues showed defective directional growth on soil to different extent, with the most severe and the most *PMElox*-like phenotype observed with expression in XPP cells (**Figure 21**). In contrast, the phenotypes in primary root differ widely (**Table 4**), suggesting dissimilar regulatory mechanisms in growth control of below- and above-ground tissues. While ubiquitous expression of *PMEI5* phenocopied *PMElox* in nearly all aspects of root growth, other cell type/tissue-specific lines only shared partially those phenotypes. With *PMEI5* expression under control of the *RLP44* promoter, the loss of CWI is induced in epidermis, LRC, stele/vasculature. Thus, the cell wall changes could be sensed locally

**Table 4. Phenotype summary of cell type/tissue-specific lines regarding the expression domain of *PMEI5* in comparison to *RLP44*.**

Transgenic line	Expression domain	<i>RLP44</i> expression in the cell type/tissue	5 DAG seedling root phenotype						
			Seedling root waving	Seedling root waving suppression by <i>rlp44<sup>enu2</sup></i>	Oblique cell wall	Oblique cell wall suppression by <i>rlp44<sup>enu2</sup></i>	Reduced RAM	QC/SCN disruption	QC/SCN disruption suppression by <i>rlp44<sup>enu2</sup></i>
<i>PMElox</i> ( <i>p35S:PMEI5</i> )	Ubiquitous	n/a	x	x	x	x	x		n/a
<i>pUBQ10&gt;GR&gt;PMEI5</i>	Ubiquitous	n/a	x	x	x	n/a	n/a		n/a
<i>pCOBL9&gt;GR&gt;PMEI5</i>	Trichoblast	medium	x	x		n/a	n/a		n/a
<i>pGL2&gt;GR&gt;PMEI5</i>	Atrichoblast	medium		n/a		n/a	n/a		n/a
<i>pML1&gt;GR&gt;PMEI5</i>	Entire epidermis	high	x	x		n/a	n/a		n/a
<i>pCO2&gt;GR&gt;PMEI5</i>	Beginning of cortex	low		n/a	x	partially	x	x	
<i>pCASP1&gt;GR&gt;PMEI5</i>	Differentiating and mature endodermis	absent		n/a		n/a	n/a		n/a
<i>pXPP1&gt;GR&gt;PMEI5</i>	Xylem pole pericycle	medium	x	x		n/a	n/a		n/a
<i>pRLP44&gt;GR&gt;PMEI5</i>	Stele, epidermis, LRC	high		n/a		n/a	n/a		n/a

and the RLP44/BRI1-mediated regulation could act cell-autonomously to ensure plant survival and cause the similar phenotype as PMElox. However, the major phenotypes of PMElox caused by this compensatory regulation such as seedling root waving and oblique cell walls have not been observed in *pRLP44>GR>PMEI5* (**Figure 20, 21B and F, 22P; Table 4**). The absence of apparent PMElox-like phenotypes would suggest that there exists a distinct regulatory mechanism in the case of cell type/tissue-specific loss of CWI, or, the induced expression of *PMEI5* was below a threshold that is sufficient to trigger a certain phenotype. Unlike *pRLP44>GR>PMEI5*, phenotypes provoked by ectopic expression of *PMEI5* in other tissues provided evidence for specific biological functions of cell wall and its surveillance in cell type/tissue specific context. In addition, phenotypes observed outside the domain of *PMEI5* expression in neighboring or even more distant zones indicated not only cell-autonomous but also non cell-autonomous responses to the cell wall perturbation. As exemplified by *pCO2>GR>PMEI5*, with expression of *PMEI5* only in the beginning of the cortex file, exhibited oblique cell walls and disrupted tissue patterning phenotype both within and outside the expression domain of *PMEI5* (**Figure 22J**). One might assume that, localized to the extracellular domain, *PMEI5* protein would be able to move to the adjacent cells and exert its effect cell-autonomously. However, this possibility is very unlikely because of the high density and complexity of the cell wall polysaccharides network. Besides, the expression of *PMEI5* in the neighboring cells/tissues of cortex, such as *pML1>GR>PMEI5* and *pRLP44>GR>PMEI5*, did not result in the same phenotype, strongly arguing for a non cell-autonomous effect.

### ***3. RLP44 and BRI1 might have distinct role in cell-autonomous regulation of root morphology upon cell wall perturbation.***

An undulating growth pattern along the gravity vector typically observed in wild-type when grown on tilted plate with impenetrable agar surface is called root waving ([Okada and Shimura, 1990](#); [Oliva et al., 2007](#); [Migliaccio et al., 2009](#); **Figure 5A**). Although root waving is often observed together with root skewing or slanting, which indicates a deviation from the direction of gravity vector ([Simmons et al., 1995](#); [Oliva et al., 2007](#)), they are believed to be uncoupled processes ([Buer et al., 2003](#); [Oliva et al., 2007](#)). Root waving has been described as gravity-related touch responses ([Thompson et al., 2004](#)), result of root tropisms such as thigmotropism, phototropism, chemotropism, and hydrotropism ([Kutschera et al., 2012](#); [Moriwaki et al., 2014](#); [Sato et al., 2014](#)). Besides, numerous candidate genes have been reported to be involved in the underlying molecular mechanisms, many of which are known to intervene in hormone pathways, such as ethylene and auxin ([Buer et al., 2003](#); [Ratherord et al., 1998](#)), cytoskeleton organization ([Ratherord et al., 1996](#); [Sedbrook et al., 2004](#); [Oliva et al., 2007](#)), cell expansion ([Yuen et al., 2003, 2005](#)), phosphorylation and signalling ([Deruère et al., 1999](#); [Santner et al., 2006](#)), and cell wall structure ([Sedbrook et al., 2002](#)). As no signalling pathway has been demonstrated to be solely

responsible for root waving, it seems that a combination of several co-ordinated mechanisms are involved in this phenotype. A recent study has identified 11 additional genes involved in root waving based on transcriptome data under different tilted growth conditions (Schultz et al., 2017). A majority of those candidate genes are associated with salt, sugar and hormone sensing mechanisms that are upstream of cell division, expansion and cell wall remodelling. Notably, several of those genes have overlapping expression domains with *RLP44*: *MIOX4* is expressed in root hairs, stele and LRC; *ASN1* is expressed in root hairs; *SIS* is up-regulated in the columella cells, root cap, and epidermis during salt stress; *SEN1* is expressed in mature and developing root hairs; *SWEET 11* is present in the mature vascular tissue. In addition, *MIOX4* is involved in oxidation of UPD-glucuronic acid precursors, which is essential for cell wall polysaccharide biosynthesis, and *PAP24* is predicted to be in the extracellular space and has metal ion binding activities (Enders et al., 2011; Li et al., 2002). A few other genes are responsive to phytohormones: *AT2G25150* is auxin and cytokinin responsive and has been reported to have activity in cell divisions (Luo et al., 2009; Zimmermann et al., 2004); *SEN1* is downregulated in the presence of auxin (Brady et al., 2007). Moreover, it has been reported that the root waving can be provoked by treatment with the most active form of BR, 24-epi-brassinolide (BL), in wild-type but not in *comfortably numb 1 (cnu1)*, the suppressor mutant of *PMElox* carrying mutation in the kinase domain of *BRI1*. Treatment with bikinin, a chemical that inhibits the negative regulator of BR signalling *BIN2* and thus activates the signaling cascade downstream of *BRI1*, induced root waving in both wild-type and *cnu1* (Wolf et al., 2012b). These results suggested that the negative feedback to BL biosynthesis by enhanced BR signalling is affected and is causative for the *PMElox* root waving phenotype.

Although gravitropism as well as other environmental signalling mechanisms have a profound impact on root waving, it does not seem to be the case in our transgenic lines with cell type/tissue-specific expression of *PMEI5* as the plates were placed vertically and the growth conditions are not supposed to cause any environmental stresses (**Material & Methods §2**). In spite of this, we still obtained some hints about the role of cell identity and *RLP44/BRI1*-mediated growth regulation in root growth pattern.

Root waving independently occurred when *PMEI5* expression was induced in various cell types/tissues that harbour *RLP44* expression. Loss of CWI in the entire epidermal tissue caused *PMElox*-like root waving (**Figure 20**) without any other growth defect. This observation is in line with the previous suggestion that locally enhanced *RLP44/BRI1*-mediated growth regulation in epidermis might be responsible for the compensatory responses and the resulted impaired root morphology. Furthermore, expression of *PMEI5* in trichoblast cells and atrichoblast cells separately resulted in root waving only when expression was driven in trichoblast cells (**Figure 20**). In this context, as *RLP44* is expressed in both cell types, it seemed to be implicated in the cell wall sensing specifically in trichoblast cells. But the resulting root waving might also be caused by an imbalanced mechanical strength between neighboring cells in the epidermal tissue,

or by an altered function of trichoblast cells that is required for normal root morphology. Arguing against the former, re-establishing the mechanical balance between trichoblast and atrichoblast cells by crossing *pCOBL9>GR>PMEI5* with *pGL2>GR>PMEI5* did not restore the regular straight root morphology (**Figure 26B**), leading to a consideration of the role of trichoblast cells in maintaining root morphology. Interestingly, it has been reported that the root waving observed in wild-type when grown on tilted plate is caused by epidermal cell file rotation along the root, which could be completely suppressed by loss-of-function alleles of *ROOT HAIR DEFECTIVE 3 (RHD3)*, a gene implicated in root hair development regulation and anisotropic cell expansion (Wang et al., 1997; Yuen et al., 2005). The RHD3 protein is involved in the control of vesicle trafficking between the endoplasmic reticulum and the Golgi apparatus (Wang et al., 1997). This observation thus suggested a role of trichoblast cell-specific transcriptional regulation in root morphology (Yuen et al., 2005). Therefore, the root waving evoked by *PMEI5* expression in trichoblast cells (*pCOBL9>GR>PMEI5*) provided evidence for RLP44-mediated, cell type-specific cell wall sensing and its downstream transcriptional regulation. *RLP44* expression is largely enriched in the differentiated vascular tissue and expanded to the surrounding pericycle cells (**Figure 18**). Triggering the loss of CWI in a subgroup of XPP cells strikingly caused similar root waving by either inducible (**Figure 20**) or constitutive (**Figure 15B**) expression of *PMEI5*. The expression of *PMEI5* in two distant and distinctive cell types separately resulted in the same growth phenotype, which suggests a role of cell-autonomously activated RLP44-mediated cell wall sensing and the downstream, non cell-autonomous regulation of root growth in response to cell wall perturbation. Conversely, in plants expressing *PMEI5* in the cortex initials and the transit amplifying cortex cells as well as the differentiating and mature endodermis, respectively, root waving has not been observed (**Figure 20**). Thus, it seems that the root waving occurred when *PMEI5* expression domain coincidence with that of *RLP44*, suggesting a role of cell-autonomous cell wall sensing by RLP44 in root growth regulation.

The attempt to suppress root waving in cell type/tissue-specific lines by *rlp44<sup>cnu2</sup>* or *bri1<sup>cnu4</sup>*, two mutations associated to PMElox phenotype suppression (Wolf et al., 2014; Holzwart et al., unpublished), suggested a partially overlapping role of RLP44 and BRI1 in root morphogenesis (**Figure 32**). The suppression of root waving in *pCOBL9>GR>PMEI5* and *pUBQ10>GR>PMEI5* by *rlp44<sup>cnu2</sup>* but not *bri1<sup>cnu4</sup>* might suggest the importance of trichoblast cell identity and the related cell wall sensing via RLP44 in root morphogenesis rather than BRs signalling. As root waving in *pML1>GR>PMEI5* might result from altered trichoblast cell wall properties and the local effect of RLP44/BRI1-mediated regulatory mechanisms in the whole epidermal tissue, it has been suppressed by both mutations. Additional studies in our group gathered evidence showing that *bri1<sup>cnu4</sup>* mutation might have negative effect on RLP44 function and that it does not exhibit strong BR signalling-deficient phenotypes (Holzwart et al., unpublished). Thus, the suppression of root waving by *bri1<sup>cnu4</sup>* in *pML1>GR>PMEI5* and

*pXPP>GR>PMEI5* could be a result of BRI1<sup>cnu4</sup>-mediated RLP44 activity in those tissues with high RLP44 accumulation. The strikingly persisting root waving in *pUBQ10>GR>PMEI5* with the presence of *bri1<sup>cnu4</sup>* mutation showed completely opposite result compared to the suppressor mutant *comfortably numb 4 (cnu4)* of PMElox, for which no likely explanation could be found so far.

#### **4. RLP44/BRI1-mediated CWS affects RAM growth through regulation of transition domain via other hormone signalling and responses.**

The *Arabidopsis* primary root is divided into three distinct regions along its longitudinal axis based on developmental state featured by different cell activities: the meristematic zone, the closest to the quiescent center (QC) and stem cell niche (SCN), where cells are actively dividing and give rise to new meristematic cells; the elongation zone, where cells cease to divide and start elongating; the differentiation zone, in which cells reach their final size and start to differentiate and acquire specific functions such as root hair cells, mature endodermal cells with casparian strip, and highly lignified vessel cells (Dolan et al., 1993; Petricka et al., 2012). It is noteworthy that a transition domain exists between the meristematic zone and elongation zone. In this domain, cells grow at a similarly low rate as meristematic cells but also with a very low division potential. The position of this transition domain determines the size of the meristem (Beemster and Baskin, 1998; Petricka et al., 2012; Ivanov and Dubrovsky, 2013). The primary root growth is a result of co-ordinated meristematic cell division in the RAM, the subsequent cell elongation, and differentiation (Ivanov and Dubrovsky, 2013; Takatsuka et al., 2014). Many studies showed that plants affected in primary root growth often exhibited altered root zonation, especially between the meristem zone and elongation zone, pointing out the importance of the transition domain (Dello Ioio et al., 2007; Ubeda-Tomás et al., 2009; González-García et al., 2010; Hacham et al., 2011; Meijón et al., 2014). The determination of this transition domain is supposed to be driven by positional information of the cells, which itself is believed to be conferred by signalling gradients (Grieneisen et al., 2012; De Vos et al., 2014). In accordance with this, a large body of evidence has revealed the role of hormone signalling, such as auxin, brassinosteroids (BRs), cytokinins and gibberellins, in root meristem size determination (Grieneisen et al., 2007; Galinha et al., 2007; Dello Ioio et al., 2007, 2008; Di Mambro et al., 2017; Petricka et al., 2012). It has been described that mutants affected in BRs perception and signalling had small meristem due to defective cell cycle progression and cell expansion (Hacham et al., 2011). However, PMElox has been reported to have enhanced BR signalling (Wolf et al., 2012b) and a smaller meristem size, which seemed to result from a premature transition of meristematic cells from division to elongation rather than a decreased cell division activity, as revealed by EdU staining (Figure 10).

Exogenous cytokinin treatment resulted in a decreased RAM size with significantly fewer meristematic cells. This is consistent with the observation that the triple cytokinin biosynthetic mutants *ipt3*, *ipt5*, *ipt7*, which lacks cytokinin in the vasculature of the elongation/differentiation

zone, showed increased RAM cell number. This suggests that Cytokinin controls RAM size by limiting cell differentiation rate from the vasculature of the transition zone (Dello Iorio et al., 2007). Depletion of endogenous cytokinin in all tissues of the transition zone in the auxin efflux triple mutant *pin1, 3, 7* did not alter the RAM size, suggesting the necessity of having a proper auxin distribution for cytokinin effect in RAM size control (Dello Iorio et al., 2007). On the other hand, cytokinins are reported to promote cell division in the vascular tissue (Bishopp et al., 2011), showing diverging roles of those hormones in different aspects of root growth regulation. In addition, it has been revealed that the cytokinin- and auxin-mediated regulations of RAM size did converge at genetic level (Dello Iorio et al., 2007, 2008; Di Mambro et al., 2017).

Further investigation of cytokinin signalling showed a decrease of ARR5-related negative regulation of cytokinin responses and possibly a reduced cytokinin signalling (Figure 12A, B). Cytokinin activates *SHY/IAA3* gene through AHK3-ARR1 two component signalling pathway, which in turn reduces auxin responses and negatively regulates the expression of *PIN* genes that are known to localize to the basal membrane to direct the rootward auxin flow (Dello Iorio et al., 2007, 2008; Wang and Estelle, 2014; Vieten et al., 2005; Blilou et al., 2005). The altered auxin distribution leads to cell differentiation in all tissues of the transition zone in the RAM, thus limits RAM size. Conversely, auxin accumulation triggers degradation of SHY2/IAA3 protein and sustains expression of *PIN*s (Vieten et al., 2005; Dello Iorio et al., 2007, 2008). Recent updates on this cytokinin-auxin interaction model revealed that, in addition to the negative regulation of *PIN*s, another ARR1 direct target gene *GH3.17* triggers auxin degradation and forms an auxin minimum in the topmost cells of the RAM, which also contributes to the determination of the transition zone and controls the RAM size (Di Mambro et al., 2017). Furthermore, *ARR5* expression in the stele promotes cell division, indicating a role of specific cell type/tissue in hormonal growth control (Bishopp et al., 2011). Accumulation of *PIN7* seemed to be decreased in the RAM of *PMElox* along the longitudinal axis but not radially (Figure 12G, K). Further up in the differentiation zone, *PIN7* showed a slight extended distribution covering not only procambial cells but also protoxylem cells (Figure 12J, N). Interestingly, examination of a group of cell identity markers did not reveal aberrant cell fate specification in most of the tissues with the exception that, in *PMElox* only one group of xylem pole pericycle (XPP) cells has been observed (Figure 14C, D) instead of two groups that are opposite each other at an angle of 180° (Figure 14A, B). Given the adjacent position between protoxylem and XPP cells, whether the extended *PIN7* distribution into protoxylem cells, and the likely resulted auxin accumulation in the neighbouring XPP cells, contributed to the impairment of XPP cell specification is an interesting question. It has been described that the formation of the auxin maximum in the xylem axis of the *Arabidopsis* root vascular tissue is mediated by the *PIN* class of auxin efflux carriers. The cytokinin-regulated *PIN* distribution forces auxin out of the procambial cells into the xylem cells and promotes their specification (Mähönen et al., 2006; Bishopp et al., 2011). XPP cells are at the basis of lateral root initiation, as they are recruited to become founder cells, which upon activation start to divide and

give rise to lateral root primordia. This initiation is believed to be triggered by local auxin accumulation (Dubrovsky et al., 2006, 2007; el-Showk et al., 2015). Therefore, the altered cytokinin-auxin interaction might have influence on XPP cell specifications, which in turn affect lateral organ formation in *PMElox*.

Taken together, the ubiquitous loss of CWI in *PMElox* might indirectly result in reduced meristem size and XPP cell specification due to impaired cytokinin and auxin signalling as well as responses, but how is this impairment caused by the loss of CWI still remains elusive. At tissue level, loss of CWI triggered in the beginning of the cortex (*pCO2>GR>PMEI5*) did not result in as dramatic reduction in RAM size as in *PMElox* (**Figure 23**). As evidenced by qRT-PCR analysis, all cell type/tissue-specific lines did not seem to have dramatically altered level of BR signalling (**Figure 31**). Does the loss of CWI in cell type/tissue-specific context also alter meristem size and if yes, is the influence also associated to cytokinin and auxin signalling and/or responses, need to be thoroughly studied.

### ***5. Cell wall properties affect cell division and tissue patterning in both cell-autonomous and non cell-autonomous manner possibly by interfering with BR and auxin responses.***

Cell divisions shape the plant by contributing to tissue growth and patterning, as well as organ formation (Dupuy et al., 2010; Uyttewaal et al., 2012; Petricka et al., 2012). Cell proliferation is achieved through successive symmetric cell divisions with strictly defined division plane (Besson et al., 2011; Rasmussen et al., 2013). Asymmetric divisions give rise to daughter cells with distinct size and identity, which are instrumental for cell fate specification, tissue patterning as well as many other developmental processes. Therefore, their division plane orientation also needs to be tightly controlled (Abrash and Bergmann, 2009). Although the cell wall has pivotal functions in cell division (Lloyd, 1991; Lipka et al., 2015; Smith, 2001; Rasmussen et al., 2013), observations of severe defect in cell division plane orientation have not been reported for many cell wall biosynthetic mutants (MacKinnon et al., 2005; Desprez et al., 2015; Bouton et al., 2002; Cavalier et al., 2008). Contrarily, mutants affected in cell division steps such as preprophase band (PPB) and cell plate formation often show disturbed division plane and oblique cell walls (Lipka et al., 2014; Müller et al., 2006; Walker et al., 2007; Rasmussen et al., 2010; Zuo et al., 2000). Thus, cell wall properties might not directly influence cell division plane determination but rather in an indirect way or through wall mechanics (Louveau et al., 2016). Both *PMElox* and *pCO2>GR>PMEI5* exhibited oblique cell walls in the longitudinally patterned cell files of the RAM, with the latter showing additionally a disrupted QC/SCN organization presumably resulted from a series of mis-orientated cell divisions (**Figure 5D, F; R16J, 20A**). The cortical division site (CDS) marker POK1 was recruited to and remained at the plasma membrane throughout the division cycle, revealing a shift of the CDS position, which caused an oblique transverse cell wall as its

formation has been guided by phragmoplast to fuse at the shifted CDS with the parental wall (**Figure 8B**). This observation suggested a failure of *PMElox* cells to maintain a proper CDS and a division plane. However, what caused the CDS shift within the plasma membrane remains unclear. In a hypothetical scenario, proteins that mark the position of CDS, such as POK1, POK2 and TAN could be at least partially connected to the cell wall, and the perturbation in cell wall properties might alter this connection and thus impair the capacity of maintaining CDS position within the plasma membrane. Another possibility, although less likely, is that the disrupted cell wall caused an imbalance in mechanical stress and a different growth rate between the cell walls of a given cell, resulting in unequal displacement of the CDS. To test the first hypothesis, it would be insightful to trigger plasmolysis in *PMElox* and wild-type plants carrying the POK1 marker and track its position during the mitotic cycle. As evidence regarding tissue-level changes in the cell wall is lacking, we cannot further speculate about how a disrupted cell wall in *PMElox* might influence tensile stress between individual cells. However, given the heterogeneity of cell wall composition and structure in different tissues, inhibition of pectate- $\text{Ca}^{2+}$  crosslink formation could potentially alter cell wall mechanics in distinctive ways. In order to shed more light on the impact of altered cell wall properties on tissue patterning, immunolabelling of different cell wall components using anti-wall carbohydrate antibodies on root cross sections has been ongoing. In addition, a lately developed pectin fingerprinting technique with MALDI-Q/TOF (INRA, Versailles, France) has been exploited to reveal in more detailed way changes in pectins and the results could be analyzed in the near future.

Despite the lack of information about their altered cell wall compositions, *PMElox* and *pCO2>GR>PMEI5* should experience cell wall disruptions in distinctive domains. In the latter, only the first few cortex cells following the cortex/endodermis initial (CEI) were affected in pectin modification (**Figure 18**). The cortex cells positioned in the distal RAM, progeny of cells that were affected in cell wall properties, might still have *PMEI5* activity and or cell wall defects after exiting the *pCO2*-driven expression domain of *PMEI5*. Thus, the oblique cell walls within the cortex file are presumably due to cell-autonomous effect of cell wall perturbation. Conformable with this, time-course induction of *pCO2>GR>PMEI5* showed that the oblique cell walls and the likely resulting defective tissue patterning around the beginning of cortex cell file appeared two days after induction, a time frame too short for cells to progress from initials to the distal meristematic zone, while the oblique cell walls in cortex cells of distal RAM were not observed yet (**Figure 25**). On the other hand, oblique walls in cells of other tissues than cortex might be caused non cell-autonomously by either cell-to-cell communication or mechanical imbalance. In contrast, *PMElox* showed oblique cell walls only in the longitudinal cell files without having any disrupted tissue organization in the proximal meristem surrounding the QC/SCN (**Figure 5D**) but over-differentiated columella stem cells (CSC) (**Figure 11B**). This diverging manifestation of *PMEI5*-triggered cell division defect and disrupted tissue patterning in *PMElox* and *pCO2>GR>PMEI5* RAM indicated a potential role of cell identity in division plane control in the responses to cell wall disruption.

Intriguingly, examination of two marker lines indicated a loss of QC identity in *pCO2>GR>PMEI5* (**Figure 28**), which strengthened this hypothesis.

Although the tissue patterning defect in the proximal meristem of *pCO2>GR>PMEI5* seemed to be a consequence of locally impaired mechanical balance between adjacent cells, F1 plants of a cross between *pCO2>GR>PMEI5* and *pRPL44>GR>PMEI5* did not much ameliorate the phenotype (**Figure 27D**). However, F1 plants of a cross between *pCO2>GR>PMEI5* and *pCO2>GR>bin2-1* alleviated the QC/SCN disruption, suggesting a role of BR signalling (**Figure 27E**). This could be further supported by a partial suppression of the QC/SCN disruption by *bri1<sup>cnu4</sup>* but not *rlp44<sup>cnu2</sup>* (**Figure 33D, H**). However, *pCO2>GR>PMEI5* did not exhibit apparent alteration in BR signalling as suggested by qRT-PCR result (**Figure 31**). Such an observation could also be due to a diluted expression changes masked by the presence of many other cells/tissues that did not express *PMEI5*. In addition, BRs have been shown to be associated with ectopic cell division plane orientations (Jang et al., 2000) and BR signalling might play a role in auxin maximum patterning (Nakamura et al., 2003). The formation of the auxin maximum around the QC allows the establishment of a gradient of the PLT transcription factors, which maintains the expression of PIN carriers that are crucial for SCN positioning (Blilou et al., 2005; Galinha et al., 2007; Vanneste and Friml, 2009; Liu et al., 2017). The slightly decreased and outward diffusing pattern of auxin maxima in the area of QC and SCN indicated a decreased auxin response (output) (**Figure 29D**) while the auxin input was rather stable in this area (**Figure 29C**), which corroborated the likely loss of QC identity. Additionally, the enriched auxin input in all RAM tissues, excluding the proximal meristem, might contribute to the observed oblique cell wall formation, as auxin is known to be related to cell division control. The altered PIN7 distribution in the outer columella cell layer of *PMEI*ox meristem (**Figure 12G, K**) provided additional evidence for auxin-related responses to the loss of CWI. Nevertheless, BRs might also regulate SCN homeostasis on their own, apart from their interactions with auxin (González-García et al., 2011). Collectively, the causal relationship between the cell wall disruption and the cell identity change as well as defective tissue patterning is still obscure and requires further investigation.

In conclusion, in this study we have further revealed the impact of cell wall homeostasis on *Arabidopsis* primary root growth, especially in root morphogenesis, meristem size control, division plane determination through CDS maintenance, and tissue patterning. The RLP44/BRI1-mediated CWS in the case of ubiquitous loss of CWI does not seem to exert the same regulatory role in cell type/tissue-specific context and both cell-autonomous and non cell-autonomous regulation are involved in the responses to cell wall perturbation. We also collected evidence showing that, upon cell wall disruption, responses mediated by BRs as well as their crosstalks with cytokinin and auxin can potentially influence RAM growth and patterning. At the tissue level, we showed that cell wall and its surveillance in a given cell type/tissue has specific biological functions as manifested by diverse growth responses to the loss of CWI in a give cell type or tissue. Besides,

other mechanisms than RLP44/BRI1-mediated CWS might be in play for ensuring plant growth upon cell wall disruption. To unravel the underlying molecular mechanism implicated in the responses to loss of CWI, cell type/tissue-specific transcription analysis is being undertaken with the hope of discovering candidate genes that are responsive to cell wall-related triggers.



## Material & Methods

### 1. Green Gate cloning, plant transformation and transgenic line selection.

All constructs were produced by using GreenGate cloning (Lampropoulos et al., 2013) with modules and primers listed in **Table S2**. Primers for the cloning of sequence of interest with GreenGate module-specific overhangs are explained in **Figure 34**. Cloning has been carried out with Q5® High-Fidelity DNA Polymerase (NEB #M0491) with reaction mix and PCR cycles listed in **Table 5 and 6**. The amplified PCR product has been column-purified by using GeneJET PCR Purification Kit (ThermoFisher #K0701) and then digested with *Eco31I* FD restriction enzyme (ThermoFisher #FD0293) at 37°C for 15 minutes with reaction mix listed in **7**. Digested products were again column-purified as described above. Empty vectors have been digested and purified separately by following the same instructions. Digested and purified insert and vector are ligated by using Instant Sticky-end Ligase Master Mix (NEB #M0370) as instructed by the manufacturer.

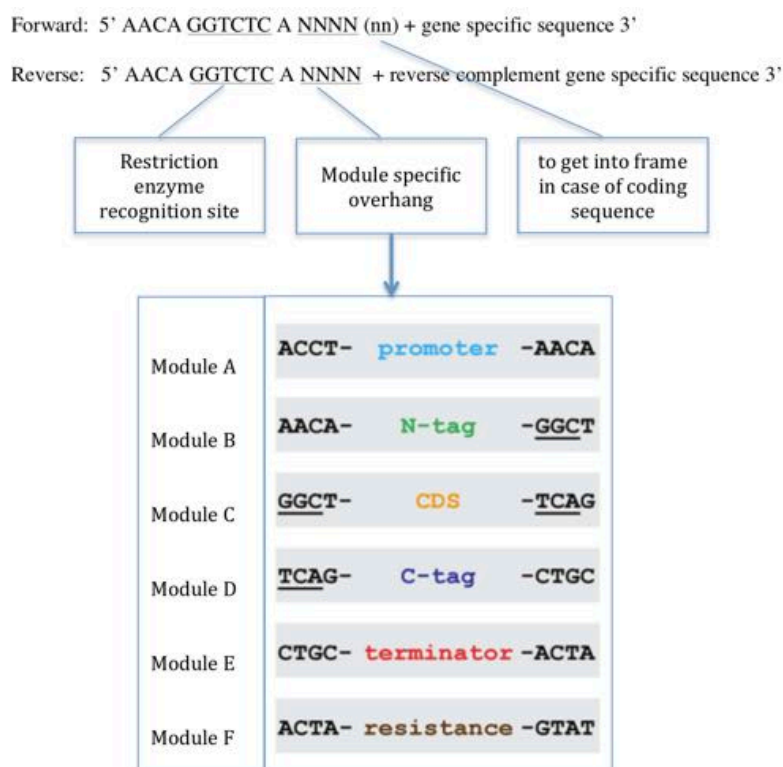


Figure 34. Design of cloning primers with GreenGate overhangs.

Table 5. Q5 cloning PCR reaction mix.

Reagent	Volume (µL)
5x Q5 reaction buffer	10
10 mM dNTP	1
10 µM primer_Fwd	2.5
11 µM primer_Rev	2.5
DNA template	1 ng - 1 µg
Q5 enzyme	0.5 µL
ddH <sub>2</sub> O	fill up to 50 µL

Table 6. Q5 cloning PCR reaction cycles.

Temperature (°C)	Duration	Number of cycles
98	30 sec	x 35
98	10 sec	
50 - 72	30 sec	
72	20 - 30 sec/kb	
72	2 min	
4	∞	

The ligated product was then transformed into chemically competent *E.coli* strain DH5 $\alpha$  or XL1-blue and cultivated in LB medium supplied with antibiotics in accordance with the resistance of the module (**Table S1**). Positive colonies have been confirmed with single colony PCR by using primers that bind to either vector backbone or inserted sequence (**Table S3**). Amplified plasmids have been extracted from single colonies by using GeneJET Plasmid Miniprep Kit (ThermoFisher #K0502), inserted sequence has been further verified by sequencing conducted at Eurofins Genomics. Confirmed entry modules are ligated into intermediate vector by running GreenGate reaction ( **Table 8, 5; Figure 35**). The intermediate module plasmids are amplified, extracted and verified as described before. The assembly of two expression cassettes each carried by one intermediate vector was achieved by running the same GreenGate reaction and simply replacing the entry module and empty intermediate vector by purified intermediate module and empty destination vector, respectively. The sequence of final plasmid has been double verified by colony PCR and digestion test, and then transformed into *Agrobacterium tumefaciens* strain ASE (pSOUP+) carrying resistance to chloramphenicol, kanamycin and tetracycline. All constructs were transformed by the floral dip method as described in [Clough and Bent, 1998](#) and adapted from [Zhang et al., 2006](#)

**Table 7. *Eco31I* digestion reaction mix.**

Reagent	Volume ( $\mu$ L)
10x fast digest buffer	3 $\mu$ L
Purified PCR product	0.2 $\mu$ g
<i>Eco31I</i> FD	1 $\mu$ L
ddH <sub>2</sub> O	fill up to 30 $\mu$ L

**Table 8. GreenGate reaction mix.**

Reagent	Volume ( $\mu$ L)
Entry module	1.5 $\mu$ L each
Empty intermediate module	1 $\mu$ L
FD buffer	2 $\mu$ L
10 mM ATP	1.5 $\mu$ L
T4 DNA ligase	1 $\mu$ L
<i>Eco31I</i> FD	1 $\mu$ L

**Table 9. GreenGate reaction cycles.**

Temperature ( $^{\circ}$ C)	Duration	Number of cycles
37	2 min	x 30
16	2 min	
50	5 min	
80	5 min	

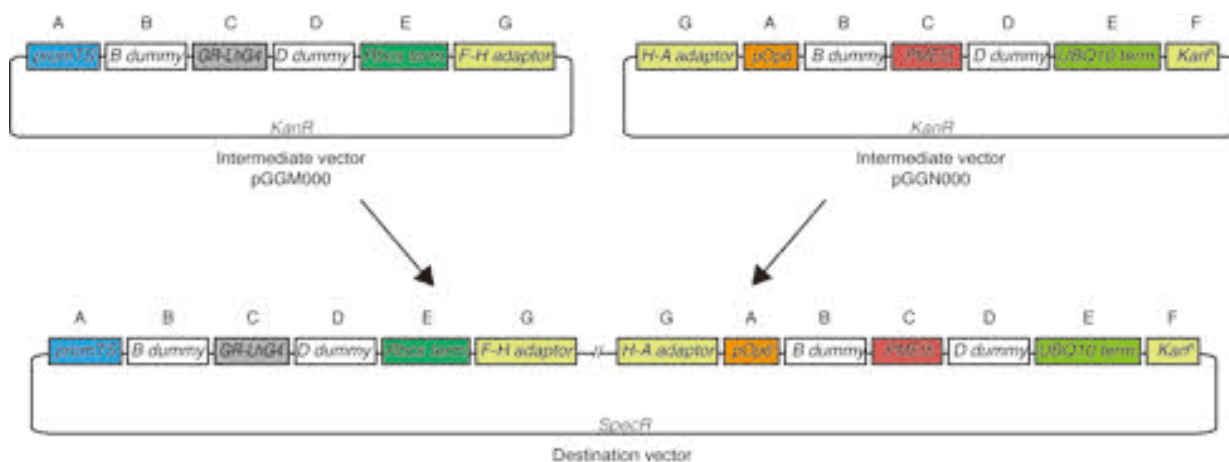


**Figure 35. Scheme representing ligation of GreenGate modules.** Entry modules (indicated with capital letters A - G) are ligated into an intermediate module (M000 or N000) to form one expression cassette. The subsequent assembly gathers two expression cassettes into one destination vector (Z001). Based on Lampropoulos et al., 2013.

into *Arabidopsis thaliana* Col-0. Transformant selection has been done on growth medium supplied with either kanamycin or sulfonamide according to the resistance cassette carried on the T-DNA. Homozygous stable lines with single insertion have been obtained and used in the subsequent studies.

## 2. Plant materials and growth conditions.

All *Arabidopsis* seed were sterilized with approximately 1.3% (v/v) sodium hypochlorite (NaOCl) diluted in 70% ethanol for 3 minutes, then washed twice with 100% ethanol and dried in laminar flow hood. Seeds were sowed out on plate with growth medium containing half-strength (1/2) Murashige & Skroog (MS) medium (Duchefa), 1% D-sucrose (Car Roth) and 0.9% phytoagar (Duchefa) with pH adjusted to 5.8 with KOH. After 2 days stratification at 4°C in darkness, plates were placed vertically in long day conditions (16h light/ 8h dark cycles) with equal light conditions (approximately 100  $\mu\text{E m}^{-2}\text{s}^{-1}$ ) for 5 days. All analyses have been carried out on seedling of 5-day-old. For dexamethasone (Dex) induction on plate, desired amount of Dex (Signam-Aldrich #D4902) was added to the growth medium, equal volume of dimethyl sulfoxide (DMSO) has been added to the control plate. For Dex induction on soil, 30  $\mu\text{M}$  Dex has been used to spray the above ground plant body and to water every other day starting from 3 days after transfer of seedling on soil. All plants are grown on soil under long day conditions (16h light/ 8h dark cycles) at 23°C with 65% humidity. Sources of seeds of marker lines as well as other transgenic lines that have not been produced in this study are listed in **Table 10**.

**Table 10. Source of lines that are not produced in this study.**

Name of the line	Number in lab stock	Source
Col-0	#183	S. Wolf lab
PM10a	#180	Wu et al., 2012b
PM10a	#181	Wu et al., 2012b
gfp:atgus2	#264	Wu et al., 2014
gus:tom1	#428	Wu et al., 2012b
gus:tom4	#441	S. Wolf lab
gus:GFP:GUS:YFP	#342	S. Wolf lab
YFP:YFP1	#407	S. Meyer lab
gus:GUS:GUS:GUS	#474	J. Lohmann lab
gus:GUS:GUS:GUS	#394	S. Wolf lab
gus:YFP:YFP:YFP	#465	J. Lohmann lab
gus:GUS:GUS:GFP	#520	B. Schrepf lab
gus:GUS:GFP	#476	T. Grub lab
gus:GUS:GFP	#480	T. Grub lab
G376	#485	J. Hauptf line
G386	#528	J. Hauptf line
gus:GUS:GUS	#534	A. Maizel lab
gus:GUS:GFP	#535	A. Maizel lab
gus:GUS:GUS:Tomato:GUS:GUS:Tomato	#576	Schäfer and Lopez-Salazar et al., 2018
gus:GUS:GUS:YFP (Sand line)	#574	Margolis-Bueno et al., 2019
gus:GUS:GUS:YFP	#536	A. Maizel lab
gus:GUS:GUS:Tomato:GUS:GUS:Tomato:GUS:GUS:Tomato:GUS:GUS:Tomato	#557	D. Weiers lab

## 3. Genomic DNA extraction and genotyping.

Homozygosity has been confirmed by genotyping PCR followed by production digestion and separation on agarose gel. In brief, freshly harvest plant tissue has been frozen in liquid nitrogen and then grounded by using Tissue Lyser II (Quiagen). 200  $\mu\text{L}$  of gDNA extraction buffer

(150 mM Tris-HCL, pH 8; 250 mM NaCl, 25 mM EDTA, 0.5% SDS) was added to the grounded sample. The solution was thoroughly mixed and then pinned down at room temperature at 14 000 g for 15 minutes. 150 µL of the cleared supernatant was transferred to a new tube and 150 µL isopropanol has been added. The mixture was again centrifuged at 14 000 g for 10 minutes and the supernatant was discarded without disturbing the DNA pellet. Next, 1 mL of 70% ethanol has been added to the pellet and the sample was centrifuged at the same speed for 10 minutes. After removing the supernatant, the pellet has been dried under the laminar flow hood. At the end gDNA pellet was resuspended in 40 µL of a buffer containing 10 mM Tris-HCl, pH 8 and 0.5 mM EDTA. *rlp44<sup>cnu2</sup>* and *bri1<sup>cnu4</sup>* mutation homozygosity has been confirmed by using CAPS marker with primers listed in **Table S1**, and were further digested with HinfI and BseII, respectively. According to the number of copy of the transgene, the digestion resulted in fragment with different sizes that can be separated on 3% agarose gel as follows: plants with non *rlp44<sup>cnu2</sup>* mutation had 3 bands with 127, 91 and 42 bp; plants heterozygous for *rlp44<sup>cnu2</sup>* mutation had 4 bands with 169, 127, 91 and 42 bp; plants homozygous for *rlp44<sup>cnu2</sup>* mutation had only 2 bands with 169 and 91 bp. For *bri1<sup>cnu4</sup>*, wild-type had 3 bands with 499, 336 and 318 bp; heterozygous plants had 4 bands with 767, 499, 336 and 318 bp; homozygous plants had only 2 bands with 767 and 336 bp.

#### 4. Microscopy analysis.

Microscopic analyses have been carried out with Zeiss LSM 510 Meta and Leica TCS SP5 laser scanning confocal microscope. Laser lines used for excitation and emission wave-length that are collected for different fluorophores are listed in **Table 11**.

#### 5. EdU staining.

Seedling were harvested at 5 DAG and mitotically active cells have been marked by using Click-iT™ EdU Alexa Fluor™ 488 Imaging Kit (ThermoFisher #C10337) and following manufacture's instructions and as described in [Perilli et al., 2013](#). Stained seedlings were mounted in PBS buffer and imaged under Leica TCS SP5 II confocal laser scanning microscope with exaction at 488 nm and emission collected between 480 nm and 550 nm.

#### 6. Microtubule immunolabelling.

Seedlings at 5 DAG were fixed with 0.5x MTSBT buffer (25 mM PIPES, 2.5 mM EGTA, 2.5 mM MgSO<sub>4</sub>, 0.1% triton X-100, pH 7 adjusted with KOH) diluted in 4% paraformaldehyde for 1 hour under vacuum. Samples were washed with 0.5x MTSBT buffer for 10 minutes and then treated with 80% methanol for 10 minutes and washed again with 0.5x MTSBT buffer. The cell

**Table 11. Excitation and emission wave-length of fluorophores used in this study .**

Fluorophores	Excitation (nm)	Emission (nm)
mTurquoise2	458	460 - 520
GFP/Alexa 488	488	490 - 530
YFP/Venus	514	520 - 560
RFP	561	560 - 620
mCherry	561	
tdTomato	561	
Cy3	561	
Propidium iodide	488	600 - 670
FM4-64	561	675 - 790

wall was digested with solution containing 25 mM MES (pH 5.4), 8 mM CaCl<sub>2</sub>, 600 mM mannitol, 0.02% pectolyase (Duchefa) and 0.1% macerozyme (Duchefa) for 30 minutes at 37 °C. Samples were then washed with PBS buffer added with 50 mM glycine. Washed samples were incubated with primary antibody anti- $\alpha$ -tubulin (Sigma-Aldrich #T9026) in PBS and 50 mM glycine overnight at 4 °C. After being washed for 10 minutes as described above, samples were incubated with secondary antibody goat anti-mouse IgG Alexa fluor 488 (Molecular Probes #A11001) for 1 hour at 37 °C. After a final wash for 10 minutes, samples were mounted in VECTASHIELD Antifade Mounting Medium with DAPI (Vector Laboratories #H-1200).

### 7. mPS-PI staining.

Staining of cell outline with propidium iodide (PI, Sigma-Aldrich #P4170) with modified pseudo-PI staining method has been performed as described in [Truernit et al., 2008](#) with modifications. Seedlings at 5 DAG were fixed in solution containing 50% methanol and 10% acetic acid for 3 days at 4 °C. Samples were then washed twice with H<sub>2</sub>O and incubated in 1% periodic acid (Sigma-Aldrich #P0430) at room temperature for 40 minutes. Samples were washed twice with H<sub>2</sub>O and then stained with 100  $\mu$ g/mL PI freshly diluted in Schiff's reagent (100 mM sodium metabisulphite, 75 mM HCl). Stained samples were transferred onto microscope slides covered by chlorohydrate solution (4 g chloral hydrate, 1 mL glycerol, 2 mL H<sub>2</sub>O) and incubated overnight at room temperature in a closed environment. Excess of chlorohydrate solution was removed and several drops of Hoyer's solution (3 g gum arabic, 20 g chloral hydrate, 2 g glycerol, 5 mL H<sub>2</sub>O) was added to the samples, which were at the end covered gently by cover splits and stayed at room temperature for 3 days before imaging.

### 8. Histology: GUS staining and basic fuchsin staining of stem cross sections.

Plants of reporter lines driving expression of the gene encoding  $\beta$ -glucuronidase were stained as follows. In 1 mL of Na<sub>2</sub>HPO<sub>4</sub>/NaH<sub>2</sub>PO<sub>4</sub> buffer (pH 7) were added 25  $\mu$ L of potassium ferrocyanide (K<sub>4</sub>Fe(CN)<sub>6</sub> 3H<sub>2</sub>O), 25  $\mu$ L of potassium hexacyanoferrate (K<sub>3</sub>Fe(CN)<sub>6</sub>) and 10  $\mu$ L of 100 mM X-GlcA (Sigma-Aldrich #B6650). About 5 to 10 seedlings were incubated in the mixed solution at 37 °C overnight in the darkness. A clearing process has been done by following steps in **Table 12** and samples are mounted in 50% glycerol on slides. Stained samples were imaged with Zeiss Axiovision epifluorescence microscope.

**Table 12. Clearing steps after GUS staining.**

Solution	Time (min)	Temperature (°C)
4% HCl + 20% methanol	25	60
7% NaOH in 60% ethanol	15	25
40% ethanol	10	
20% ethanol	10	
10% ethanol	10	
25% glycerol in 10% ethanol	10	

Cross sections of the basal stem has been stained with basic fuchsin (Sigma-Aldrich #857343). Stem fragments have been fixed with FAA fixative (50% ethanol, 5% (v/v) acetic acid 3.7% (v/v) formaldehyde) and then dehydrated through a series of ethanol (70%, 90%, 90%,

99.8% + eosin, 99.8%, absolute) followed by three cycles of clearing with xylene. Samples were then infiltrated with paraffin wax and embedded in a wax bloc. Cross sections with 10  $\mu\text{m}$  thickness were obtained by using Leica RM2255 rotatory microtome. Sections were washed with Roti®-Histol (Carl Roth #6640) for 10 minutes twice, and rehydrated with a ethanol series (absolute, absolute, 95%, 85%, 50%, 30%, H<sub>2</sub>O, H<sub>2</sub>O) for 1 minute each. Dried sections were subsequently stained with 0.001% basic fuchsin for 1 minute, washed in H<sub>2</sub>O twice and dehydrated successively in 95% and absolute ethanol, and mounted in 50% glycerol for imaging under Zeiss Axiovision epifluorescence microscope.

### 9. qRT-PCR.

Seedling roots were harvested at 5 DAG and directly frozen in liquid nitrogen. After tissue grounding, RNA extraction has been carried out by using GeneMATRIX Universal RNA Purification Kit (EURx #3598) and following manufacture's instructions. Purified RNA has been used to synthesize cDNA first with the reaction mix in step 1 incubated at 65 °C for 5 minutes then on ice

**Table 13. cDNA synthesis reaction mix.**

Step 1		Step 2	
Reagent	Volume/Mass	Reagent	Volume/Mass
RNA	1 $\mu\text{g}$	5x RT buffer	2 $\mu\text{g}$
10 mM dNTP	0.625 $\mu\text{L}$	RNase inhibitor 40 u/ $\mu\text{L}$	0.25 $\mu\text{L}$
40 $\mu\text{M}$ oligodT primer	0.625 $\mu\text{L}$	100 mM DTT	0.5 $\mu\text{L}$
ddH <sub>2</sub> O	fill up to 7 $\mu\text{L}$	Reverse Transcriptase	0.25 $\mu\text{L}$

**Table 14. qRT-PCR reaction mix.**

Reagent	Volume ( $\mu\text{L}$ )
10x PCR buffer	1.5
50 mM MgCl <sub>2</sub>	0.2
10 mM dNTP	0.3
100 $\mu\text{M}$ primer_Fwd	0.05
100 $\mu\text{M}$ primer_Rev	0.05
Sybr Green (1:400)	0.15
Junp Start polymerase	0.3
ddH <sub>2</sub> O	7.45
cDNA template	5 (1:40 dilution)

**Table 15. qRT-PCR reaction cycles.**

Temperature (°C)	Duration	Number of cycles
95	6 min	
95	30 sec	x 45
59	20 sec	
72	30 sec	
Melt curve		
55-59 °C	1 °C per step	

for 5 minutes. The reaction mix in step 2 was then added to each tube and incubated at 42 °C for 1 hour and then 85 °C for 5 minutes (**Table 13**). qRT-PCR reaction has been performed as indicated in **Table 14 and 15**.

Supplemental information

Table S1. List of primers for sequencing and qRT-PCR.

Primer name	Experiment	Fwd primer	Rev primer
pCOB19_MR1		n/a	tgctcaatcactatctdctc
pGL2_MR		n/a	gggttgccggtgatactg
B-dummy_F		gtatctcgttcgactggtaaccac	ttgtatcccgctgactgtaatac
GR-Lh4G_MR		ctagcaaacgggttaacggtatacgg	n/a
D-dummy_F		gtggatccctgataaccctaac	gtggatccctgataaccctaac
RbcS_term_R		gtggcaaatggtggccctcaatg	ggaccatatactcctcaactc
UBQ10_term_R		n/a	ctatccgggataatacaaggcc
H-A_35g/ter_F	sequencing	gacatagatgctcctgtaaca	n/a
PME15_R		n/a	ttagggtcaaacgctgttga
KanR_R		n/a	ccggagaaacctgctggcaat
A-CO20_F		gctcaatgcaataatggag	ctgctgtaatgagatgcaacc
MW200_F		agacctcaactaaacctgaag	cgcttccgctgtaaatctggc
Z001_F		acctctgggctctctgg	cgattttgtagtctctgac
(p44-4_CAP8_(p44 <sup>int</sup> )) bet <sup>int</sup>	genotyping	aattcacaactctcaatcac	ctgaccggataatctgtaac
		gccaatgcaataatggag	tcaggagctcatgtagtaca
PME15 (AG231435) qRT-PCR	qRT-PCR	acgtgctttaattgcatgaacg	gaagtcacaattcccaagctg
(AA19_(AG115540))		gggttcaactgcatatccgttaaca	ccggtagatctccgatctttaca



Table S2 (follow-up). List of primers and modules for GreenGate cloning.

Intermediate module (single expression cassette)				Module composition					
Vector backbone	Plasmid number	G module	A module	B module	C module	D module	E module	F module	G module
M000	pS19017		UBQ10						
	pS19014		pM1						
	pS19026		pCOB1.9						
	pS19017	n/a		B-dummy	GR-LK04	D-dummy	Rbca_term	n/a	F-H adaptor
	pS19025								
	pS19032								
	pS19033								
M000	pS19038	H-A adaptor	pOp6	B-dummy	PME3 bn2.1	D-dummy	UBQ10_term	KanR	n/a
	pS19039								

Destination module (two expression cassettes on one F-DNA)				Module composition				
Vector backbone	Plasmid number	Plasmid name	A module	B module	C module	D module	E module	F module
Z001	pS19032	pUBQ10-GR-PME15	pOp6					
	pS19011	pM1-GR-PME3						
	pS19014	pCOB1.9-GR-PME15						
	pS19015	pGL2-GR-PME15						
	pS19013	pCO2-GR-PME15			pS19031			
	pS19029	pCASP1-GR-PME15						
	pS19010	pRFP-GR-PME3						
	pS19016	pRFP4-GR-PME15						
	pS19024	pUBQ10-GR-bn2-1						
	pS19037	pM1-GR-bn2-0						
	pS19035	pCOB1.9-GR-bn2-1						
	pS19038	pGL2-GR-bn2-1						
	pS19034	pCO2-GR-bn2-1						
	pS19040	pCASP1-GR-bn2-1						
pS19033	pRFP-GR-bn2-1							
pS19038	pRFP4-GR-bn2-1							
pS19025	GFP reporter line							
pS19054	Venus reporter line							



## Reference

- Abrash, E.B. & Bergmann, D.C., 2009. Asymmetric Cell Divisions: A View from Plant Development. *Developmental Cell*, 16(6), pp.783–796.
- Aida, M. et al., 2004. The PLETHORA Genes Mediate Patterning of the Arabidopsis Root Stem Cell Niche. *Cell*, 119(1), pp.109–120.
- Albrecht, C. et al., 2012. Brassinosteroids inhibit pathogen-associated molecular pattern-triggered immune signaling independent of the receptor kinase BAK1. *Proceedings of the National Academy of Sciences*, 109(1), pp.303–308.
- An, C. & Mou, Z., 2011. Salicylic Acid and its Function in Plant Immunity. *Journal of Integrative Plant Biology*, 53(6), pp.412–428.
- Ana Sanz et al., 2018. The CWI Pathway: Regulation of the Transcriptional Adaptive Response to Cell Wall Stress in Yeast. *Journal of Fungi*, 4(1), pp.1–12.
- Antoniadi, I. et al., 2015. Cell-Type-Specific Cytokinin Distribution within the Arabidopsis Primary Root Apex. *THE PLANT CELL ONLINE*, 27(7), pp.1955–1967.
- Atta, R. et al., 2009. Pluripotency of Arabidopsis xylem pericycle underlies shoot regeneration from root and hypocotyl explants grown in vitro. *The Plant Journal*, 57(4), pp.626–644.
- Bai, M.-Y. et al., 2012. Brassinosteroid, gibberellin and phytochrome impinge on a common transcription module in Arabidopsis. *Nature Cell Biology*, 14(8), pp.810–817.
- Baluska, F. et al., 2003. Cytoskeleton-plasma membrane-cell wall continuum in plants. Emerging links revisited. *Plant Physiology*, 133(2), pp.482–491.
- Beeckman, T. & De Smet, I., 2014. Quick guide. *Current Biology*, 24(10), pp.R378–R379.
- Beemster, G.T.S. & Baskin, T.I., 1998. Analysis of cell division and elongation underlying the developmental acceleration of root growth in Arabidopsis thaliana. *Plant Physiology*, 116(4), pp.1515–1526.
- Belkhadir, Y. & Jaillais, Y., 2015. The molecular circuitry of brassinosteroid signaling. *New Phytologist*, 206(2), pp.522–540.
- Bennett, T. & Scheres, B., 2010. *Root Development—Two Meristems for the Price of One?* Elsevier.
- Bernardo-García, S. et al., 2014. BR-dependent phosphorylation modulates PIF4 transcriptional activity and shapes diurnal hypocotyl growth. *Genes & Development*, 28(15), pp.1681–1694.
- Besson, S. & Dumais, J., 2011. Universal rule for the symmetric division of plant cells. *Proceedings of the National Academy of Sciences*, 108(15), pp.6294–6299.
- Bielach, A. et al., 2012. Spatiotemporal Regulation of Lateral Root Organogenesis in Arabidopsis by Cytokinin. *THE PLANT CELL ONLINE*, 24(10), pp.3967–3981.
- Bindon, K.A., Bacic, A. & Kennedy, J.A., 2012. Tissue-Specific and Developmental Modifications of Grape Cell Walls Influence the Adsorption of Proanthocyanidins. *Journal of Agricultural and Food Chemistry*, 60(36), pp.9249–9260.
- Birnbaum, K.D., 2016. How many ways are there to make a root? *Current Opinion in Plant Biology*, 34, pp.61–67.
- Bishopp, A. et al., 2011. A Mutually Inhibitory Interaction between Auxin and Cytokinin Specifies Vascular Pattern in Roots. *Current Biology*, 21(11), pp.917–926.
- Blilou, I. et al., 2005. The PIN auxin efflux facilitator network controls growth and patterning in Arabidopsis roots. *Nature*, 433(7021), pp.39–44.
- Boisson-Dernier, A. et al., 2009. Disruption of the pollen-expressed FERONIA homologs ANXUR1 and ANXUR2 triggers pollen tube discharge. *Development (Cambridge, England)*, 136(19), pp.3279–3288.
- Bojar, D. et al., 2014. Crystal structures of the phosphorylated BRI1 kinase domain and implications for brassinosteroid signal initiation. *The Plant Journal*, 78(1), pp.31–43.
- Bonachela, J.A. et al., 2015. Termite mounds can increase the robustness of dryland ecosystems to climatic change. *Science*, 347(6222), pp.651–655.
- Bouton, S., 2002. QUASIMODO1 Encodes a Putative Membrane-Bound Glycosyltransferase Required for Normal Pectin Synthesis and Cell Adhesion in Arabidopsis. *THE PLANT CELL ONLINE*, 14(10), pp.2577–2590.

- Bowman, S.M. & Free, S.J., 2006. The structure and synthesis of the fungal cell wall. *BioEssays*, 28(8), pp.799–808.
- Brady, S.M. et al., 2007. A high-resolution root spatiotemporal map reveals dominant expression patterns. *Science*, 318(5851), pp.801–806.
- Braidwood, L., Breuer, C. & Sugimoto, K., 2013. My body is a cage: mechanisms and modulation of plant cell growth. *New Phytologist*, 201(2), pp.388–402.
- Braybrook, S.A. & Peaucelle, A., 2013. Mechano-Chemical Aspects of Organ Formation in *Arabidopsis thaliana*: The Relationship between Auxin and Pectin M. Grebe, ed. *PLoS ONE*, 8(3), pp.e57813–10.
- Brutus, A. et al., 2010. A domain swap approach reveals a role of the plant wall-associated kinase 1 (WAK1) as a receptor of oligogalacturonides. *Proceedings of the National Academy of Sciences of the United States of America*, 107(20), pp.9452–9457.
- Buer, C.S., Wasteneys, G.O. & Masle, J., 2003. Ethylene modulates root-wave responses in *Arabidopsis*. *Plant Physiology*, 132(2), pp.1085–1096.
- Burg, S.P., 1973. Ethylene in Plant Growth. *Proceedings of the National Academy of Sciences*, 70(2), pp.591–597.
- Burton, R.A., Gidley, M.J. & Fincher, G.B., 2010. Heterogeneity in the chemistry, structure and function of plant cell walls. *Nature Chemical Biology*, 6(10), pp.724–732.
- Cai, Z. et al., 2014. GSK3-like kinases positively modulate abscisic acid signaling through phosphorylating subgroup III SnRK2s in *Arabidopsis*. *Proceedings of the National Academy of Sciences of the United States of America*, 111(26), pp.9651–9656.
- Caño-Delgado, A.I. et al., 2004. BRL1 and BRL3 are novel brassinosteroid receptors that function in vascular differentiation in *Arabidopsis*. *Development (Cambridge, England)*, 131(21), pp.5341–5351.
- Caño-Delgado, A.I. et al., 2003. Reduced cellulose synthesis invokes lignification and defense responses in *Arabidopsis thaliana*. *The Plant Journal*, 34(3), pp.351–362.
- Casamitjana-Martínez, E. et al., 2003. Root-Specific CLE19 Overexpression and the *sol1/2* Suppressors Implicate a CLV-like Pathway in the Control of *Arabidopsis* Root Meristem Maintenance. *Current Biology*, 13(16), pp.1435–1441.
- Cattaneo, P. & Hardtke, C.S., 2017. BIG BROTHER Uncouples Cell Proliferation from Elongation in the *Arabidopsis* Primary Root. *Plant and Cell Physiology*, 58(9), pp.1519–1527.
- Cederholm, H.M., Iyer-Pascuzzi, A.S. & Benfey, P.N., 2012. Patterning the primary root in *Arabidopsis*. *Wiley interdisciplinary reviews. Developmental biology*, 1(5), pp.675–691.
- Chen, J. & Yin, Y., 2017. WRKY transcription factors are involved in brassinosteroid signaling and mediate the crosstalk between plant growth and drought tolerance. *Plant Signaling & Behavior*, 12(11), p.e1365212.
- Cheng, Y., Zhu, W., Chen, Y., Ito, S., Asami, T. & Wang, X., 2014. Brassinosteroids control root epidermal cell fate via direct regulation of a MYB-bHLH-WD40 complex by GSK3-like kinases. *eLife*, 3, pp.366–17.
- Chinchilla, D. et al., 2007. A flagellin-induced complex of the receptor FLS2 and BAK1 initiates plant defence. *Nature*, 448(7152), pp.497–500.
- Cho, H., 2013. A secreted peptide acts on BIN2-mediated phosphorylation of ARFs to potentiate auxin response during lateral root development. *Nature Cell Biology*, 16(1), pp.66–76.
- Clouse, S.D. & Sasse, J.M., 1998. BRASSINOSTEROIDS: Essential Regulators of Plant Growth and Development. *Annual Review of Plant Physiology and Plant Molecular Biology*, 49(1), pp.427–451.
- Clouse, S.D., Langford, M. & McMorris, T.C., 1996. A Brassinosteroid-Insensitive Mutant in *Arabidopsis thaliana* Exhibits Multiple Defects in Growth and Development. *Plant Physiology*, 111(3), pp.671–678.
- C.L.1991, Development, How does the cytoskeleton read the laws of geometry in aligning the division plane of plant cells?
- Cosgrove, D.J., 2000a. Expansive growth of plant cell walls. *Plant physiology and biochemistry : PPB*, 38(1-2), pp. 109–124.
- Cosgrove, D.J., 2005. Growth of the plant cell wall. *Nature reviews. Molecular cell biology*, 6(11), pp.850–861.
- Cosgrove, D.J., 2000b. Loosening of plant cell walls by expansins. *Nature*, 407(6802), pp.321–326.
- Cosgrove, D.J., 2016. Plant cell wall extensibility: connecting plant cell growth with cell wall structure, mechanics, and the action of wall-modifying enzymes. *Journal of Experimental Botany*, 67(2), pp.463–476.

- Cosgrove, D.J., 2015. ScienceDirect Plant expansins: diversity and interactions with plant cell walls. *Current Opinion in Plant Biology*, 25, pp.162–172.
- Cosgrove, D.J., 2014. ScienceDirect Re-constructing our models of cellulose and primary cell wall assembly. *Current Opinion in Plant Biology*, 22, pp.122–131.
- Cosgrove, D.J. & Jarvis, M.C., 2012. Comparative structure and biomechanics of plant primary and secondary cell walls. *Frontiers in Plant Science*, 3.
- Cui, H. & Benfey, P.N., 2009. Interplay between SCARECROW, GA and LIKE HETEROCHROMATIN PROTEIN 1 in ground tissue patterning in the Arabidopsis root. *The Plant Journal*, 58(6), pp.1016–1027.
- Cvrcková, F. et al., 1995. Ste20-like protein kinases are required for normal localization of cell growth and for cytokinesis in budding yeast. *Genes & Development*, 9(15), pp.1817–1830.
- D'Agostino, I.B., Deruère, J. & Kieber, J.J., 2000. Characterization of the response of the Arabidopsis response regulator gene family to cytokinin. *Plant Physiology*, 124(4), pp.1706–1717.
- D, D.S. & B, L.P., 2010. FERONIA Is a Key Modulator of Brassinosteroid and Ethylene Responsiveness in Arabidopsis Hypocotyls. *MOLECULAR PLANT*, 3(3), pp.626–640.
- Daher, F.B. & Braybrook, S.A., 2015. How to let go: pectin and plant cell adhesion. *Frontiers in Plant Science*, 6, pp.1–8.
- Davière, J.-M. & Achard, P., 2013. Gibberellin signaling in plants. *Development (Cambridge, England)*, 140(6), pp.1147–1151.
- de Lucas, M. et al., 2008. A molecular framework for light and gibberellin control of cell elongation. *Nature*, 451(7177), pp.480–484.
- De Rybel, B. et al., 2013. A bHLH Complex Controls Embryonic Vascular Tissue Establishment and Indeterminate Growth in Arabidopsis. *Developmental Cell*, 24(4), pp.426–437.
- De Vos, D. et al., 2014. Putting Theory to the Test: Which Regulatory Mechanisms Can Drive Realistic Growth of a Root? S. X. Sun, ed. *PLoS Computational Biology*, 10(10), pp.e1003910–19.
- Decreux, A. & Messiaen, J., 2005. Wall-associated Kinase WAK1 Interacts with Cell Wall Pectins in a Calcium-induced Conformation. *Plant and Cell Physiology*, 46(2), pp.268–278.
- DECREUX, A. et al., 2006. In vitro characterization of the homogalacturonan-binding domain of the wall-associated kinase WAK1 using site-directed mutagenesis. *Phytochemistry*, 67(11), pp.1068–1079.
- Delamarre, L., 2005. Differential Lysosomal Proteolysis in Antigen-Presenting Cells Determines Antigen Fate. *Science*, 307(5715), pp.1630–1634.
- Derbyshire, P., McCann, M.C. & Roberts, K., 2007. Restricted cell elongation in Arabidopsis hypocotyls is associated with a reduced average pectin esterification level. *BMC Plant Biology*, 7(1), pp.31–12.
- Deruère, J. et al., 1999. The RCN1-encoded A subunit of protein phosphatase 2A increases phosphatase activity in vivo. *The Plant Journal*, 20(4), pp.389–399.
- Desprez, T. et al., 2007. Organization of cellulose synthase complexes involved in primary cell wall synthesis in Arabidopsis thaliana. *Proceedings of the National Academy of Sciences*, 104(39), pp.15572–15577.
- Dhonukshe, P. et al., 2005. *BMC Biology*. *BMC biology*, 3(1), pp.11–15.
- Di Mambro, R. et al., 2017. Auxin minimum triggers the developmental switch from cell division to cell differentiation in the Arabidopsis root. *Proceedings of the National Academy of Sciences*, 114(36), pp.E7641–E7649.
- Di Matteo, A., 2005. Structural Basis for the Interaction between Pectin Methyltransferase and a Specific Inhibitor Protein. *THE PLANT CELL ONLINE*, 17(3), pp.849–858.
- Dick-Pérez, M. et al., 2011. Structure and Interactions of Plant Cell-Wall Polysaccharides by Two- and Three-Dimensional Magic-Angle-Spinning Solid-State NMR. *Biochemistry*, 50(6), pp.989–1000.
- Ding, S.-Y., Zhao, S. & Zeng, Y., 2013. Size, shape, and arrangement of native cellulose fibrils in maize cell walls. *Cellulose*, 21(2), pp.863–871.
- Dinneny, J.R. et al., 2008. Cell identity mediates the response of Arabidopsis roots to abiotic stress. *Science*, 320(5878), pp.942–945.
- Doblin, M.S. et al., 2002. Cellulose biosynthesis in plants: from genes to rosettes. *Plant and Cell Physiology*, 43(12), pp.1407–1420.

- Doco, T. et al., 2003. Polysaccharides from grape berry cell walls. Part II. Structural characterization of the xyloglucan polysaccharides. *Carbohydrate Polymers*, 53(3), pp.253–261.
- Dodsworth, S., 2009. A diverse and intricate signalling network regulates stem cell fate in the shoot apical meristem. *Developmental Biology*, 336(1), pp.1–9.
- Dolan, L., 2005. Positional information and mobile transcriptional regulators determine cell pattern in the Arabidopsis root epidermis. *Journal of Experimental Botany*, 57(1), pp.51–54.
- Dolan, L. et al., Cellular organisation of the Arabidopsis thaliana root. *dev.biologists.org*
- Domagalska, M.A. et al., 2007. Attenuation of brassinosteroid signaling enhances FLC expression and delays flowering. *Development (Cambridge, England)*, 134(15), pp.2841–2850.
- Drisch, R.C. & Stahl, Y., 2015. Function and regulation of transcription factors involved in root apical meristem and stem cell maintenance. *Frontiers in Plant Science*, 6, pp.1–8.
- Dubrovsky, J.G. et al., 2008. Auxin acts as a local morphogenetic trigger to specify lateral root founder cells. *Proceedings of the National Academy of Sciences of the United States of America*, 105(25), pp.8790–8794.
- Dubrovsky, J.G. et al., 2006. Lateral Root Initiation in Arabidopsis: Developmental Window, Spatial Patterning, Density and Predictability. *Annals of Botany*, 97(5), pp.903–915.
- Dubrovsky, J.G. et al., 2000. Pericycle cell proliferation and lateral root initiation in Arabidopsis. *Plant Physiology*, 124(4), pp.1648–1657.
- Dupuy, L., Mackenzie, J. & Haseloff, J., 2010. Coordination of plant cell division and expansion in a simple morphogenetic system. *Proceedings of the National Academy of Sciences*, 107(6), pp.2711–2716.
- El-Shawk, S. et al., 2015. Parsimonious Model of Vascular Patterning Links Transverse Hormone Fluxes to Lateral Root Initiation: Auxin Leads the Way, while Cytokinin Levels Out T. Beeckman, ed. *PLoS Computational Biology*, 11(10), pp.e1004450–40.
- Ellis, C. & Turner, J.G., 2001. The Arabidopsis Mutant *cev1* Has Constitutively Active Jasmonate and Ethylene Signal Pathways and Enhanced Resistance to Pathogens. *The Plant cell*, 13(5), p.1025.
- Endres, S. & Tenhaken, R., 2011. Down-regulation of the myo-inositol oxygenase gene family has no effect on cell wall composition in Arabidopsis. *Planta*, 234(1), pp.157–169.
- Fan, M. et al., 2014. The bHLH Transcription Factor HBI1 Mediates the Trade-Off between Growth and Pathogen-Associated Molecular Pattern-Triggered Immunity in Arabidopsis. *THE PLANT CELL ONLINE*, 26(2), pp.828–841.
- Fernandes, A.N., the, L.T.P.O.2011, Nanostructure of cellulose microfibrils in spruce wood. *National Academy Sciences*
- Finkelstein, R., 2013. Abscisic Acid Synthesis and Response. *The Arabidopsis Book*, 11, pp.e0166–36.
- Fleming, A.J., 2005. The co-ordination of cell division, differentiation and morphogenesis in the shoot apical meristem: a perspective. *Journal of Experimental Botany*, 57(1), pp.25–32.
- Fletcher, J.C., 2002. Coordination of cell proliferation and cell fate decisions in the angiosperm shoot apical meristem. *BioEssays*, 24(1), pp.27–37.
- Francis, K.E., Lam, S.Y. & Copenhaver, G.P., 2006. Separation of Arabidopsis Pollen Tetrads Is Regulated by QUARTET1, a Pectin Methyltransferase Gene. *Plant Physiology*, 142(3), pp.1004–1013.
- Fridman, Y. et al., 2014. Root growth is modulated by differential hormonal sensitivity in neighboring cells. *Genes & Development*, 28(8), pp.912–920.
- Fridman, Y. et al., 2016. High Resolution Quantification of Crystalline Cellulose Accumulation in Arabidopsis Roots to Monitor Tissue-specific Cell Wall Modifications. *Journal of visualized experiments : JoVE*, (111), pp.e53707–e53707.
- Friedrichsen, D.M. et al., 2000. Brassinosteroid-insensitive-1 is a ubiquitously expressed leucine-rich repeat receptor serine/threonine kinase. *Plant Physiology*, 123(4), pp.1247–1256.
- Friml, J. et al., 2002. AtPIN4 mediates sink-driven auxin gradients and root patterning in Arabidopsis. *Cell*, 108(5), pp.661–673.
- Fry, S.C. et al., 1992. Xyloglucan endotransglycosylase, a new wall-loosening enzyme activity from plants. *Biochemical Journal*, 282 ( Pt 3)(Pt 3), pp.821–828.
- Furner, J., Development, J.P.1992, Cell fate in the shoot apical meristem of Arabidopsis thaliana. *dev.biologists.org*

- Galinha, C. et al., 2007. PLETHORA proteins as dose-dependent master regulators of Arabidopsis root development. *Nature*, 449(7165), pp.1053–1057.
- Gallagher, K.L. et al., 2004. Mechanisms Regulating SHORT-ROOT Intercellular Movement. *Current Biology*, 14(20), pp.1847–1851.
- Gallego-Bartolomé, J. et al., 2012. Molecular mechanism for the interaction between gibberellin and brassinosteroid signaling pathways in Arabidopsis. *Proceedings of the National Academy of Sciences*, 109(33), pp.13446–13451.
- Gampala, S.S. et al., 2007. An Essential Role for 14-3-3 Proteins in Brassinosteroid Signal Transduction in Arabidopsis. *Developmental Cell*, 13(2), pp.177–189.
- Gifford, M.L. et al., 2008. Cell-specific nitrogen responses mediate developmental plasticity. *Proceedings of the National Academy of Sciences of the United States of America*, 105(2), pp.803–808.
- González-García, M.-P. et al., 2011. Brassinosteroids control meristem size by promoting cell cycle progression in Arabidopsis roots. *Development (Cambridge, England)*, 138(5), pp.849–859.
- Gravino, M. et al., 2015. Ethylene production in Botrytis cinerea- and oligogalacturonide-induced immunity requires calcium-dependent protein kinases. *The Plant Journal*, 84(6), pp.1073–1086.
- Gray, W.M., 2004. Hormonal Regulation of Plant Growth and Development. *PLoS Biology*, 2(9), pp.e311–4.
- Grieneisen, V.A. et al., 2007. Auxin transport is sufficient to generate a maximum and gradient guiding root growth. *Nature*, 449(7165), pp.1008–1013.
- Grieneisen, V.A. et al., 2012. Morphogengineering roots: comparing mechanisms of morphogen gradient formation. *BMC systems biology*, 6(1), p.37.
- Gudesblat, G.E. et al., 2012. SPEECHLESS integrates brassinosteroid and stomata signalling pathways. *Nature Cell Biology*, 14(5), pp.548–554.
- Guerrero, G., Fugelstad, J. & Bulone, V., 2010. What Do We Really Know about Cellulose Biosynthesis in Higher Plants? *Journal of Integrative Plant Biology*, 52(2), pp.161–175.
- Hacham, Y. et al., 2011. Brassinosteroid perception in the epidermis controls root meristem size. *Development (Cambridge, England)*, 138(5), pp.839–848.
- Hamann, T., 2014. The Plant Cell Wall Integrity Maintenance Mechanism—Concepts for Organization and Mode of Action. *Plant and Cell Physiology*, 56(2), pp.215–223.
- Hammes, U.Z., 2016. Novel roles for phyto-sulfonamide signalling in plant-pathogen interactions. *Plant, Cell & Environment*, 39(7), pp.1393–1395.
- Han, Z., Sun, Y. & Chai, J., 2014. ScienceDirect Structural insight into the activation of plant receptor kinases. *Current Opinion in Plant Biology*, 20, pp.55–63.
- Hanano, S. et al., 2006. Multiple phytohormones influence distinct parameters of the plant circadian clock. *Genes to Cells*, 11(12), pp.1381–1392.
- Harholt, J., Suttangkakul, A. & Vibe Scheller, H., 2010. Biosynthesis of Pectin. *Plant Physiology*, 153(2), pp.384–395.
- Hartwig, T. et al., Brassinosteroid control of sex determination in maize. *National Academy Sciences*
- Haruta, M. et al., 2014. A Peptide Hormone and Its Receptor Protein Kinase Regulate Plant Cell Expansion. *Science*, 343(6169), pp.408–411.
- Haswell, E.S. et al., 2008. Two MscS Homologs Provide Mechanosensitive Channel Activities in the Arabidopsis Root. *Current Biology*, 18(10), pp.730–734.
- He, J.-X. et al., 2002. The GSK3-like kinase BIN2 phosphorylates and destabilizes BZR1, a positive regulator of the brassinosteroid signaling pathway in Arabidopsis. *Proceedings of the National Academy of Sciences*, 99(15), pp. 10185–10190.
- He, Z. et al., 2000. Perception of brassinosteroids by the extracellular domain of the receptor kinase BRI1. *Science*, 288(5475), pp.2360–2363.
- Helariutta, Y. et al., 2000. The SHORT-ROOT gene controls radial patterning of the Arabidopsis root through radial signaling. *Cell*, 101(5), pp.555–567.
- HEMATY, K. & Hofte, H., 2008. Novel receptor kinases involved in growth regulation. *Current Opinion in Plant Biology*, 11(3), pp.321–328.

- Heremans, J.P. et al., 2008. Enhancement of Thermoelectric Efficiency in PbTe by Distortion of the Electronic Density of States. *Science*, 321(5888), pp.554–557.
- Hernández-Blanco, C. et al., 2007. Impairment of cellulose synthases required for Arabidopsis secondary cell wall formation enhances disease resistance. *THE PLANT CELL ONLINE*, 19(3), pp.890–903.
- Hématy, K. et al., 2007. A Receptor-like Kinase Mediates the Response of Arabidopsis Cells to the Inhibition of Cellulose Synthesis. *Current Biology*, 17(11), pp.922–931.
- Holzwardt, E. et al., 2018. Integration of Brassinosteroid and Phytosulfokine Signalling Controls Vascular Cell Fate in the Arabidopsis Root. pp.1–18.
- Hove, ten, C.A., Lu, K.J. & Weijers, D., 2015. Building a plant: cell fate specification in the early Arabidopsis embryo. *Development (Cambridge, England)*, 142(3), pp.420–430.
- Höfte, H., 2015. The Yin and Yang of Cell Wall Integrity Control: Brassinosteroid and FERONIA Signaling. *Plant and Cell Physiology*, 56(2), pp.224–231.
- Hutchison, C.E. & Kieber, J.J., 2002. Cytokinin Signaling in Arabidopsis. *THE PLANT CELL ONLINE*, 14(suppl 1), pp.S47–S59.
- Hwang, I. & Sheen, J., 2001. Two-component circuitry in Arabidopsis cytokinin signal transduction. *Nature*, 413(6854), pp.383–389.
- Hyodo, H. et al., 2013. Tissue Specific Localization of Pectin–Ca<sup>2+</sup> Cross-Linkages and Pectin Methyl-Esterification during Fruit Ripening in Tomato (*Solanum lycopersicum*) R. Balestrini, ed. *PLoS ONE*, 8(11), pp.e78949–10.
- Ibañez, C. et al., 2018. Brassinosteroids Dominate Hormonal Regulation of Plant Thermomorphogenesis via BZR1. *Current Biology*, pp.1–17.
- Imamura, A. et al., 1998. Response regulators implicated in His-to-Asp phosphotransfer signaling in Arabidopsis. *Proceedings of the National Academy of Sciences*, 95(5), pp.2691–2696.
- Ioio, Dello, R. et al., 2008. A genetic framework for the control of cell division and differentiation in the root meristem. *Science*, 322(5906), pp.1380–1384.
- Ioio, Dello, R. et al., 2007. Cytokinins Determine Arabidopsis Root-Meristem Size by Controlling Cell Differentiation. *Current Biology*, 17(8), pp.678–682.
- Iqbal, N. et al., 2017. Ethylene Role in Plant Growth, Development and Senescence: Interaction with Other Phytohormones. *Frontiers in Plant Science*, 08(9), pp.6484–19.
- Ito, T. et al., 2014. Plant GSK3 proteins regulate xylem cell differentiation downstream of TDIF–TDR signalling. *Nature Communications*, 5, pp.1–11.
- Ivanov, V.B. & Dubrovsky, J.G., 2013. Longitudinal zonation pattern in plant roots: conflicts and solutions. *Trends in Plant Science*, 18(5), pp.237–243.
- Jaillais, Y. & Chory, J., 2010. Unraveling the paradoxes of plant hormone signaling integration. *Nature structural & molecular biology*, 17(6), pp.642–645.
- Jaillais, Y. & Vert, G., 2012. Brassinosteroids, gibberellins and light-mediated signalling are the three-way controls of plant sprouting. *Nature Cell Biology*, 14(8), pp.788–790.
- Jaillais, Y., Belkhadir, Y., et al., 2011a. Extracellular leucine-rich repeats as a platform for receptor/coreceptor complex formation. *Proceedings of the National Academy of Sciences of the United States of America*, 108(20), pp.8503–8507.
- Jaillais, Y., Hothorn, M., et al., 2011b. Tyrosine phosphorylation controls brassinosteroid receptor activation by triggering membrane release of its kinase inhibitor. *Genes & Development*, 25(3), pp.232–237.
- Jang, J.C. et al., 2000. A critical role of sterols in embryonic patterning and meristem programming revealed by the fackel mutants of Arabidopsis thaliana. *Genes & Development*, 14(12), pp.1485–1497.
- Kauschmann, A. et al., Genetic evidence for an essential role of brassinosteroids in plant development. *Wiley Online Library*.
- Keegstra, K., 2010. Plant Cell Walls. *Plant Physiology*, 154(2), pp.483–486.
- Khan, M. et al., 2013. Brassinosteroid-regulated GSK3/Shaggy-like kinases phosphorylate mitogen-activated protein (MAP) kinase kinases, which control stomata development in Arabidopsis thaliana. *Journal of Biological Chemistry*, 288(11), pp.7519–7527.

- Khan, N.A., 2005. The influence of exogenous ethylene on growth and photosynthesis of mustard (*Brassica juncea*) following defoliation. *Scientia Horticulturae*, 105(4), pp.499–505.
- Kidner, C. et al., 2000. Clonal analysis of the *Arabidopsis* root confirms that position, not lineage, determines cell fate. *Planta*, 211(2), pp.191–199.
- Kieber, J.J. & Schaller, G.E., 2014. Cytokinins. *The Arabidopsis Book*, 12, p.e0168.
- Kim, G., Dhar, S. & Lim, J., 2017. The SHORT-ROOT regulatory network in the endodermis development of *Arabidopsis* roots and shoots. *Journal of Plant Biology*, 60(4), pp.306–313.
- Kim, T.-W. et al., 2012. Brassinosteroid regulates stomatal development by GSK3-mediated inhibition of a MAPK pathway. *Nature*, 482(7385), pp.419–422.
- Kim, T.-W. et al., 2009. Brassinosteroid signal transduction from cell-surface receptor kinases to nuclear transcription factors. *Nature Cell Biology*, 11(10), pp.1254–1260.
- Kim, T.-W. et al., 2011. The CDG1 Kinase Mediates Brassinosteroid Signal Transduction from BRI1 Receptor Kinase to BSU1 Phosphatase and GSK3-like Kinase BIN2. *Molecular Cell*, 43(4), pp.561–571.
- Kohorn, B.D., 2016. Cell wall-associated kinases and pectin perception. *Journal of Experimental Botany*, 67(2), pp.489–494.
- Kohorn, B.D. et al., 2009. Pectin activation of MAP kinase and gene expression is WAK2 dependent. *The Plant Journal*, 60(6), pp.974–982.
- Kondo, Y. et al., 2014. Plant GSK3 proteins regulate xylem cell differentiation downstream of TDIF-TDR signalling. *Nature Communications*, 5, p.3504.
- Kondo, Y., Hirakawa, Y. & Fukuda, H., 2013. Chapter 14 TDIF. In *Chapter 230 Neurotrophic Peptides*. pp. 71–75.
- Krecek, P. et al., 2009. The PIN-FORMED (PIN) protein family of auxin transporters. *Genome biology*, 10(12), p.249.
- Kuppusamy, K.T., Chen, A.Y. & Nemhauser, J.L., 2009a. Steroids are required for epidermal cell fate establishment in *Arabidopsis* roots. *Proceedings of the National Academy of Sciences of the United States of America*, 106(19), pp.8073–8076.
- Kutschera, U. & Niklas, K.J., 2007. The epidermal-growth-control theory of stem elongation: An old and a new perspective. *Journal of Plant Physiology*, 164(11), pp.1395–1409.
- Lampropoulos, A. et al., 2013. GreenGate - A Novel, Versatile, and Efficient Cloning System for Plant Transgenesis P. J. Janssen, ed. *PLoS ONE*, 8(12), pp.e83043–15.
- Laplaze, L. et al., 2007. Cytokinins Act Directly on Lateral Root Founder Cells to Inhibit Root Initiation. *THE PLANT CELL ONLINE*, 19(12), pp.3889–3900.
- Laskowski, M. et al., 2008. Root System Architecture from Coupling Cell Shape to Auxin Transport D. Weigel, ed. *PLoS Biology*, 6(12), pp.e307–15.
- Lee, D.J. et al., 2007. Genome-wide expression profiling of ARABIDOPSIS RESPONSE REGULATOR 7 (ARR7) overexpression in cytokinin response. *Molecular genetics and genomics : MGG*, 277(2), pp.115–137.
- Lee, H.-S. et al., 2015. Brassinazole resistant 1 (BZR1)-dependent brassinosteroid signalling pathway leads to ectopic activation of quiescent cell division and suppresses columella stem cell differentiation. *Journal of Experimental Botany*, 66(15), pp.4835–4849.
- Li, D. et al., 2002. Purple Acid Phosphatases of *Arabidopsis thaliana*. *Journal of Biological Chemistry*, 277(31), pp.27772–27781.
- Li, J. & Chory, J., 1997. A Putative Leucine-Rich Repeat Receptor Kinase Involved in Brassinosteroid Signal Transduction. *Cell*, 90(5), pp.929–938.
- Li, J. & Chory, J., 1999. Review article. Brassinosteroid actions in plants. *Journal of Experimental Botany*, 50(332), pp.275–282.
- Li, J. & Nam, K.H., 2002. Regulation of brassinosteroid signaling by a GSK3/SHAGGY-like kinase. *Science*, 295(5558), pp.1299–1301.
- Li, J. et al., 2001. BIN2, a new brassinosteroid-insensitive locus in *Arabidopsis*. *Plant Physiology*, 127(1), pp.14–22.
- Li, S.-B. et al., 2016. A Review of Auxin Response Factors (ARFs) in Plants. *Frontiers in Plant Science*, 7(742), pp.137–7.

- Li, Z., Chakraborty, S. & Xu, G., 2017. Differential CLE peptide perception by plant receptors implicated from structural and functional analyses of TDIF-TDR interactions B. Kobe, ed. *PLoS ONE*, 12(4), p.e0175317.
- Liang, Z. et al., 2015. Calpain-Mediated Positional Information Directs Cell Wall Orientation to Sustain Plant Stem Cell Activity, Growth and Development. *Plant and Cell Physiology*, 56(9), pp.1855–1866.
- Liao, C.-Y. et al., 2015. Reporters for sensitive and quantitative measurement of auxin response. *Nature Methods*, 12(3), pp.207–210.
- Lindeboom, J. et al., 2008. Cellulose microfibril deposition: coordinated activity at the plant plasma membrane. *Journal of microscopy*, 231(2), pp.192–200.
- Lindner, H. et al., 2012. CrRLK1L receptor-like kinases: not just another brick in the wall. *Current Opinion in Plant Biology*, 15(6), pp.659–669.
- Liners, F. et al., 1989. Monoclonal Antibodies against Pectin: Recognition of a Conformation Induced by Calcium. *Plant Physiology*, 91(4), pp.1419–1424.
- Lipka, E. et al., 2014. The Phragmoplast-Orienting Kinesin-12 Class Proteins Translate the Positional Information of the Preprophase Band to Establish the Cortical Division Zone in *Arabidopsis thaliana*. *The Plant cell*, 26(6), pp.2617–2632.
- Lipka, E., Herrmann, A. & Mueller, S., 2015. Mechanisms of plant cell division. *Wiley interdisciplinary reviews. Developmental biology*, 4(4), pp.391–405.
- Liu, Y. et al., 2017. Symplastic communication spatially directs local auxin biosynthesis to maintain root stem cell niche in *Arabidopsis*. *Proceedings of the National Academy of Sciences*, 114(15), pp.4005–4010.
- Louveaux, M. et al., 2016. Cell division plane orientation based on tensile stress in *Arabidopsis thaliana*. *Proceedings of the National Academy of Sciences*, 113(30), pp.E4294–E4303.
- Lozano-Durán, R. et al., 2013. The transcriptional regulator BZR1 mediates trade-off between plant innate immunity and growth. *eLife*, 2, pp.303–15.
- Luo, J. et al., 2009. A Novel Polyamine Acyltransferase Responsible for the Accumulation of Spermidine Conjugates in *Arabidopsis* Seed. *THE PLANT CELL ONLINE*, 21(1), pp.318–333.
- Ma, N. et al., 2013. Overexpression of OsEXPA8, a Root-Specific Gene, Improves Rice Growth and Root System Architecture by Facilitating Cell Extension M. J. Bennett, ed. *PLoS ONE*, 8(10), pp.e75997–10.
- Ma, X. et al., 2016. SERKING Coreceptors for Receptors. *Trends in Plant Science*, 21(12), pp.1017–1033.
- MacKinnon, I.M. et al., 2006. Cell-wall structure and anisotropy in procuste, a cellulose synthase mutant of *Arabidopsis thaliana*. *Planta*, 224(2), pp.438–448.
- Malinovsky, F.G., 2014. The role of the cell wall in plant immunity. pp.1–12.
- Malinovsky, F.G. et al., 2014. Antagonistic regulation of growth and immunity by the *Arabidopsis* basic helix-loop-helix transcription factor homolog of brassinosteroid enhanced expression2 interacting with increased leaf inclination1 binding bHLH1. *Plant Physiology*, 164(3), pp.1443–1455.
- Mandava, N., 1988. Plant Growth-Promoting Brassinosteroids. *Annual Review of Plant Physiology and Plant Molecular Biology*, 39(1), pp.23–52.
- Marquès-Bueno, M.M. et al., 2016. A versatile Multisite Gateway-compatible promoter and transgenic line collection for cell type-specific functional genomics in *Arabidopsis*. *The Plant Journal*, 85(2), pp.320–333.
- Matsubayashi, Y., 2006. Disruption and Overexpression of *Arabidopsis* Phytosulfokine Receptor Gene Affects Cellular Longevity and Potential for Growth. *Plant Physiology*, 142(1), pp.45–53.
- Mähönen, A.P. et al., 2006. Cytokinins Regulate a Bidirectional Phosphorelay Network in *Arabidopsis*. *Current Biology*, 16(11), pp.1116–1122.
- McCann, M.C. et al., 1993. Orientation of macromolecules in the walls of elongating carrot cells. *Journal of Cell Science*, 106 ( Pt 4), pp.1347–1356.
- Meijón, M. et al., 2013. Genome-wide association study using cellular traits identifies a new regulator of root development in *Arabidopsis*. *Nature Publishing Group*, 46(1), pp.77–81.
- Migliaccio, F., Fortunati, A. & Tassone, P., 2014. *Arabidopsis* root growth movements and their symmetry. *Plant Signaling & Behavior*, 4(3), pp.183–190.
- Mirabet, V. et al., 2011. The Role of Mechanical Forces in Plant Morphogenesis. *Annual Review of Plant Biology*, 62(1), pp.365–385.

- Miyashima, S. et al., 2012. Review Stem cell function during plant vascular development. *The EMBO Journal*, 32(2), pp.178–193.
- Miyazaki, S. et al., 2009. ANXUR1 and 2, Sister Genes to FERONIA/SIRENE, Are Male Factors for Coordinated Fertilization. *Current Biology*, 19(15), pp.1327–1331.
- MOHNEN, D., 2008. Pectin structure and biosynthesis. *Current Opinion in Plant Biology*, 11(3), pp.266–277.
- Moore, I. et al., 1998. A transcription activation system for regulated gene expression in transgenic plants. *Proceedings of the National Academy of Sciences*, 95(1), pp.376–381.
- Moriwaki, T. et al., 2014. GNOM regulates root hydrotropism and phototropism independently of PIN-mediated auxin transport. *Plant Science*, 215-216, pp.141–149.
- Möller, B.K. et al., 2017. Auxin response cell-autonomously controls ground tissue initiation in the early Arabidopsis embryo. *Proceedings of the National Academy of Sciences*, 114(12), pp.E2533–E2539.
- Müller, S., Han, S. & Smith, L.G., 2006. Two Kinesins Are Involved in the Spatial Control of Cytokinesis in Arabidopsis thaliana. *Current Biology*, 16(9), pp.888–894.
- Müller, J. et al., 2009. Arabidopsis MPK6 is involved in cell division plane control during early root development, and localizes to the pre-prophase band, phragmoplast, trans-Golgi network and plasma membrane. *The Plant Journal*, 61(2), pp.234–248.
- Müssig, C., Shin, G.-H. & Altmann, T., 2003. Brassinosteroids promote root growth in Arabidopsis. *Plant Physiology*, 133(3), pp.1261–1271.
- Nakagawa, Y. et al., 2007. Arabidopsis plasma membrane protein crucial for Ca<sup>2+</sup> influx and touch sensing in roots. *Proceedings of the National Academy of Sciences*, 104(9), pp.3639–3644.
- Nakamura, A. et al., 2003. Brassinolide induces IAA5, IAA19, and DR5, a synthetic auxin response element in Arabidopsis, implying a cross talk point of brassinosteroid and auxin signaling. *Plant Physiology*, 133(4), pp.1843–1853.
- Nakashima, K. & Yamaguchi-Shinozaki, K., 2013. ABA signaling in stress-response and seed development. *Plant Cell Reports*, 32(7), pp.959–970.
- Newman, R.H., Hill, S.J. & Harris, P.J., 2013. Wide-Angle X-Ray Scattering and Solid-State Nuclear Magnetic Resonance Data Combined to Test Models for Cellulose Microfibrils in Mung Bean Cell Walls. *Plant Physiology*, 163(4), pp.1558–1567.
- Nishitani, K. & Demura, T., 2015. Editorial: An Emerging View of Plant Cell Walls as an Apoplastic Intelligent System. *Plant and Cell Physiology*, 56(2), pp.177–179.
- Nissen, K.S., Willats, W.G.T. & Malinovsky, F.G., 2016. Understanding CrRLK1L Function: Cell Walls and Growth Control. *Trends in Plant Science*, 21(6), pp.516–527.
- Norman, A.W., Mizwicki, M.T. & Norman, D.P.G., 2004. Steroid-hormone rapid actions, membrane receptors and a conformational ensemble model. *Nature reviews. Drug discovery*, 3(1), pp.27–41.
- Novotny, V., 2006. Why Are There So Many Species of Herbivorous Insects in Tropical Rainforests? *Science*, 313(5790), pp.1115–1118.
- O'Neill, M.A., ALBERSHEIM, P. & DARVILL, A., 1990. *12 The Pectic Polysaccharides of Primary Cell Walls*,
- Oh, E. et al., 2014. Cell elongation is regulated through a central circuit of interacting transcription factors in the Arabidopsis hypocotyl. *eLife*, 3, p.601.
- Oh, E., Zhu, J.-Y. & Wang, Z.-Y., 2012. Interaction between BZR1 and PIF4 integrates brassinosteroid and environmental responses. *Nature Cell Biology*, 14(8), pp.802–809.
- Oh, M.-H., 2005. Ordered Liquid Aluminum at the Interface with Sapphire. *Science*, 310(5748), pp.661–663.
- Oh, M.-H. et al., 2009. Tyrosine phosphorylation of the BRI1 receptor kinase emerges as a component of brassinosteroid signaling in Arabidopsis. *Proceedings of the National Academy of Sciences of the United States of America*, 106(2), pp.658–663.
- Okada, K. & Shimura, Y., 1990. Reversible root tip rotation in Arabidopsis seedlings induced by obstacle-touching stimulus. *Science*, 250(4978), pp.274–276.
- Oliva, M. & Dunand, C., 2007. Waving and skewing: how gravity and the surface of growth media affect root development in Arabidopsis. *New Phytologist*, 176(1), pp.37–43.

- Pan, W. & Kastin, A.J., 2013. Chapter 230 Neurotrophic Peptides. In *A.J.Kastin Handbook of Biologically Active Peptides 1st ed. 2006 Academic Press 0-12-369442-6 1640 pp.*, Hardback, Price: £ 135.00, \$ 229.95, € 195. Elsevier, pp. 1682–1687.
- Pandey, G.K., 2017. *Mechanism of Plant Hormone Signaling Under Stress, 2 Volume Set* G. K. Pandey, ed., Hoboken, NJ, USA: John Wiley & Sons, Inc.
- Paniagua, C. et al., 2014. Fruit softening and pectin disassembly: an overview of nanostructural pectin modifications assessed by atomic force microscopy. *Annals of Botany*, 114(6), pp.1375–1383.
- Parizot, B. et al., 2012. In silico analyses of pericycle cell populations reinforce their relation with associated vasculature in Arabidopsis. *Philosophical transactions of the Royal Society of London. Series B, Biological sciences*, 367(1595), pp.1479–1488.
- Park, Y.B. & Cosgrove, D.J., 2012. A Revised Architecture of Primary Cell Walls Based on Biomechanical Changes Induced by Substrate-Specific Endoglucanases. *Plant Physiology*, 158(4), pp.1933–1943.
- Pauli, S. et al., 2004. The Cauliflower Mosaic Virus 35S Promoter Extends into the Transcribed Region. *Journal of Virology*, 78(22), pp.12120–12128.
- Peaucelle, A. et al., 2008. Arabidopsis Phyllotaxis Is Controlled by the Methyl-Esterification Status of Cell-Wall Pectins. *Current Biology*, 18(24), pp.1943–1948.
- Peaucelle, A., Braybrook, S.A. & Hoefte, H., 2012. Cell wall mechanics and growth control in plants: the role of pectins revisited. *Frontiers in Plant Science*, 3.
- Peaucelle, A., Braybrook, S.A., et al., 2011a. Pectin-Induced Changes in Cell Wall Mechanics Underlie Organ Initiation in Arabidopsis. *Current Biology*, 21(20), pp.1720–1726.
- Peaucelle, A., Louvet, R., et al., 2011b. The transcription factor BELLRINGER modulates phyllotaxis by regulating the expression of a pectin methylesterase in Arabidopsis. *Development (Cambridge, England)*, 138(21), pp.4733–4741.
- Pelletier, S. et al., 2010. A role for pectin de-methylesterification in a developmentally regulated growth acceleration in dark-grown Arabidopsis hypocotyls. *New Phytologist*, 188(3), pp.726–739.
- Pelloux, J., RUSTERUCCI, C. & MELLEROWICZ, E., 2007. New insights into pectin methylesterase structure and function. *Trends in Plant Science*, 12(6), pp.267–277.
- Perilli, S. et al., 2013. RETINOBLASTOMA-RELATED Protein Stimulates Cell Differentiation in the Arabidopsis Root Meristem by Interacting with Cytokinin Signaling. *THE PLANT CELL ONLINE*, 25(11), pp.4469–4478.
- Petricka, J.J., Winter, C.M. & Benfey, P.N., 2012. Control of Arabidopsis root development. *Annual Review of Plant Biology*, 63, pp.563–590.
- Pillitteri, L.J., Guo, X. & Dong, J., 2016. Asymmetric cell division in plants: mechanisms of symmetry breaking and cell fate determination. *Cellular and Molecular Life Sciences*, 73(22), pp.4213–4229.
- Poppenberger, B. et al., 2011. CESTA, a positive regulator of brassinosteroid biosynthesis. *The EMBO Journal*, 30(6), pp.1149–1161.
- Radoeva, T. et al., 2016. Molecular characterization of Arabidopsis GAL4/UAS enhancer trap lines identifies novel cell type-specific promoters. *Plant Physiology*, pp.pp.00213.2016–13.
- Rahni, R. & Birnbaum, K.D., 2016. Plant Cell Shape: Trafficking Gets Edgy. *Developmental Cell*, 36(4), pp.353–354.
- Rasmussen, C.G., Sun, B. & Smith, L.G., 2010. Tangled localization at the cortical division site of plant cells occurs by several mechanisms. *Journal of Cell Science*, 124(2), pp.270–279.
- Rasmussen, C.G., Wright, A.J. & Müller, S., 2013. The role of the cytoskeleton and associated proteins in determination of the plant cell division plane. *The Plant Journal*, 75(2), pp.258–269.
- Reiter, W.D., Chapple, C. & Somerville, C.R., 1997. Mutants of Arabidopsis thaliana with altered cell wall polysaccharide composition. *The Plant Journal*, 12(2), pp.335–345.
- Ribeiro, R.C., Kushner, P.J. & Baxter, J.D., 1995. The nuclear hormone receptor gene superfamily. *Annual review of medicine*, 46(1), pp.443–453.
- Ridley, B.L., O'Neill, M.A. & Mohnen, D., 2001. Pectins: structure, biosynthesis, and oligogalacturonide-related signaling. *Phytochemistry*, 57(6), pp.929–967.
- Roland, J.C., 1978. Cell wall differentiation and stages involved with intercellular gas space opening. *Journal of Cell Science*, 32, pp.325–336.

- Roy, R. & Bassham, D.C., 2014. Root growth movements: Waving and skewing. *Plant Science*, 221-222, pp.42–47.
- Rutherford, R., Gallois, P. & Masson, P.H., 1998. Mutations in *Arabidopsis thaliana* genes involved in the tryptophan biosynthesis pathway affect root waving on tilted agar surfaces. *The Plant Journal*, 16(2), pp.145–154.
- Sabatini, S. et al., 1999. An auxin-dependent distal organizer of pattern and polarity in the *Arabidopsis* root. *Cell*, 99(5), pp.463–472.
- Sablowski, R., 2016. Coordination of plant cell growth and division: collective control or mutual agreement? *Current Opinion in Plant Biology*, 34, pp.54–60.
- Samalova, M., Brzobohaty, B. & Moore, I., 2005. pOp6/LhGR: a stringently regulated and highly responsive dexamethasone-inducible gene expression system for tobacco. *The Plant Journal*, 41(6), pp.919–935.
- Santner, A.A. & Estelle, M., 2009. Recent advances and emerging trends in plant hormone signalling. *Nature*, 459(7250), pp.1071–1078.
- Santner, A.A. & Watson, J.C., 2006. The WAG1 and WAG2 protein kinases negatively regulate root waving in *Arabidopsis*. *The Plant Journal*, 45(5), pp.752–764.
- Sato, E.M. et al., 2014. New insights into root gravitropic signalling. *Journal of Experimental Botany*, 66(8), pp.2155–2165.
- Sauter, M., 2015. Phytosulfokine peptide signalling. *Journal of Experimental Botany*, 66(17), pp.5161–5169.
- Savaldi-Goldstein, S., Peto, C. & Chory, J., 2007. The epidermis both drives and restricts plant shoot growth. *Nature*, 446(7132), pp.199–202.
- Saxena, I.M. & Brown, R.M., 2005. Cellulose biosynthesis: current views and evolving concepts. *Annals of Botany*, 96(1), pp.9–21.
- Scheffers, D.-J. & Pinho, M.G., 2005. Bacterial cell wall synthesis: new insights from localization studies. *Microbiology and Molecular Biology Reviews*, 69(4), pp.585–607.
- Scheller, H.V. & Ulvskov, P., 2010. Hemicelluloses. *Annual Review of Plant Biology*, 61(1), pp.263–289.
- Scheres, B. et al., Embryonic origin of the *Arabidopsis* primary root and root meristem initials. *dev.biologists.org*
- Schultz, E.R. et al., 2017. Skewing in *Arabidopsis* roots involves disparate environmental signaling pathways. pp.1–16.
- Sedbrook, J.C., 2002. The *Arabidopsis* SKU5 Gene Encodes an Extracellular Glycosyl Phosphatidylinositol-Anchored Glycoprotein Involved in Directional Root Growth. *THE PLANT CELL ONLINE*, 14(7), pp.1635–1648.
- Sedbrook, J.C. et al., 1998. Molecular genetics of root gravitropism and waving in *Arabidopsis thaliana*. *Gravitational and space biology bulletin : publication of the American Society for Gravitational and Space Biology*, 11(2), pp. 71–78.
- Sedbrook, J.C. et al., 2004. The *Arabidopsis* sku6/spiral1 gene encodes a plus end-localized microtubule-interacting protein involved in directional cell expansion. *THE PLANT CELL ONLINE*, 16(6), pp.1506–1520.
- Seifert, G.J. & Blaukopf, C., 2010. Irritable Walls: The Plant Extracellular Matrix and Signaling. *Plant Physiology*, 153(2), pp.467–478.
- Sénéchal, F. et al., 2014. Homogalacturonan-modifying enzymes: structure, expression, and roles in plants. *Journal of Experimental Botany*, 65(18), pp.5125–5160.
- Shan, X., Yan, J. & Xie, D., 2012. Comparison of phytohormone signaling mechanisms. *Current Opinion in Plant Biology*, 15(1), pp.84–91.
- Shapiro, B.E. et al., 2015. Analysis of cell division patterns in the *Arabidopsis* shoot apical meristem. *Proceedings of the National Academy of Sciences*, 112(15), pp.4815–4820.
- Shi, B. et al., 2018. Feedback from Lateral Organs Controls Shoot Apical Meristem Growth by Modulating Auxin Transport. *Developmental Cell*, 44(2), pp.204–216.e6.
- Shi, H. et al., 2013. BR-SIGNALING KINASE1 physically associates with FLAGELLIN SENSING2 and regulates plant innate immunity in *Arabidopsis*. *The Plant cell*, 25(3), pp.1143–1157.
- Shiu, S.H. & Bleecker, A.B., 2003. Expansion of the receptor-like kinase/Pelle gene family and receptor-like proteins in *Arabidopsis*. *Plant Physiology*, 132(2), pp.530–543.
- Shiu, S.H. & Bleecker, A.B., 2001. Plant receptor-like kinase gene family: diversity, function, and signaling. *Science's STKE : signal transduction knowledge environment*, 2001(113), pp.re22–re22.

- Simmons, C. et al., 1995. A novel root gravitropism mutant of *Arabidopsis thaliana* exhibiting altered auxin physiology. *Physiologia plantarum*, 93, pp.790–798.
- Singh, A.P. et al., 2014. Activity of the brassinosteroid transcription factors BRASSINAZOLE RESISTANT1 and BRASSINOSTEROID INSENSITIVE1-ETHYL METHANESULFONATE-SUPPRESSOR1/BRASSINAZOLE RESISTANT2 blocks developmental reprogramming in response to low phosphate availability. *Plant Physiology*, 166(2), pp.678–688.
- Singh, M., Gupta, A. & Laxmi, A., 2017. Glucose and Brassinosteroid Signaling Network in Controlling Plant Growth and Development Under Different Environmental Conditions. In G. K. Pandey, ed. *Mechanism of Plant Hormone Signaling Under Stress, 2 Volume Set*. Hoboken, NJ, USA: John Wiley & Sons, Inc., pp. 443–469.
- Singh, S. et al., 2017. Sirtinol, a Sir2 protein inhibitor, affects stem cell maintenance and root development in *Arabidopsis thaliana* by modulating auxin-cytokinin signaling components. *Nature Publishing Group*, pp.1–13.
- Smith, L.G., 2001. Plant cell division: building walls in the right places. *Nature reviews. Molecular cell biology*, 2(1), pp.33–39.
- Somerville, C.R., 2006. Cellulose Synthesis in Higher Plants. *Annual Review of Cell and Developmental Biology*, 22(1), pp.53–78.
- Somerville, C.R. et al., 2004. Toward a systems approach to understanding plant cell walls. *Science*, 306(5705), pp. 2206–2211.
- Somssich, M., Khan, G.A. & Persson, S., 2016. Cell Wall Heterogeneity in Root Development of *Arabidopsis*. *Frontiers in Plant Science*, 7, p.1242.
- Sparks, E.E. & Benfey, P.N., 2017. The contribution of root systems to plant nutrient acquisition. In *Plant Macronutrient Use Efficiency*. Elsevier, pp. 83–92.
- Stahl, Y. & Simon, R., 2010. Plant primary meristems: shared functions and regulatory mechanisms. *Current Opinion in Plant Biology*, 13(1), pp.53–58.
- Steeves, T.A. & Sussex, I.M., 2009. *Patterns in plant development* 2nd ed., Cambridge: Cambridge University Press.
- Sun, Yadong et al., 2013. Structure reveals that BAK1 as a co-receptor recognizes the BRI1-bound brassinolide. *Nature Publishing Group*, 23(11), pp.1326–1329.
- Sun, Yu et al., 2010. Integration of Brassinosteroid Signal Transduction with the Transcription Network for Plant Growth Regulation in *Arabidopsis*. *Developmental Cell*, 19(5), pp.765–777.
- Takatsuka, H. & Umeda, M., 2014. Hormonal control of cell division and elongation along differentiation trajectories in roots. *Journal of Experimental Botany*, 65(10), pp.2633–2643.
- Tamaoki, D. et al., 2014. Jasmonic acid and salicylic acid activate a common defense system in rice. *Plant Signaling & Behavior*, 8(6), pp.e24260–3.
- Tameshige, T. et al., 2015. Cell walls as a stage for intercellular communication regulating shoot meristem development. *Frontiers in Plant Science*, 6, pp.447–10.
- Tan, L. et al., 2012. Arabinogalactan-proteins and the research challenges for these enigmatic plant cell surface proteoglycans. *Frontiers in Plant Science*, 3, p.140.
- Tang, J., Han, Z. & Chai, J., 2016. Q&A: what are brassinosteroids and how do they act in plants? *BMC biology*, 14(1), p.113.
- Tang, W. et al., 2011. PP2A activates brassinosteroid-responsive gene expression and plant growth by dephosphorylating BZR1. *Nature Cell Biology*, 13(2), pp.124–131.
- Taylor-Teeple, M. et al., 2015. An *Arabidopsis* gene regulatory network for secondary cell wall synthesis. *Nature*, 517(7536), pp.571–575.
- Thomas, L.H. et al., 2012. Structure of Cellulose Microfibrils in Primary Cell Walls from Collenchyma. *Plant Physiology*, 161(1), pp.465–476.
- Thompson, M.V. & Holbrook, N.M., 2004. Root-gel interactions and the root waving behavior of *Arabidopsis*. *Plant Physiology*, 135(3), pp.1822–1837.
- Thummel, C.S. & Chory, J., 2002. Steroid signaling in plants and insects—common themes, different pathways. *Genes & Development*, 16(24), pp.3113–3129.

- Tian, H. et al., 2014. The key players of the primary root growth and development also function in lateral roots in Arabidopsis. *Plant Cell Reports*, 33(5), pp.745–753.
- To, J.P.C. & Kieber, J.J., 2008. Cytokinin signaling: two-components and more. *Trends in Plant Science*, 13(2), pp.85–92.
- To, J.P.C. et al., 2004. Type-A Arabidopsis response regulators are partially redundant negative regulators of cytokinin signaling. *THE PLANT CELL ONLINE*, 16(3), pp.658–671.
- To, J.P.C., Deruère, J., Maxwell, B.B., Morris, V.F., Hutchison, C.E., Ferreira, F.J., Schaller, G.E. & Kieber, J.J., 2007. Cytokinin Regulates Type-A Arabidopsis Response Regulator Activity and Protein Stability via Two-Component Phosphorelay. *THE PLANT CELL ONLINE*, 19(12), pp.3901–3914.
- Tor, M., Lotze, M.T. & Holton, N., 2009. Receptor-mediated signalling in plants: molecular patterns and programmes. *Journal of Experimental Botany*, 60(13), pp.3645–3654.
- Truernit, E. et al., 2008. High-Resolution Whole-Mount Imaging of Three-Dimensional Tissue Organization and Gene Expression Enables the Study of Phloem Development and Structure in Arabidopsis. *THE PLANT CELL ONLINE*, 20(6), pp.1494–1503.
- Ubeda-Tomás, S. et al., 2009. Gibberellin Signaling in the Endodermis Controls Arabidopsis Root Meristem Size. *Current Biology*, 19(14), pp.1194–1199.
- Ubeda-Tomás, S., Beemster, G.T.S. & Bennett, M.J., 2012. Hormonal regulation of root growth: integrating local activities into global behaviour. *Trends in Plant Science*, 17(6), pp.326–331.
- Uehara, T. et al., 2010. Daughter cell separation is controlled by cytokinetic ring-activated cell wall hydrolysis. *The EMBO Journal*, pp.1–11.
- Uyttewaal, M. et al., 2012. Mechanical Stress Acts via Katanin to Amplify Differences in Growth Rate between Adjacent Cells in Arabidopsis. *Cell*, 149(2), pp.439–451.
- Van Dam, D., 2007. A.J.Kastin Handbook of Biologically Active Peptides 1st ed. 2006 Academic Press 0-12-369442-6 1640 pp., Hardback. *Clinical Neurology and Neurosurgery*, 109(5), p.477.
- van den Berg, C. et al., 1995. Cell fate in the Arabidopsis root meristem determined by directional signalling. *Nature*, 378(6552), pp.62–65.
- Vanneste, S. & Friml, J., 2009. Auxin: A Trigger for Change in Plant Development. *Cell*, 136(6), pp.1005–1016.
- Vieten, A. et al., 2005. Functional redundancy of PIN proteins is accompanied by auxin-dependent cross-regulation of PIN expression. *Development (Cambridge, England)*, 132(20), pp.4521–4531.
- Vilarrasa-Blasi, J. et al., 2014. Regulation of Plant Stem Cell Quiescence by a Brassinosteroid Signaling Module. *Developmental Cell*, 30(1), pp.36–47.
- Wachsman, G., Sparks, E.E. & Benfey, P.N., 2015. Genes and networks regulating root anatomy and architecture. *New Phytologist*, 208(1), pp.26–38.
- Wakabayashi, K., Hoson, T. & Huber, D.J., 2003. Methyl de-esterification as a major factor regulating the extent of pectin depolymerization during fruit ripening: a comparison of the action of avocado (*Persea americana*) and tomato (*Lycopersicon esculentum*) polygalacturonases. *Journal of Plant Physiology*, 160(6), pp.667–673.
- Walker, K.L., Müller, S., Moss, D., Ehrhardt, D.W. & Smith, L.G., 2007. Arabidopsis TANGLED identifies the division plane throughout mitosis and cytokinesis. *Current Biology*, 17(21), pp.1827–1836.
- Wallace, A.F. et al., 2013. Microscopic Evidence for Liquid-Liquid Separation in Supersaturated CaCO<sub>3</sub> Solutions. *Science*, 341(6148), pp.885–889.
- Wang, H. et al., 2017. Abscisic Acid Signaling Inhibits Brassinosteroid Signaling through Dampening the Dephosphorylation of BIN2 by ABI1 and ABI2. *MOLECULAR PLANT*, pp.1–34.
- Wang, H. et al., 1997. The ROOT HAIR DEFECTIVE3 gene encodes an evolutionarily conserved protein with GTP-binding motifs and is required for regulated cell enlargement in Arabidopsis. *Genes & Development*, 11(6), pp. 799–811.
- Wang, J. et al., 2014. Structural insights into the negative regulation of BRI1 signaling by BRI1-interacting protein BKI1. *Nature Publishing Group*, 24(11), pp.1328–1341.
- Wang, R. & Estelle, M., 2014. Diversity and specificity: auxin perception and signaling through the TIR1/AFB pathway. *Current Opinion in Plant Biology*, 21, pp.51–58.

- Wang, W., Bai, M.-Y. & Wang, Z.-Y., 2014. The brassinosteroid signaling network — a paradigm of signal integration. *Current Opinion in Plant Biology*, 21, pp.147–153.
- Wang, X. et al., 2008. Sequential Transphosphorylation of the BRI1/BAK1 Receptor Kinase Complex Impacts Early Events in Brassinosteroid Signaling. *Developmental Cell*, 15(2), pp.220–235.
- Wang, Y. et al., 2013. Strigolactone/MAX2-Induced Degradation of Brassinosteroid Transcriptional Effector BES1 Regulates Shoot Branching. *Developmental Cell*, 27(6), pp.681–688.
- Wang, Z.-Y. et al., 2012. Brassinosteroid signaling network and regulation of photomorphogenesis. *Annual review of genetics*, 46(1), pp.701–724.
- Wang, Z.-Y. et al., 2001. BRI1 is a critical component of a plasma-membrane receptor for plant steroids. *Nature*, 410(6826), pp.380–383.
- Wang, Z.-Y. et al., 2002. Nuclear-localized BZR1 mediates brassinosteroid-induced growth and feedback suppression of brassinosteroid biosynthesis. *Developmental Cell*, 2(4), pp.505–513.
- West, A.H. & Stock, A.M., 2001. Histidine kinases and response regulator proteins in two-component signaling systems. *Trends in biochemical sciences*, 26(6), pp.369–376.
- Willis, L. et al., 2016. Cell size and growth regulation in the Arabidopsis thaliana apical stem cell niche. *Proceedings of the National Academy of Sciences of the United States of America*, 113(51), pp.E8238–E8246.
- Wolf, S., Mouille, G. & Jérôme, P.J., 2009. Homogalacturonan Methyl-Esterification and Plant Development. *MOLECULAR PLANT*, 2(5), pp.851–860.
- Wolf, S. & Hofte, H., 2014. Growth Control: A Saga of Cell Walls, ROS, and Peptide Receptors. *THE PLANT CELL ONLINE*, 26(5), pp.1848–1856.
- Wolf, S. et al., 2014. A receptor-like protein mediates the response to pectin modification by activating brassinosteroid signaling. *Proceedings of the National Academy of Sciences*, 111(42), pp.15261–15266.
- Wolf, S., Hématy, K. & Höfte, H., 2012a. Growth Control and Cell Wall Signaling in Plants. *Annual Review of Plant Biology*, 63(1), pp.381–407.
- Wolf, S., Mravec, J., et al., 2012b. Plant Cell Wall Homeostasis Is Mediated by Brassinosteroid Feedback Signaling. *Current Biology*, 22(18), pp.1732–1737.
- Woodward, A.W. & Bartel, B., 2005. Auxin: regulation, action, and interaction. *Annals of Botany*, 95(5), pp.707–735.
- Wormit, A. et al., 2012. Osmosensitive Changes of Carbohydrate Metabolism in Response to Cellulose Biosynthesis Inhibition. *Plant Physiology*, 159(1), pp.105–117.
- Yabuuchi, T. et al., 2015. Preprophase band formation and cortical division zone establishment: RanGAP behaves differently from microtubules during their band formation. *Plant Signaling & Behavior*, 10(9), pp.e1060385–11.
- Yang, D.C. et al., 2011. An ATP-binding cassette transporter-like complex governs cell-wall hydrolysis at the bacterial cytokinetic ring. *Proceedings of the National Academy of Sciences of the United States of America*, 108(45), pp.E1052–60.
- Yang, W., et al., 2016. Regulation of Meristem Morphogenesis by Cell Wall Synthases in Arabidopsis. *Current Biology*, pp.1–34.
- Yapo, B.M. et al., 2007. Pectins from citrus peel cell walls contain homogalacturonans homogenous with respect to molar mass, rhamnogalacturonan I and rhamnogalacturonan II. *Carbohydrate Polymers*, 69(3), pp.426–435.
- Ye, H. et al., 2017. RD26 mediates crosstalk between drought and brassinosteroid signalling pathways. *Nature Communications*, 8, p.14573.
- Ye, Q. et al., 2010. Brassinosteroids control male fertility by regulating the expression of key genes involved in Arabidopsis anther and pollen development. *Proceedings of the National Academy of Sciences*, 107(13), pp.6100–6105.
- Yeats, T.H. et al., 2016. Cellulose Deficiency Is Enhanced on Hyper Accumulation of Sucrose by a H<sup>+</sup>-Coupled Sucrose Symporter. *Plant Physiology*, 171(1), pp.110–124.
- Yin, Y. et al., 2005. A New Class of Transcription Factors Mediates Brassinosteroid-Regulated Gene Expression in Arabidopsis. *Cell*, 120(2), pp.249–259.
- Yin, Y. et al., 2002. BES1 accumulates in the nucleus in response to brassinosteroids to regulate gene expression and promote stem elongation. *Cell*, 109(2), pp.181–191.

- Yoneda, A. et al., 2005. Decision of Spindle Poles and Division Plane by Double Preprophase Bands in a BY-2 Cell Line Expressing GFP-Tubulin. *Plant and Cell Physiology*, 46(3), pp.531–538.
- Yu, X. et al., 2008. Modulation of brassinosteroid-regulated gene expression by Jumonji domain-containing proteins ELF6 and REF6 in Arabidopsis. *Proceedings of the National Academy of Sciences of the United States of America*, 105(21), pp.7618–7623.
- Yuen, C.Y.L. et al., 2005. Loss-of-function mutations of ROOT HAIR DEFECTIVE3 suppress root waving, skewing, and epidermal cell file rotation in Arabidopsis. *Plant Physiology*, 138(2), pp.701–714.
- Yuen, C.Y.L. et al., 2003. WVD2 and WDL1 modulate helical organ growth and anisotropic cell expansion in Arabidopsis. *Plant Physiology*, 131(2), pp.493–506.
- Zeng, C. et al., 2010. Evaluation of 5-ethynyl-2'-deoxyuridine staining as a sensitive and reliable method for studying cell proliferation in the adult nervous system. *Brain Research*, 1319, pp.21–32.
- Zhang, D. et al., 2013. Transcription factor HAT1 is phosphorylated by BIN2 kinase and mediates brassinosteroid repressed gene expression in Arabidopsis. *The Plant Journal*, 77(1), pp.59–70.
- Zhang, Y., Iakovidis, M. & Costa, S., 2016. Control of patterns of symmetric cell division in the epidermal and cortical tissues of the Arabidopsis root. *Development (Cambridge, England)*, 143(6), pp.978–982.
- Zhang, Z. et al., 2016. TOR Signaling Promotes Accumulation of BZR1 to Balance Growth with Carbon Availability in Arabidopsis. *Current Biology*, pp.1–18.
- Zhao, Y., 2010. Auxin Biosynthesis and Its Role in Plant Development. *Annual Review of Plant Biology*, 61(1), pp.49–64.
- Zhu, J.-Y., Sae-Seaw, J. & Wang, Z.-Y., 2013. Brassinosteroid signalling. *Development (Cambridge, England)*, 140(8), pp.1615–1620.
- Zimmermann, P. et al., 2004. GENEVESTIGATOR. Arabidopsis microarray database and analysis toolbox. *Plant Physiology*, 136(1), pp.2621–2632.
- Zipfel, C., 2014. Plant pattern-recognition receptors. *Trends in Immunology*, 35(7), pp.345–351.
- Zuo, J. et al., 2000. KORRIGAN, an Arabidopsis endo-1,4-beta-glucanase, localizes to the cell plate by polarized targeting and is essential for cytokinesis. *THE PLANT CELL ONLINE*, 12(7), pp.1137–1152.
- Zwanenburg, B., Pospíšil, T. & Zeljković, S.Ć., 2016. Strigolactones: new plant hormones in action. *Planta*, 243(6), pp.1311–1326.
- Zykwinska, A.W., 2005. Evidence for In Vitro Binding of Pectin Side Chains to Cellulose. *Plant Physiology*, 139(1), pp.397–407.

## Acknowledgement

The first and most important, I am deeply grateful to Dr. Sebastian Wolf, you gave me this opportunity to go a step further in science which was also a very important turning point in my life. Your kind and generous help for not only science but also personal life in Heidelberg was beyond a nice boss. The inspirations I have got from you will have an endless and profound impact on my life, no matter where I am and what I do. I also owe my deep gratitude to my thesis defense committee members, Prof. Dr. Karin Schumacher, Prof. Dr. Alexis Maizel and Prof. Dr. Rüdiger Hell, your scientific suggestions supported me through the entire Ph.D. and your passion as well as sparkle in but also beyond science deeply infected me.

My heartfelt appreciation goes to the entire AG Wolf (Dr. Borja Garnelo Gómez, Eleonore Holzward, Ann-Kathrin Schürholz, Philippe Golfier, John Walden, Hannah Walter, and all the former members and students), the most amazing group I have ever been a part of. Borja, the Spanish sunshine, mon 'compagnon d'armes', les mémoires qu'on a créés, les voyages et les bêtises qu'on a faits ensemble ne seront jamais oubliés. Eli, the lovely hamster, you have been always so helpful for whatever I need, and our mini-excursion to café botanik with a beer in the middle of a working day is one of the best highlights of my Ph.D. memories. AKS, my bird lady, a big big thank you for all you have done for me, you are always there when I need, and we have done so much together that I don't even know how to summarize, in one word, my life in Heidelberg will be with no colour without you. Wolfies, all the moments, tears, laugh, gossip, ... .., all what we created together, and of course the awesome science, will stay in my heart forever.

I would also like to offer my special thanks to all members of AG Schumacher, AG Maizel and Ines Steins, all my floor members, for your generous technical and administrative support and the best working atmosphere in COS.

I would particularly like to thank Prof. Dr. Thomas Rausch, for hosting our group in his lab in the beginning of my Ph.D. I would like to thank Angelika Wundlich for helping me with all the German paper work when I just arrived in Heidelberg and did not say a word in German (well, except Guten Tag and Danke), and also for your sunny smile, as always. Heike Steininger, my dear Heike, the best technician ever, my bench mate for half a year, the competitor for the messiest bench in the lab, I will definitely miss your hearty laughter. Tatjana Peskan-Berghöfer, one of the gentlest people I have ever known, you are a bright scientist and a wonderful co-worker. Philippe, thanks for generously providing me your 'three squirrels' nuts when I was dying from hunger but still insisting on writing my thesis. Wan Zhang, my deliver girl of hotpot sauce, even though I will not receive it before my submission, you are still my hero. Zoe Zhong, it is amazing to meet you here, thanks for correcting my Cantonese, I wish you all the happiness for your life.

I would like to give my sweet thanks to Apolonio Huerta, for our conversations about work, life, love and everything, for hosting in Zürich, for sharing all my feelings; my sweet smart Jana Askani, you have always been so sweet to me; M. Görkem Patir Nebioglu and Dr. Upendo Lupanga, for our crazy drinking/partying/traveling time together; Béatrice Berthet, tu es une fille magnifique, bien plus magnifique que tout le monde le croyait, je te dois un grand merci pour tout les soutiens que tu m'as généreusement offerts. Zhaoxue Ma, my lab gossip swapper, I will live my young spirit as you wished for my birthday. Michael Stitz, my best badminton partner and adversary, you made badminton the funnest sport in my life in Heidelberg.

I will never ever forget about those who enlightened my life outside science in Heidelberg. Dr. Yihan Dong, a private friend and the best food-mate, without you my happiness will not become true. Cyril Legrand, mon petit lapin blanc, tu es un pote incroyable, le lapin le plus beau, le plus mignon et le plus adorable que j'ai jamais vu. Yi Xiao, my dearest 二姐, my faithful hotpot and cooking fan, the unforgettable one, no word can describe our friendship, you know it. Loïc Schweicher, Monsieur Loïc Pas de Raison, hope we can keep annoying each other for endless years. You guys, I really feel like being at home when I am with you.

Jun Dong and Daqing Li, you are the best parents in the world, in the galaxy, in the whole universe. Thanks for letting me do what I wanted to, thanks for understanding me and supporting me for every single decision that I made in my life. My every success in the past and future has your sweat and blood in it.

The last, I put you the last just because I need a lot of time to organize my words for you. Shanshan Wang, my beloved 哇噻噻, my most precious treasure, you made me find the meaning of my life. We have been through a lot and we have grown up a lot together, and we have both discovered the best of ourselves ever. I cannot wait to see the next step of our life, it is going to be more than awesome, I know it.